
CHAPTER

- 6 -

ENGINE MANAGEMENT SYSTEM INSTALLATION

Before the ANN stability controller was developed, additional hardware was installed into the test vehicle to enable real-time data acquisition and control. One particular problem was that the requirements of electronic reduction of engine power for traction control could not be met with the factory fitted engine electronic control unit (ECU). As such, and with the observation that hydrogen conversion of the engine would not be possible with the factory ECU either, the decision was made to replace it with an aftermarket ECU.

To this end, the following chapter describes the MoTeC ECU installation process, as well as detailing the engine sensor calibrations, ECU configuration and engine tuning.

6.1 Test Vehicle Limitations

The test vehicle is factory fitted with an electronic engine management system. This system was considered inadequate for this investigation based on a number of goal limitations, as noted below.

- a. Flexibility of the unit. The factory system is specifically designed for the standard vehicle without flexibility of use in mind. The system cannot be “re-tuned” outside of a very small range, significantly increasing the tuning complications if anything is done that is out of the ordinary.
- b. Intellectual property of the unit. The engine control unit, and the tuning data it contains, remains the intellectual property of Toyota, with only service information and basic wiring diagrams available [125, 126, 127]. As a result it is extremely difficult to get information on its internal functions and the algorithms it performs.
- c. Potential for adverse operation. As the internal operation of the controller is unknown, it is not possible to predict the outcomes of augmenting the current arrangement or introducing new systems. This not only makes it difficult to determine the accuracy of results, but may cause unexpected consequences. This, obviously, has safety ramifications, but may also cause severe engine damage and possibly void any experimental research.
- d. Adding engine sensors. The factory system is designed in such a way that it is not possible to add any new devices or sensors, other than Toyota supplied ones where available. This means that it is not possible to incorporate any new sensors into the engine control.
- e. Adding additional engine control. This investigation requires an ability to limit the amount of power the engine produces. This can be done in a number of ways (including injection cut, ignition cut, ignition retard and cam retard), but to avoid engine damage requires a high level of control [128]. The factory system does not allow for this at all and, due to its “black box” nature, it is highly questionable if any “add on” system will operate as anticipated.

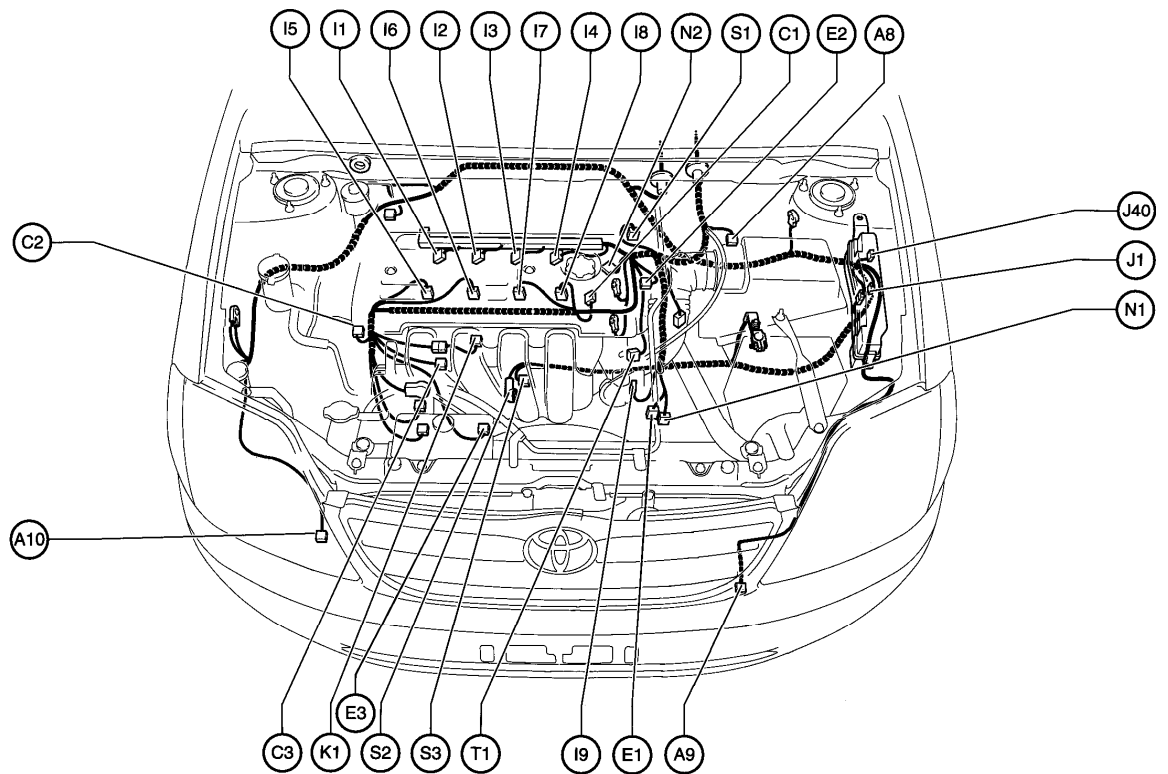
- f. Future research limitations. The “Intelligent Car” projects require a vehicle that is highly flexible, and this investigation aim to support this goal. The factory system, however, does not allow for any flexibility with regard to the engine, and offers a severe hindrance to the intended outcome.
- g. Hydrogen conversion. The “HART” hydrogen conversion that is to take place after the conclusion of this investigation will not be supported by the factory system. Another stated goal of this investigation is to install systems that integrate with the equipment required for each, which any factory engine management system “add on” will not do.

As a result of these numerous restrictions, it was decided to install an aftermarket engine management system. Such systems are commonly used in racing circles and are freely available, with great variation in both quality and price. To ensure the greatest flexibility and performance for the “Intelligent Car” projects, and to ensure sufficient control options for the “HART” hydrogen conversion, the decision was made to purchase MoTeC’s M400 engine management system. This system has very high flexibility and, most importantly for this investigation, contains numerous inputs to affect additional engine control in many different respects. Specification for the unit can be found in the Appendix.

The M400 was installed in a “piggy back” arrangement, which allows fast and simple conversion back to the Toyota system, and is detailed below.

6.2 Factory ECU

Almost all modern vehicles are factory fitted with electronically controlled fuel injection in some form, and often combine this with electronically controlled ignition. The 2002 Toyota Corolla test vehicle is no exception, with its 1ZZ-FE VVTi engine incorporating individual cylinder injections and ignition systems. This in turn necessitates the use of a factory fitted engine management electronic control unit, which will be referred to hereafter as the “Factory ECU”. This ECU measures an array of parameters from the engine and controls one ignition and two injection parameters for each cylinder, being ignition timing, injection timing and the injection pulse width (which determines the amount of fuel). Many of the system components are given in Figure 6.1.



A 8 Air Flow Meter	I 1 Ignition Coil and Igniter No. 1	J 1 Junction Connector
A 9 Airbag Sensor Front LH	I 2 Ignition Coil and Igniter No. 2	J 40 Junction Connector
A10 Airbag Sensor Front RH	I 3 Ignition Coil and Igniter No. 3	K 1 Knock Sensor
C 1 Camshaft Position Sensor	I 4 Ignition Coil and Igniter No. 4	N 1 Neutral Start SW
C 2 Camshaft Timing Oil Control Valve	I 5 Injector No.1	N 2 Noise Filter (Ignition)
C 3 Crankshaft Position Sensor	I 6 Injector No.2	S 1 Speed Sensor (Combination Meter)
E 1 ECT Solenoid	I 7 Injector No.3	S 2 Starter
E 2 EFI Water Temp. Sensor	I 8 Injector No.4	S 3 Starter
E 3 Engine Oil Pressure SW	I 9 ISC Valve	T 1 Throttle Position Sensor

Figure 6.1: Factory installed engine management system components; non-exhaustive [modified from 125]

These are not the only engine parameters that require control. The “VVTi” of the engine name stands for “Variable Valve Timing – intelligent”, and inspection of the engine shows that the inlet cam pulley contains a mechanism by which the timing of the cam can be advanced. This allows for more sensitivity in the engine control by allowing the inlet cam to be advanced to affect the volumetric efficiency of the engine and to augment the fuel timing. The “intelligent” refers to the way the factory ECU controls the cam and, while Toyota do not provide this information publicly, it would seem a reasonable assumption that the control is based on exhaustive empirical testing that incorporates steady state and dynamic engine conditions with the possibility of some predictive capability.

Still, these are not the only engine parameters that the factory ECU controls. The ECU performs secondary engine control for items such as the idle valve, fuel pump, radiator fan, lambda sensor heater and starter motor, as well powering all of the engine sensors.

It controls other features such as the engine immobiliser, airbag and air conditioning systems, as well as the driver display of warning lights and vehicle and engine speed. Additionally, many of these systems are, or could be, interrelated and moving a single sensor input or modifying the systems that communicate with the factory ECU may cause unpredictable results.

It would be preferable to maintain the factory ECU for functions that are not directly related to engine control. Therefore, to remove the chance of malfunction, the factory ECU should be left installed in the vehicle with its original wiring configuration. The only required modification would be to cut the control signals from the factory ECU, which are simple one-way digital signals, and connect them to the new aftermarket ECU.

6.3 MoTeC ECU

MoTeC are regarded as one of the international leaders in engine management systems, as their products reaching across many different applications. They are most noted as one of the best automobile racing engine management producers in the world. MoTeC also prides itself on outstanding customer support (regardless of the age of the product, which is ideal in a university environment), provides regular training in its hardware and has a continuing software development program. In addition the company is Australian initiated, Australian owned and Australian based, and provides a discount price for the University of Tasmania.

The University of Tasmania has an established relationship with MoTeC, having previously purchased four engine management systems from them, as well as other equipment that will be used in this investigation. As a result, there is a great deal of experience within the University with MoTeC products, myself having had reasonable experience with MoTeC's M4 ECU.

The M400 differs considerably in functionality to the M4, which is its predecessor. Not the least is the fact that the M4 was configurable through MS DOS[®] while the M400 is MS Windows[®] based, marking a considerable step forward. The M400 also has vastly increased functionality, and is summarised in Figure 6.2.

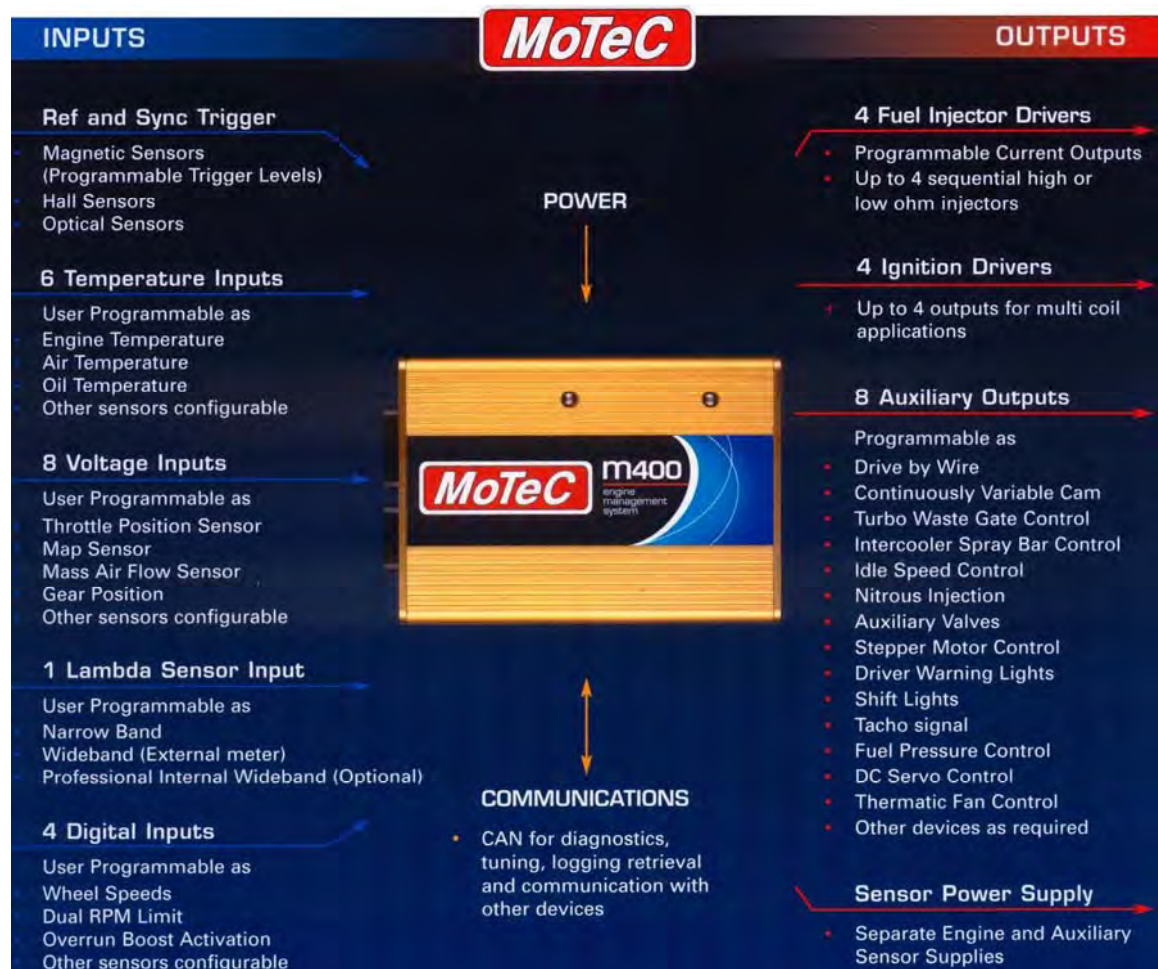


Figure 6.2: M400 engine management system specification summary [129]

Compared to the M4, the M400 provides additional scope for optical ref and sync triggers, 3 more temperature inputs, 5 more voltage inputs, 2 more digital inputs and 4 more auxiliary outputs. The additional auxiliary outputs provide additional functions, including continuously variable cam control, second stage injection control (two injectors per cylinder), electronic throttle control (drive by wire), fuel pressure control, DC servo control and stepper motor control. The M400 incorporates CAN bus communications, providing significantly faster data streaming than its RS232 predecessor.

The M4 would severely limit the performance of the test vehicle engine, and significantly reduce functionality for future research. By providing cam control, the M400 not only makes the best use of the features of the engine, but also provides additional scope for the proposed hydrogen conversion. This is because petrol internal combustion engines that are converted to hydrogen often run into serious problems involving cam overlap. Most petrol engines have a level of overlap, which is when the

cylinder inlet and exhaust valves are opened at the same time, because it increases the airflow in and out of the engine and increases power. In a hydrogen-converted engine, however, the hot exhaust gases can ignite the hydrogen rich inlet air due to its much lower limit of flammability, and produce backfiring. This not only generates very poor engine performance, but it burns the valves out very quickly. By providing cam advance control these problems of valve overlap can be avoided, and the inlet cams can be tuned for optimum performance.

The ability of the M400 to control second stage injection is an extremely useful feature for hydrogen conversion. This feature provides that ability to run two separate injectors per cylinder, and control them separately. Normally this feature is used to control one small and one large injector on engines with wildly varying fuel demands, with the small injector providing minimum fuelling near idle and the large injector providing maximum fuelling for power. This is done because of the mechanical limitations of the injectors, which either cannot provide sufficiently fine pulse resolution for minimum required fuelling, or simply cannot inject enough fuel when demanded. This feature is very useful for hydrogen conversion, as previous work done by the University of Tasmania has suggested that a single hydrogen injector per cylinder will not provide sufficient fuelling for the range of operation of the engine. The work also suggests that the hydrogen may need to be injected in much shorter pulses than is normally acceptable in petrol engines. By providing two stage injection the M400 provides this capability for future research.

The inclusion of two-stage injection within the M400 gives rise to the possibility of converting the engine to a hybrid type. By running one choice of fuel through the first injector, and another choice through the second it is possible to run each fuel separately or in combination. In the case of the proposed hydrogen conversion, this could mean running a petrol/hydrogen system. The engine could then, at the flick of a switch, go from running on hydrogen to running on petrol. This would provide significant versatility due to the extreme lack of hydrogen refuelling stations. Further, the engine could be converted to run as a hydrogen/petrol hybrid, running on a combination of each. In this case, for instance, the engine could be tuned to run on hydrogen only when city driving and to run on predominately petrol when accelerating hard. This would provide “the best of both worlds” of the two fuels, significantly reducing emissions without any loss of peak power – while also retaining a large range of travel between refills.

The “drive by wire” function of the M400 could be exploited in future research into vehicle dynamics. In this investigation engine power will be limited using electronic injection and ignition cut only, which is considered to produce both a harsh ride and excessive wear to the engine over long periods. A better system would be a combination of throttle and injection/ignition control, whereby the injection/ignition provide instantaneous response and the throttle provides smoother power reduction with some lag. The inclusion of the electronic throttle control that the M400 provides would enable this type of system to be incorporated in the future, although a safer option would probably be electronic secondary throttle control where it is impossible for the main throttle to erroneously stay open [41].

Lastly, the inclusion of CAN bus communication within the M400 provides greatly increased data transfer rates between the ECU and other CAN devices. While the M400 is capable of logging data internally at very high rates, the CAN bus allows this data to be transmitted to other logging or control devices at reduced but still comparably high rates. This would be particularly useful when considering the large number of parameters that the M400 generates that would otherwise be very difficult to obtain. Additionally, the CAN functionality of the ECU allows it to be directly linked to a CAN “backbone”, whereby it is very easy to have a large number of devices communicating with each other.

6.4 Vehicle Sensors

The MoTeC ECU can only operate correctly if it can obtain an array of information from the engine about its condition. Particularly, it requires information on the crank position to determine accurate timing, and cam position to determine if cylinders are on compression or exhaust strokes. In addition, it requires a measure of driver-desired load, which is normally measured through throttle position, manifold pressure and/or mass airflow. Further, information on engine and air temperatures are generally used to compensate for environmental conditions. To install the MoTeC ECU correctly, a thorough understanding of how these sensors operate is necessary.

6.4.1 Manifold Air Pressure Sensor

The function of the throttle on a naturally aspirated car is to limit the amount of air that enters the engine. The engine, on the other hand, is a positive displacement air pump that

moves a specific volume of air on each cycle. Operating these two components together produces a vacuum within the intake manifold, which is measured by the manifold air pressure (MAP) sensor. This parameter is not normally measured in naturally aspirated engines, being generally limited in application to turbo and supercharged engines that, in addition, often run very high positive pressures. As such, the test vehicle is not factory fitted with a MAP sensor. Nonetheless, to provide increased research opportunities, coupled with the ease of installation, it was decided to add this sensor.

The sensor that was chosen was supplied from Bosch, and has the part number 0-261-230-030. The sensor measures absolute pressures in the 10 to 115kPa range, making it ideally suited to the Corolla's naturally aspirated engine, and has an integral air temperature sensor with a range of -40°C to 130°C . Pressure is measured using a piezoresistive pressure sensor element that is mounted to a glass base within the sensor body, as shown in Figure 6.3. One side of the sensor element is exposed to the pressure being measured, while the other is exposed to the reference vacuum enclosed between the element and the glass base. The effect on voltage from the resulting change in resistance of the element is amplified and compensated for temperature on the internal silicon chip, producing an analogue voltage pressure output. The temperature sensor resistance, which is of the negative temperature coefficient type, is proved as a sensor output to providing data on the temperature of the air within the manifold.

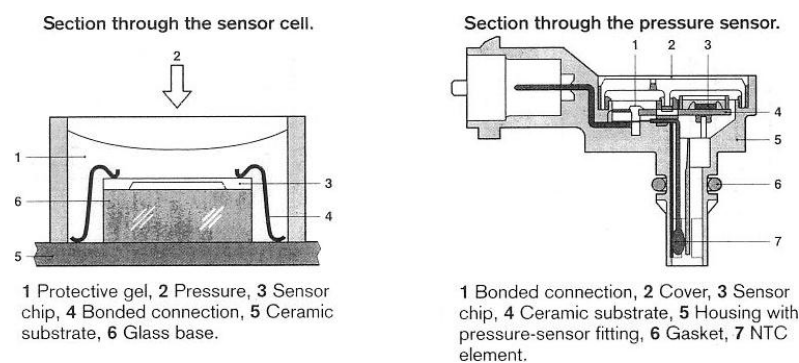


Figure 6.3: Manifold air pressure sensor construction [130]

6.4.1.1 Sensor Considerations

While the test vehicle remains naturally aspirated, the selected MAP sensor should have sufficient resolution for all operating conditions. If a turbo or supercharger is fitted in the future, which is foreseeable, it is important to realise that this sensor will have to be replaced. This is a simple process.

To install the current sensor there are only two real considerations to keep in mind. The first is that the sensor is installed in such a way as to avoid air leakage into the manifold. Any additional air will alter the engine tuning and result in a 'lean' mixture, potentially damaging the engine. The second consideration is based on the sensor design. The sensing element of the sensor, while having a protective coating, is sensitive to the accumulation of condensation. As such, it is important to place the sensor in such a way as to avoid condensation forming within the sensor. This is simply done by installing the sensor horizontally, so that the sensing element and temperature sensor face downward.

6.4.1.2 Sensor Installation

Manifold vacuum is used on most engines to control various things, and the Corolla is no exception. This simplified installation significantly and, instead of having to bore into the manifold itself, required only the addition of a "T" junction into one of the manifold vacuum tubes and routing the extra end to the sensor. The installation is pictured in Figure 6.4.



Figure 6.4: Intake manifold air pressure (MAP) sensor installation

6.4.1.2.1 Sensor Calibration

The approximate calibration data for the sensor is supplied by Bosch, and was used to calibrate the sensors. This was because the data will not be used for engine control or evaluation in this investigation, but for ANN modelling which does not require accurate calibration. The resulting sensor calibrations are therefore given in Table 6.1 and Table 6.2.

Voltage (V)	0.0	0.0	0.4	0.6	0.8	1.0	1.2	1.4	1.6	1.8	2.0	2.2	2.4
MAP (kPa)	0	5	10	15	20	25	30	35	40	45	50	55	60

2.6	2.8	3.0	3.2	3.4	3.6	3.8	4.0	4.2	4.4	4.6	5.0	5.0
65	70	75	80	85	90	95	100	105	110	115	120	125

Table 6.1: Intake manifold air pressure calibration data

Voltage (V)	0.0	0.0	1.9	2.9	3.7	4.3	4.6	4.7	4.8	4.9	4.9	4.9	4.9
Manifold Air Temp. (oC)	-50	-40	-30	-20	-10	0	10	20	30	40	50	60	70

5.0	5.0	5.0	5.0	5.0	5.0	5.1	5.1	5.1	5.1	5.1	5.1	5.1	5.1
80	90	100	110	120	130	140	150	160	170	180	190	200	

Table 6.2: Air temperature at MAP sensor calibration data (5V supply)

6.4.2 Mass Air Flow Sensor

A mass air flow (MAF) sensor was provided as a standard component within the Corolla engine bay. This sensor is provided to measure the mass of air that enters the engine before combustion, and provide the engine management system with additional information to determine correct fuel injection. The sensor in fact measures the velocity of air as it passes through a short tube and, by considering its cross sectional area, estimates the volume of air that passes through it. The sensor has an integral air temperature and humidity sensor, which can be used to convert air volume into air mass.

There are many ways to measure air velocity, and as such many different types of MAF sensors. At present the most common is the “hot wire” sensor, which the Corolla uses. This type of sensor places a wire into the air flow through a length of tube that is designed to minimise turbulence. The wire is heated to a constant temperature using a constant voltage, and cooled by the passing air flow. Since the wire has a positive temperature coefficient of resistance, this cooling causes its electrical resistance to drop. This in turn means that the sensor must apply a greater current to the hot wire to maintain it at its programmed temperature. It is this variation in the current to the hot wire that is used to determine the velocity of the air that passes through the sensor.

Measuring air speed in this way is sensitive to air temperature. Cooler air will cool the wire more, causing the sensor to sense a higher air speed. Humidity also has an effect, and as such sensors of the hot wire type often contain temperature and humidity sensors to facilitate accurate calibration. This calibration applies not only to compensation for the effects at the hot wire, but for varying air density in the air speed to mass air flow calculation. The sensor provides no direct air pressure calibration.

In the case of the test vehicle, the MAF sensor provides the engine management system with a mass air flow, air temperature and humidity signals, all of which are in the form of analogue voltages.

6.4.2.1 Sensor Considerations

There is little to consider in the use of this sensor, as it is a factory installed item. Since there were no plans to alter the amount of air flow into the engine in this investigation, or any foreseeable subsequent investigations, it is fair to assume that it has been chosen and installed to offer sufficient resolution and performance for the application.

Nonetheless, it is still important to identify exactly what the sensor is measuring. In this case the sensor is integral to the air filter (which is upstream of the throttle), and measures the air flow directly from the filter box after it has passed the air filter element. This position was probably chosen to minimise large turbulence and ensure near laminar and consistent flow through the sensor. This position gives rise to a potential error source due to air pressure, as the placement of the sensor between the air filter and the throttle would certainly cause a pressure variation. As the sensor does not compensate for pressure, and there is no pressure sensor in this area to allow external calibration, this may produce an error source.

6.4.2.2 Sensor Calibration

Toyota provides no calibration data for the MAF sensor, or the air temperature and humidity sensors integral to it. In the case of this project, the outputs of these sensors are not of great importance as they are not required for basic tuning of the MoTeC ECU. In this case, the sensor outputs will only be used in ANN models, of which calibration accuracy is not required. To this end, only approximate calibration curves shown in Table 6.3 and Table 6.4 were fitted, the MAF curve being based on the assumption that the engine will pump its entire cubic capacity of air on every stroke (i.e. no losses), and the air temperature curve coming from MoTeC. Humidity was not measured.

Voltage (V)	0.6	1.1	1.4	1.8	2.1	2.4	2.7	2.9	3.1	3.4	3.6	3.8	3.9
MAF (g/s)	0	4	8	12	16	20	24	28	32	36	40	44	48

4.1	4.3	4.4	4.5	4.7	4.8	4.9	5.0	5.1	5.2	5.3	5.4	5.5
52	56	60	64	68	72	76	80	84	88	92	96	100

Table 6.3: Mass air flow (MAF) calibration data

Voltage (V)	3.4	3.3	3.1	3.0	2.8	2.7	2.5	2.0	1.8	1.4	1.3	1.2	1.1
Ambient Air Temp. (oC)	-50	-40	-30	-20	-10	0	10	20	30	40	50	60	70

1.0	1.0	0.9	0.8	0.7	0.6	0.5	0.4	0.3	0.3	0.2	0.1	0.0
80	90	100	110	120	130	140	150	160	170	180	190	200

Table 6.4: Air temperature at MAF sensor calibration data

6.4.3 Throttle Position Sensor

The throttle position sensor is of the rotary potentiometer type, and was factory fitted to the throttle body by Toyota, as seen in Figure 6.5. The potentiometer measures the position of the throttle butterfly valve as it turns through approximately 0° full closed to 90° fully open. The sensor operates in much the same way as the steering wheel sensor above, but is directly coupled to the valve and only turns through a quarter of a turn.

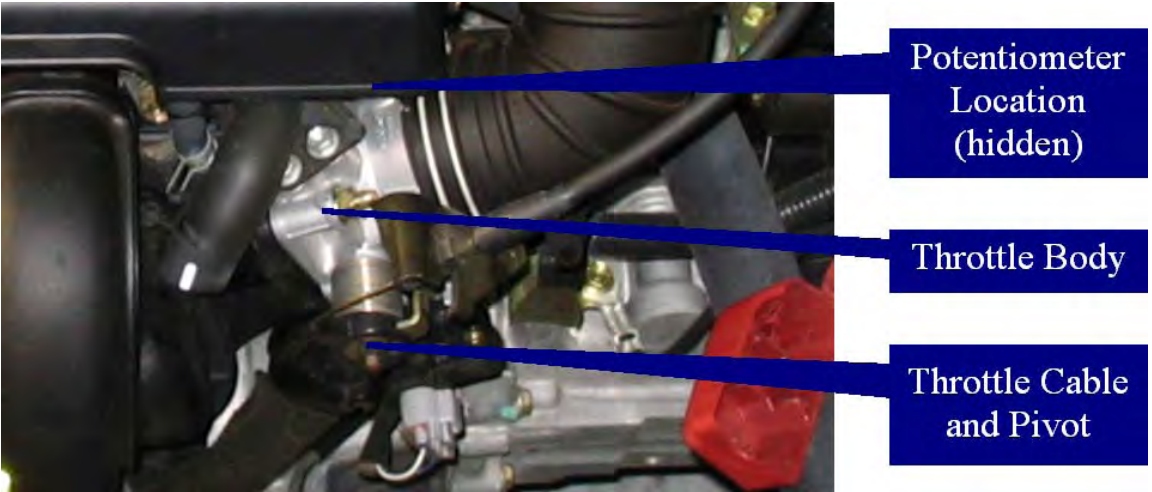


Figure 6.5: Throttle body - sensor is located at other end of the pivot

6.4.3.1 Sensor Considerations

The throttle position sensor is a very simple and highly reliable sensor and, as it is factory fitted and powered by the Toyota ECU, there are no suspected problems with it. Sources of significant error are also limited to flaws with the sensor itself to variations in supply voltage. Toyota does not proved this information, but it is fair to make the assumption that any error will be negligible.

6.4.3.2 Sensor Calibration

The accepted unit of measurement for throttle position is “percent open”. This means that 0% indicates fully closed, 100% indicates fully open, and all intermediate readings fall linearly between these two values. Only two measurements are therefore necessary for calibration, that being the sensor voltage at 0% and at 100% that were recorded as 0.60V and 4.01V respectively.

6.4.4 Engine Temperature Sensor

Engine temperature is often measured via an engine coolant temperature sensor, and these sensors are extremely common. As such, the negative temperature coefficient temperature sensor that is factory installed into the test vehicle was considered more than adequate for this measurement. The sensor measures the temperature of the engine coolant after it has circulated the engine block, and therefore gives a reasonable approximation of the temperature of the engine itself. Apart from alerting the driver if the engine is too hot, this data is critical in electronically controlled engines to determine cold start and warm up fuelling.

6.4.4.1 Sensor Calibration

The engine temperature sensor is powered from the Toyota ECU. MoTeC provided the calibration data for this sensor, saving a lengthy calibration procedure. The data that was provided is given in Table 6.5.

Voltage (V)	2.7	2.7	2.6	2.6	2.5	2.5	2.4	2.3	1.6	1.5	1.1	0.9	0.6
Engine Temp. (oC)	-50	-40	-30	-20	-10	0	10	20	30	40	50	60	70

0.5	0.3	0.3	0.1	0.0	0.0	0.0	0.0	0.0	0.0	0.0	0.0	0.0	0.0
80	90	100	110	120	130	140	150	160	170	180	190	200	

Table 6.5: Engine temperature calibration data

6.4.5 Crank and Cam Position Sensors

The crank and cam sensors are extremely important in regards to electronic engine management, and as a result are factory fitted. The crank sensor provides the engine management system with crank position and engine speed measurements, which are important to determine injection and ignition timing, as well as to establish correct fuelling and injection and ignition advances. The data from the cam sensor is integral to this, providing information on whether each piston is on a compression or exhaust stroke. In the case of the VVTi engine of the Corolla, which incorporates a cam advance mechanism, the cam sensor provides information on the cam position to the cam advance controller.

The crank and cam positions on the Corolla are measured using gear-toothed discs similar to that used for the rear wheel speed measurement discussed previously, except for two noteworthy differences.

The first exception is that the crank and cam positions are measured using magnetic sensors, not Hall sensors. Magnetic sensors differ from Hall sensors particularly because magnetic sensors have an analogue output, the voltage being produced by induction as the ferrous gear tooth passes the sensor, as shown in Figure 6.6. As such, the output voltage of the sensor rises as a tooth approaches and decreases as it moves away, the amplitude of the voltage being determined by the velocity of the tooth. This means that the data acquisition software needs to establish threshold values to determine when a tooth has “passed” the sensor, and to have an input voltage range that can cope with the range of the sensor in the operating conditions. The sensors on the Corolla have been set up so they are most accurate if this is done as the tooth approaches the sensor, called the “rising edge”.

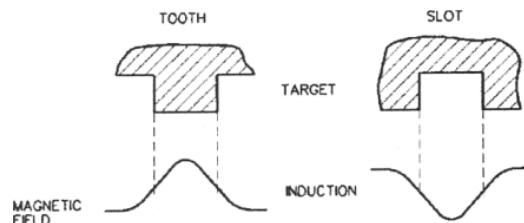


Figure 6.6: Magnetic sensor output as gear teeth pass

The second exception is that the gear toothed discs for the crank and cam sensors have missing teeth. The crank sensor consists of a disc with 36 evenly spaced teeth, two of which have been removed (missing). The cam sensor has 4 evenly spaced teeth, one of which is missing. These missing teeth perform a crucial role, by enabling the data acquisition system to construct a reference position. As the disc spins, the data acquisition system counts the period each tooth takes to pass it. When a missing tooth is encountered the period increases greatly in magnitude, telling the system that the reference position has been reached. By counting gear teeth from this reference position it is possible to then determine the angular position of the gear toothed disc precisely. By incorporating missing teeth into the measurement of crank and cam positions the engine management system can acquire data of sufficiently high quality to precisely determine engine timing.

6.5 MoTeC ECU Installation

A fourth year student originally took up the task of the MoTeC ECU installation as an honours project within the first year of this investigation. His task was to purchase the M400, which had already been selected, install it into the test vehicle, conduct basic

engine tuning and to conduct limited research into traction control. Unfortunately, delays in funding, the discovery that MoTeC had never completed this installation before and some unexpected obstacles made it clear that he would not be able to complete the project in the allotted time, and so abandoned the project with very little headway and limited results.

The main problems that arose were based around wiring, and there were many. Firstly, the wiring diagram provided by Toyota showed little information on the functionality of individual wires or ECU pins. This meant that information had to be compiled from a number of sources to try and understand what the ECU controlled, and what signals it used. This information was patchy at best, and the resulting uncertainty of the compiled information further compounded the problems faced. Further problems arose because of differences in sensor measurement and control methods used between the MoTeC and the factory ECUs. In particular, there was great uncertainty as to whether the cam and crank sensors would work with the MoTeC ECU at all, but there were also problems in that the MoTeC ECU generally drives a supply voltage to ground when controlling devices, whereas the factory ECU appears to do otherwise. In addition to all this, the factory ECU was positioned in such a location, and with very short wires, that made experimenting with the ECU wiring difficult.

Fortunately, however, a few months after the difficulties in installing the MoTeC ECU were realised and headway was slowing dramatically, MoTeC supplied some welcome news. They had just successfully fitted a M400 ECU to a 2003 ZZE-123R Corolla Sportivo, which had a very similar engine to the 1ZZ-FE in the test vehicle. After an investigation using the wiring diagram that had already been compiled, it was soon realised that the only significant practical difference between the two engines was that the Sportivo incorporated variable valve lift.

The installation details that MoTeC could now provide made the installation process much simpler from here on in. The documentation firstly specified a “piggy back” installation, which meant that factory ECU would not be removed – but rather that the MoTeC ECU would be installed in parallel. The arrangement is shown in Figure 6.7. Until this point a piggy back arrangement had not been considered in great depth because there was a very real possibility that the crank and cam magnetic sensor signals could not be split between the two ECUs.

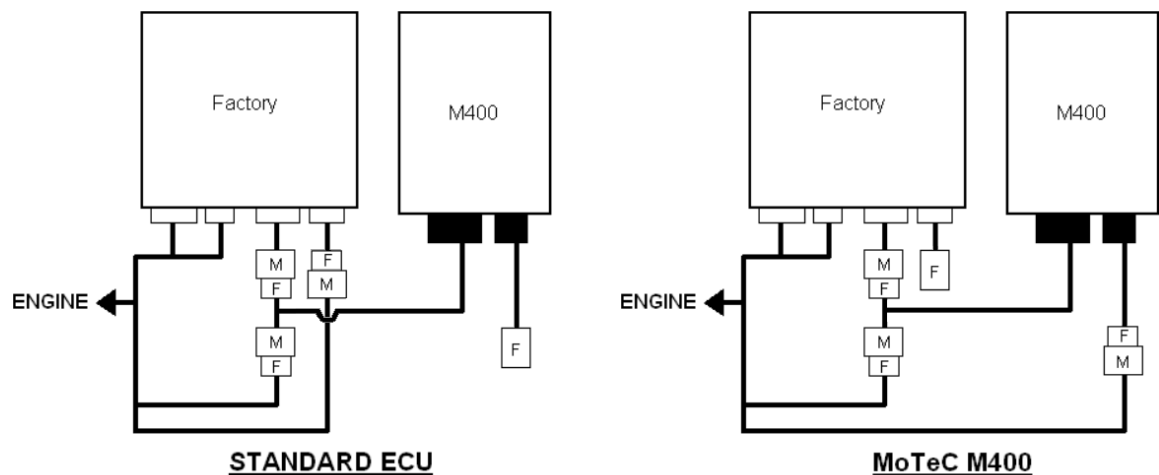


Figure 6.7: MoTeC ECU wiring schematic in “piggy back” arrangement – the engine can run on either ECU by changing the output connection

Further, the MoTeC documentation contained all of the wiring information that was needed to complete the installation, as well as the calibration data for some of the engine sensors and much of the ECU setup parameters. This proved extremely valuable and, after making a few changes to suit the test vehicle installation, provided a very clear path. These changes included the removal of the valve lift control and wideband lambda measurement (and associated heater control). They included the addition of narrowband lambda, MAP and wheel speed measurements, as well as additional wiring for external ignition/injection control, lambda meter installation and further data acquisition by another device. An “on/off” power switch and fuse running directly from the battery for the MoTeC ECU was included in the wiring to avoid the difficulties in ensuring voltage was maintained while the starter motor was running.

A complete wiring diagram was produced, as seen in Figure 6.8, and was based on these requirements. The MoTeC ECU was installed to these specifications, with careful attention made to ensure the connections were of very high quality. This was considered extremely important because of previous experience with poor connectors in racing applications, which are very prone to wearing out and breaking due to vibration. Of particular note, it is important to avoid soldering as this weakens the wire near the joint. As a result only automotive racing specific connectors were used throughout the installation, which were installed using the correct crimping tool. The installed unit is shown in Figure 6.9.

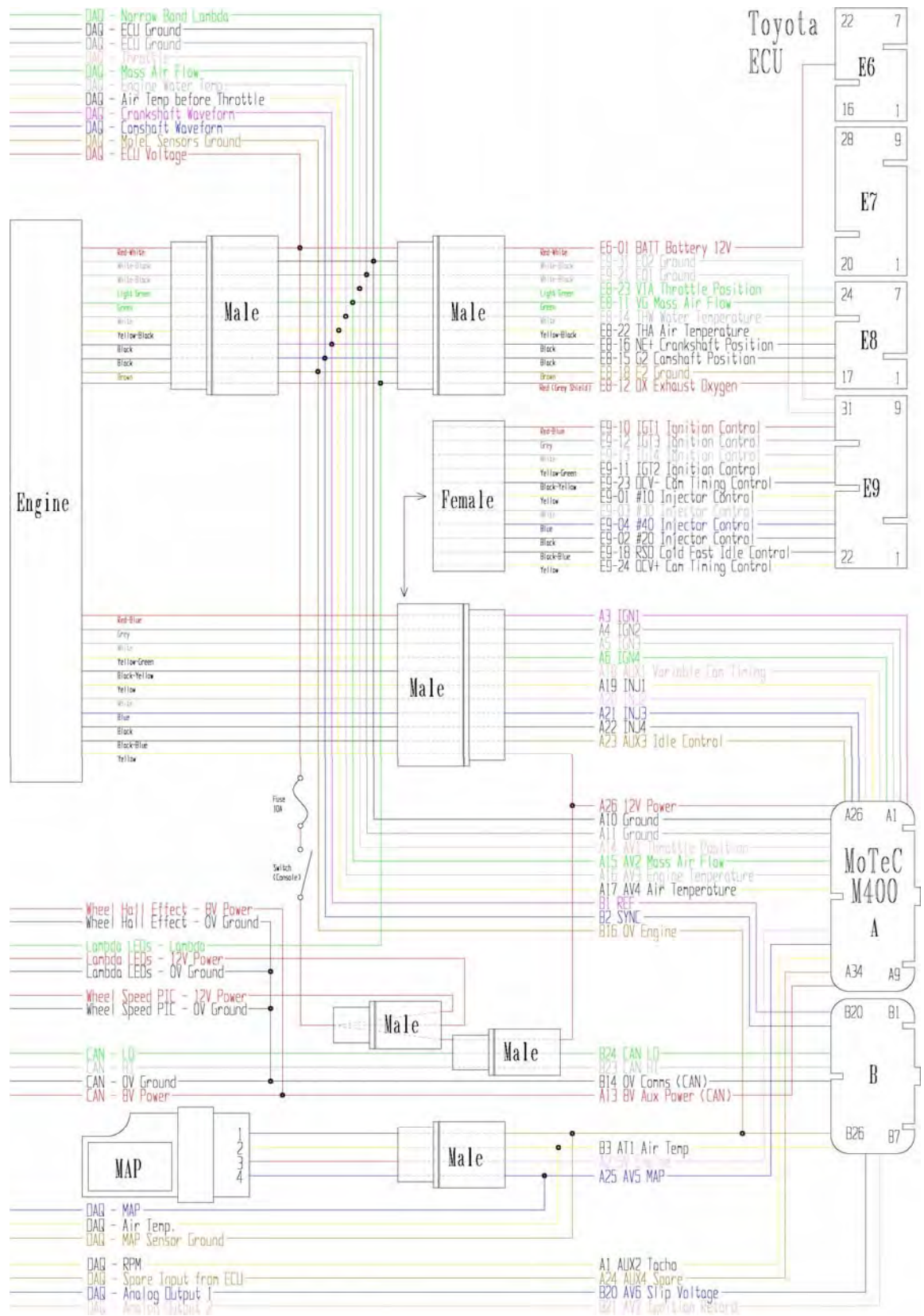


Figure 6.8: MoTeC ECU wiring diagram

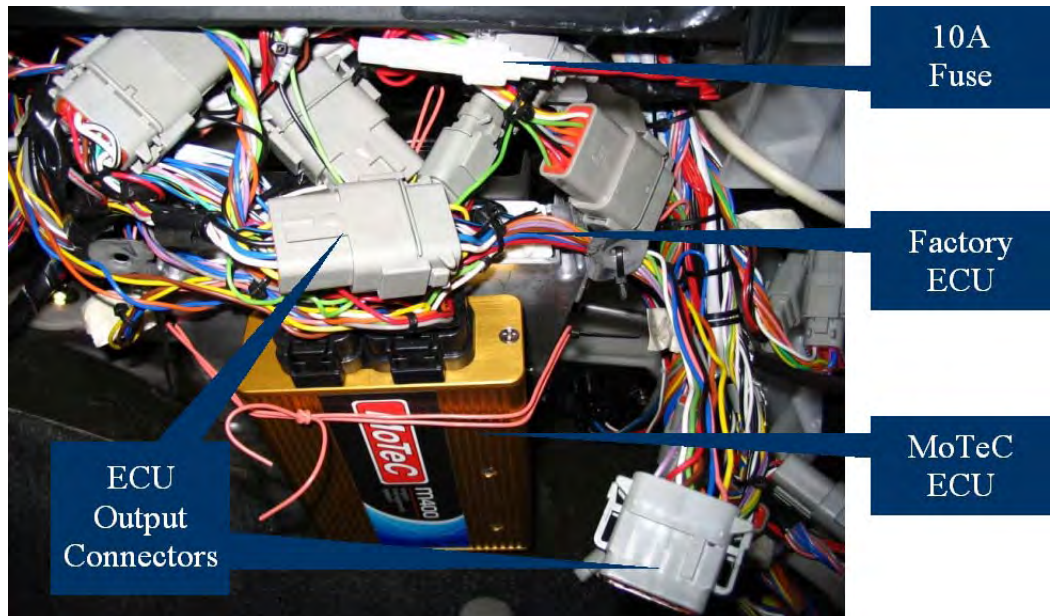


Figure 6.9: MoTeC ECU installation (located below glove box)

6.6 MoTeC ECU Configuration

With the M400 hardware was installed it was necessary to configure the ECU software correctly. This process could effectively be broken into five parts.

Firstly, the ECU had to be “enabled”. This is a code that must be entered into the ECU when first activated as a security measure. Additional codes then also had to be entered to activate a number of “upgrades” for the ECU. The M400 is normally sold as a base package containing all the hardware necessary to run all of the available upgrades, each upgrade being available through a code that can be purchased from MoTeC. In the case of this investigation the “Advanced Functions” and “Continuously Variable Cam Control” upgrades were enabled.

Secondly, all of the engine sensors were configured and calibrated. In the case of the cam and crank sensors (which are referred to by MoTeC as the “Ref” and “Sync” sensors respectively) this included specifying parameters such as data filtering, rising or falling edge triggers and trigger level.

Thirdly, the ECU general operating parameters were set. These parameters include engine type, firing order, ref and sync modes, the type of control to be used and injector and ignition specifications.

Fourthly, the auxiliary output settings were defined for the cam control valve and for the idle valve. These controllers are of a PID type, so tuning parameters include the proportional, integral and derivative gains, as well as others such as controller frequency, dead band, and high and low limits.

Finally, the supplementary functions of the ECU were set. These miscellaneous functions are not required to run the engine, but simply provide increased functionality. Function configurations included in this category include CAN address information, telemetry baud rates, constants to determine quantities of fuel used, RPM limit settings, wheel speed sensor calibration, gearbox and differential ratios to determine current gear, traction control variables, shift light limits and warning alarms.

MoTeC provided a large proportion of this information based on their Sportivo conversion, while everything else had to be inferred from the available documentation and experimentation.

6.7 MoTeC ECU Tuning

With the M400 ECU installed in the test vehicle and properly configured it became time to try and start the engine and tune it. MoTeC helped in this respect, providing “de-tuned” injection pulse width and injection and ignition timing tuning files. It is noted here that MoTeC could have provided the final tuning data from the Sportivo that probably would have correlated well with the test vehicle engine and saved considerable time. Unfortunately in this case, MoTeC deemed this information as the intellectual property of the Sportivo owner, and did not supply the information. The cam controller and idle controller PID variables mentioned above also fell into this category, and represent approximate values only.

Considering the complexity of the installation and configuration of an aftermarket ECU, getting the engine to start is a very large hurdle. While in simple terms the engine only needs to provide the right amount of fuel at the right time with an appropriately timed spark to run, the way any ECU does this requires all of its functions to work correctly. Previous, and much simpler, MoTeC installations at the University of Tasmania have taken hundreds of man-hours to correct problems highlighted by engines that simply would not run. As a testament to the conscientious and meticulous way that this

installation was carried out, however, the test vehicle engine fired on the first attempt, and with a small amount of tuning was idling within minutes!

This point represents only the very start of engine tuning, nonetheless. Tuning for any engine conditions other than idle requires load to be placed on the engine. In addition, the air/fuel ratio of the engine needs to be measured to ensure the mixture is neither too rich nor too lean. A lean mixture can create excessive heat within the exhaust gases and cause severe engine damage and increased NO_x emissions, but represents the most fuel-efficient operating condition. Rich mixtures, on the other hand, generally create the most amount of engine power per stroke, but waste a large proportion of fuel which is expelled into the exhaust unburnt. Stoichiometric mixtures, which provide exactly the correct amount of fuel to combust all of the available oxygen, fall in the middle of these two extremes and generally represent the operating condition that produces the least amount of emissions.

A well-tuned engine will take the best of these features for the given conditions, for instance by providing very rich mixture when high power is demanded from the engine, but providing a lean or stoichiometric mixture when driving slowly. Fuel injection systems allow for precise control of these mixtures for specific operating conditions, and must be tuned to suit.

This tuning requires a measurement using a sliding scale to determine if the engine is running rich, stoichiometric or lean. The amount of fuel can be adjusted to ensure the desired mixture is reached. This data is normally provided by a “Lambda” sensor, which measures the exhaust oxygen content and gives an output that is indicative of the fuel mixture. Narrowband sensors, such as the factory fitted sensor, provide an essentially binary scale of only “rich” or “lean”, while wideband sensors provide an almost linear relationship with a scale that reaches from extremely rich through to extremely lean. As such, a wideband sensor is necessary for engine tuning.

In the case of the test vehicle, MoTeC provided information suggesting that the minimum lambda value should be 0.89 (corresponding to a very rich mixture) and the maximum should be 1.05 (corresponding to a very lean mixture). A reading of 1.00 lambda always corresponds to a stoichiometric mixture of 14.7:1.

For normally aspirated engines the recommended method to determine control conditions is to construct an engine speed versus throttle position table. The correct air/fuel mixture and timing can be entered for specific engine speeds and different throttle positions. By considering the throttle position as a request from the driver for more power, it is possible to provide fueling and advance that matches the demand, as well as preserving drivability. At its most basic level, it could be assumed that little throttle indicates a desire for fuel efficiency, whereby an open throttle indicates a request for maximum available power. MoTeC name this principle “load point” which, although proportionally related to throttle position in this case, can be related to manifold air pressure (principally for turbo and supercharged engines) and inlet mass air flow.

To tune the engine, therefore, the desired lambda readings at specific throttle position and engine speed combinations must be determined. This provides the air/fuel ratio goal so correct injection duration can be determined, which is in turn augmented by injection and ignition timing.

6.7.1 Lambda Table

The M400 tuning software allows a “Lambda Table” to be constructed to determine the engine tuning goals. These goals vary depending on the intended use of the engine, and are not specific to any particular application. In the case of a drag car, for instance, very low lambda values are desired through the entire throttle and RPM range, whereas an endurance vehicle may be tuned for fuel economy to increase its range. A street car, on the other hand, requires a compromise between these two extremes.

This compromise for the test vehicle lambda table was based using statistical data. It was decided that for “normal” driving, which is defined here as everyday driving expected within a city, the countryside and freeways, a lambda value of approximately 1.0 should be used for low emissions. At very high throttle positions, which do not constitute “normal” driving and are very rare, the goal lambda value of 0.89 should be used to produce maximum power. In the region between these two extremes, which rests on the fringe of the normal driving envelope, the lambda values should form a number of intermediate steps to provide a smooth transition. Finally, in regions of the table with high RPM and low throttle where the driver obviously wants the engine to slow down, a lambda value producing minimum power without engine damage should be used, which

corresponds to a lambda value of 1.05. To determine where these figures lie it is important to statically determine what “normal” driving is.

This was a relatively simple task, and involved driving the car on public streets within the legal limits. The factory ECU was connected to control the engine, with the MoTeC ECU setup to log rpm and throttle position (this could be done because new MoTeC ECUs have the logging upgrade active for the first few hours of running time). The car was driven around the city and along a highway to an outlying town, and included a number of aggressive acceleration manoeuvres. The data, which consisted of 20 minutes of driving logged at 20Hz (24000 samples), is shown in Table 6.6, Table 6.7 and Table 6.8.

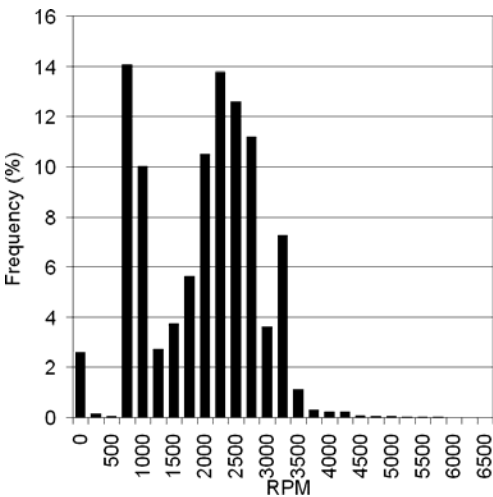


Table 6.6: RPM histogram for “normal” driving

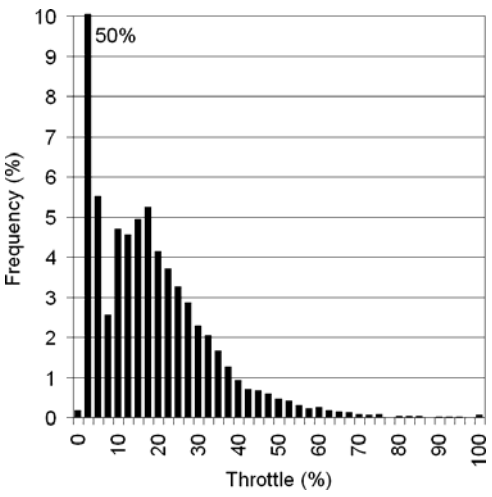


Table 6.7: Throttle histogram for “normal” driving

Almost all of the engine operation is in the 700 to 3500 RPM range, although the frequencies from 700 to 1000 RPM represent engine idle and do not have any bearing here. However, incorporating the known gear ratios shows that the 2000 RPM bin represents driving at 50km/hr in fourth gear and 60km/hr in fifth; the 2250 RPM bin represents 60km/hr in fourth and 80km/hr in fifth; and the 3000 RPM bin represents driving at 80km/hr in fourth and 100 km/hr in fifth. These are important values, as they represent all of the speed limits encountered while logging data. As a result the RPM histogram produces an approximate Bell curve within this region – with only two exceptions. The first, as noted above, is a result of engine idle around 700 RPM, while the second (the 3250 RPM bin) appears to be a result of driving in second gear at 45km/hr and third gear at 70km/hr. As such, it can be assumed that significant load was placed on the engine at these times, probably as a result of driving up a steep hill.

The throttle histogram provides useful data, and a fairly simple statistical distribution. There is an obvious logarithmic decline in frequency from 20% to 100% throttle. The two exceptions are the very high frequency in the 2.5% bin and the variable frequencies in the 5% to 17.5% throttle range. The former, which in practice also covers the 0% bin, is expected because cars must also slow down, while the latter is probably because these throttle positions do not produce enough power for the vehicle to maintain its speed.

Table 6.8 shows this data in a different way. By plotting the measured data on a XY graph more information can be derived on how the car is “normally” driven (although some “hard” driving is also included within the data). A fine point represents each measurement, so areas of black indicate high frequencies of a particular combination. The graph clearly shows the relationship between throttle and RPM. In fact, the layout of the graph is identical in format to the Lambda Table being produced, making it a valuable tool. By far the most amount of driving is done in the 1500 to 3250 RPM range at throttle positions of up to 40%. Further, at 3250 RPM there is a very clear maximum resulting from the top speed of 100km/hr (which also explains the unusual distribution in this region). By observing this graph, and by considering the points mentioned above, it was possible to determine the lambda table, which is given in Table 6.9.

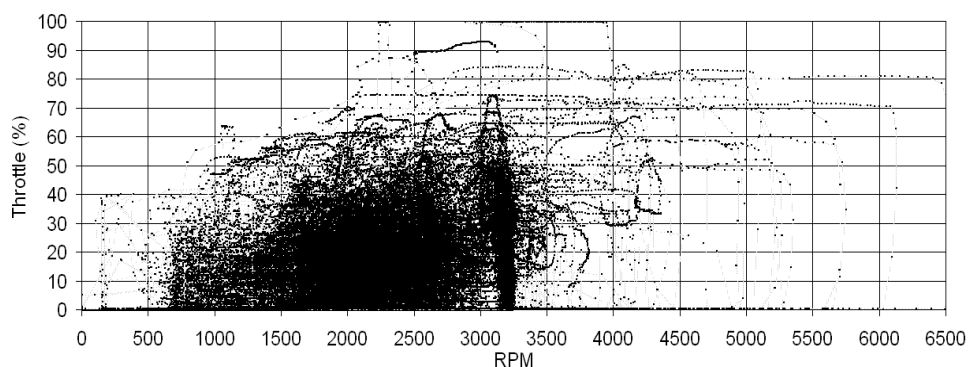


Table 6.8: RPM verses throttle plot for “normal” driving

RPM		0	500	1000	1500	2000	2500	3000	3500	4000	4500	5000	5500	6000	6500
Load %	100.0	0.90	0.90	0.90	0.90	0.90	0.89	0.89	0.89	0.89	0.89	0.89	0.89	0.89	0.89
	90.0	0.91	0.91	0.91	0.91	0.91	0.90	0.89	0.89	0.89	0.89	0.89	0.89	0.89	0.89
	80.0	0.92	0.92	0.92	0.92	0.92	0.91	0.91	0.91	0.91	0.90	0.90	0.90	0.90	0.90
	70.0	0.92	0.92	0.92	0.93	0.94	0.94	0.94	0.94	0.94	0.93	0.93	0.93	0.93	0.93
	60.0	0.92	0.93	0.93	0.96	0.97	0.97	0.97	0.97	0.97	0.96	0.96	0.96	0.96	0.96
	50.0	0.93	0.94	0.95	0.98	0.99	0.99	0.99	0.99	0.99	0.98	0.98	0.98	0.98	0.98
	40.0	0.93	0.96	0.98	0.99	1.00	1.00	1.00	1.00	1.00	0.99	0.99	0.99	0.99	0.99
	30.0	0.95	0.98	0.99	1.00	1.00	1.00	1.00	1.00	1.00	1.00	1.00	1.00	1.00	1.00
	20.0	0.98	0.99	1.00	1.00	1.00	1.00	1.00	1.00	1.00	1.00	1.00	1.00	1.00	1.00
	10.0	0.99	1.00	1.00	1.01	1.01	1.01	1.01	1.01	1.01	1.01	1.01	1.01	1.01	1.01
	0.0	1.00	1.00	1.00	1.01	1.03	1.04	1.05	1.05	1.05	1.05	1.05	1.05	1.05	1.05

Table 6.9: Lambda table for MoTeC ECU tuning (screen shot)

The table placed a lambda value of 1.00 for most of the “normal” driving conditions, but includes values up to 1.05 at the low throttle positions which do not produce sufficient power to maintain vehicle speed. Very low lambda values of 0.89 and 0.90, on the other hand, are denoted to areas that are at the extremes of the engine operation – areas that are very rarely reached during normal driving. Meanwhile, areas that form a transition between these extremes are graduated to provide a smooth curve to preserve vehicle drivability.

6.7.2 Tuning Goals

Producing a Lambda Table that represents the desired engine characteristics is an important step in tuning an engine, with this table defining many of the tuning goals.

As discussed above, the basic tuning parameters of an engine are injection pulse width, injection timing and ignition timing. In the case of the test vehicle the cam advance must also be included in the basic list. These four parameters are all interrelated, and changing one can require a change to all in order to achieve optimum performance.

This is a complicated process in itself, but tuning an engine to perform well requires a large number of “trims” to be added. These trims provide modification of these four signals to account for specific conditions that may be encountered by the engine. On the M400 a very large number of trim can be applied for functions such as:

- Engine cranking
- Cold start
- Acceleration Enrichment
- Deceleration Enleanment
- Air temperature
- Engine Temperature
- Fuel Temperature
- Fuel Pressure
- Manifold Pressure
- Gear
- Battery Voltage
- Individual Cylinder Variation
- Lambda Control
- Traction Control
- Idle Control
- RPM Limiting
- User Defined Functions

It is generally possible for any number of these trims to be active at once, which means they are all difficult to tune exactly. This is compounded by the fact that any change to the basic tuning of the engine will affect the tuning of most of the trims. This introduces a huge increase in the number of parameters that need to be considered to tune the engine well, and an exponential increase of the number of tuning combinations possible. Tuning the basic parameters and each of these trims well is a huge project, restricted in

the most part to professional racing and commercial development. This was well outside the scope of this project, and a simpler approach was adopted.

As a result of this and the financial pressure placed on the project, the “goal” of the engine performance for tuning was downgraded to a large degree. This downgrade was based on the common automobile-racing axiom that the first 95% of performance is easy to obtain, it’s the last 5% that takes all the work. Basically, this meant that only enough tuning would be completed to produce a drivable engine with a reasonable power output. This reduced the problem from months of engine tuning to only one day.

6.7.3 Chassis Dynamometer

Basic engine tuning is best done at steady state. That is, it is easiest to run the car at the desired engine speed and throttle position (called the “load site”), and use this steady operating condition to adjust all of the relevant tuning parameters to achieve optimum performance. Once this load site is tuned, it is then possible to go to all other load sites until the entire engine is tuned. Further, if it is possible to ensure that as many trim variables are constant throughout this process, then the tuning can be conducted to a high standard. This will produce a steady state tuning of the engine, which is the most basic and most important feature of engine tuning. This is because tuning variation due to engine dynamics, such as accelerating, is controlled through trims.



Figure 6.10: Test vehicle fitted to chassis dynamometer

It is very difficult, however, to tune to specific load points on the road, as it would require a variety of differently sloped hills to provide varying loads for different throttle positions and engine speeds. Instead, a chassis dynamometer (commonly referred to as a “dyno”) was used to tune the engine, as shown in Figure 6.10. This type of dynamometer allows the vehicle to be directly placed onto it, and measures the power delivered at the driven wheels. This is different from an engine dynamometer, which measures the engine power output at the flywheel and requires the engine to be removed. The results from chassis dynamometer and engine dynamometer differ by the total drive train losses, but are both suitable for engine tuning.

The chassis dynamometer consists of two rollers onto which the two driven wheels are placed. One of these rollers is capable of having a variable load applied to it, and together they provide a means to locate the tyres safely while having severe loads placed on them at a variety of speeds. Tie-down straps were used to provide additional safety, while a large fan was placed near the radiator to provide increase engine cooling. A lambda sensor was installed, pictured in Figure 6.11, using a removable length of pipe that extends well into the exhaust. By measuring the load and speed of the roller, and incorporating the gear and differential ratios of the car, the dynamometer can then determine the power produced at the wheels, the RPM and the corresponding engine torque and correlate this with lambda readings. An example of the resulting display is given in Figure 6.12.



Figure 6.11: Removable lambda sensor



Figure 6.12: Dynamometer display

The dynamometer tuning was conducted at Pro Automotive using their new “Dynologic” installation.

6.7.4 Cam Tuning

Cam tuning was conducted on the dynamometer first. To tune this thoroughly would normally require the engine to be completely tuned for a number of specific cam advances. In this way the advances at particular engine speeds and throttle positions that produced the best performance could then be selected and used. However, this approach would probably increase the tuning effort tenfold.

To reduce this amount of effort a different technique was used. It was noted that the existing tuning of the factory ECU must provide adequate variable cam advance, and this was unlikely to vary in a great way to the optimum advance used for the MoTeC ECU. With this in mind, and with the engine running on the factory ECU, the cam advance was measured for a number of different load points. This data was then copied to the cam advance tuning for the MoTeC ECU.

It should be noted here too, that in later testing with the MoTeC ECU fully tuned, it was found that the MoTeC supplied settings for the cam controller produced erratic control. This was found to be because the controller was too responsive, most notably producing “bunny hopping” when lifting off the throttle. As a result of this, the integral and derivative functions of the PID controller were removed and the proportional gain reduced. This drastically improved drivability, but can be improved further with proper investigation.

6.7.5 Injection and Ignition Tuning

Injection pulse width, injection timing and ignition timing are three highly interrelated parameters, and must be tuned in combination. The injection pulse width (which is scaled in MoTeC’s tuning software as a percentage of maximum required pulse width, called “IJPU”) controls how much fuel is injected into the manifold inlet runners. It is therefore the principle control of the air/fuel ratio, and consequently the exhaust lambda value.

Injection timing, on the other hand, defines when the fuel is injected into the manifold inlet runners. This is best visualised as a column of air and fuel being sucked into the cylinder on each inlet stroke. This column may be injected with fuel early, meaning the fuel enters the cylinder as the valve opens, or it may be injected late and enter the cylinder as the valve closes. The fuel can be injected anywhere within this column, with the width of fuel injected air being defined by the injection pulse width. In this way the fuel flow can be

controlled to produce the optimum achievable air/fuel mixing and resulting combustion efficiency, but is predominantly unaffected by throttle position. As a result, this parameter mostly defines fuel efficiency, but also has a bearing on the air/fuel ratio and lambda value.

Finally, ignition advance controls when combustion takes place by supplying a spark to the combustion chamber. Generally more ignition advance produces more power per combustion stroke – to a point. Eventually, even more advance will produce no more appreciable gains in power, and could even cause engine pre-ignition (often called “knock”). This is highly undesirable, as it is generally accompanied by significant loss in power and a very prominent likelihood of engine damage. Consequently, this parameter affects the efficiency of the engine to extract the power from combustion, but is also influenced by the air/fuel ratio and mixing.

It can be seen, that even though the three parameters are interrelated, they still predominately control different things. Injection pulse width principally controls the air/fuel ratio, injection-timing controls fuel efficiency at specific air/fuel ratios and ignition timing controls the efficiency of power extraction per stroke. With this in mind, tuning at specific load points requires an iterative procedure. The generally accepted procedure is:

Step 1: Tune the injection pulse width. This is the most significant parameter, and should be iteratively adjusted to produce the required air/fuel ratio and lambda value at the load point. The MoTeC tuning software simplifies this process by using their “Quick Lambda” function, which calculates a prediction of the correct pulse width based on the difference of the aim and measured lambdas. It should also be noted that producing a significantly lean mixture in high load conditions (by accident or otherwise) could significantly damage the engine.

Step 2: Tune the ignition timing. While looking at the dynamometer measured power output, slowly increase the ignition advance from a conservative base value. The power output should increase progressively up to a maximum value, at which it should plateau before decreasing again. If knock occurs at any stage, the ignition should not be advanced further, as it will cause engine damage. The best ignition advance (assuming no knocking occurs) is at the point where that maximum

value was first reached. As a general rule, the goal of the tuning is to produce the most amount of power with as little advance as possible.

Step 3: Tune the injection timing. This is similar in procedure as step 2, with the injection advance adjusted to find the point where the maximum amount of engine power is produced. The main differences are that it only needs to be tuned for RMP sites, and that the engine should still run adequately regardless of the advance. Nonetheless, there should be a point where the fuel will be injected into the air stream at such a time that produced the most efficient mixing for combustion, and this will correspond to a small increase in engine power.

Step 4: Repeat steps 1 to 3 for each load point until the tuning parameters converge.

Following this procedure will provide tuning data (often called an engine “map”) of a high quality. Unfortunately, an accepted number of load sites for sufficient ECU tuning are in the vicinity of at least 100, which makes this process quite tedious.

Tuning of this scale was outside of the scope of this investigation, with the only goal being to produce a drivable engine with adequate power. As such, the procedure above was only applied to a small number of load points to determine ignition and injection timing. These points were then slightly “de-tuned” for safety and interpolated across the entire tuning table, seen in Table 6.10 and Table 6.11.

		RPM	0	200	500	700	1000	1500	2000	2250	2500	2750	3000	3250
Load %	100.0	6.0	7.0	8.0	9.0	12.0	15.0	18.0	19.5	20.5	22.0	22.0	22.5	
	90.0	6.0	7.0	8.0	9.0	12.0	15.0	18.0	19.5	20.5	22.0	22.0	21.5	
	80.0	6.0	7.0	8.0	9.0	12.0	15.0	18.0	18.5	20.5	22.0	22.0	21.0	
	70.0	6.0	7.0	8.0	9.0	12.0	15.0	18.0	18.5	20.5	22.0	22.0	22.0	
	60.0	6.5	7.0	8.0	9.0	12.0	15.0	18.0	18.5	20.5	22.0	22.0	22.5	
	50.0	7.0	7.5	8.5	9.0	12.0	15.0	18.0	18.5	20.5	22.0	22.0	23.5	
	40.0	7.5	8.0	8.5	9.0	12.0	15.0	18.0	19.0	21.5	22.5	23.0	24.0	
	30.0	8.5	8.5	9.0	9.0	12.0	15.0	18.0	19.5	21.5	23.0	24.0	25.0	
	20.0	10.0	10.0	9.5	9.5	12.0	15.0	18.0	19.5	21.5	23.0	24.0	25.0	
	10.0	10.5	10.0	9.5	9.5	12.0	15.0	18.0	19.5	22.0	23.0	24.0	26.0	
0.0	10.0	10.0	9.5	9.5	12.0	15.0	15.0	19.5	22.0	24.0	24.5	26.0		

	3500	3750	4000	4250	4500	5000	5500	6000	6500	7000	9500
23.0	23.0	23.0	24.0	25.0	26.0	28.5	28.5	30.0	30.0	28.5	
21.0	22.0	23.0	24.0	25.0	26.0	27.5	25.5	25.5	27.5	27.5	
20.5	21.0	21.0	22.0	23.0	23.5	25.5	26.5	26.5	28.0	27.5	
22.0	22.5	22.5	23.5	24.0	24.5	26.5	27.5	27.5	28.5	28.5	
23.0	23.5	23.5	24.5	25.5	25.5	27.5	28.5	28.5	29.5	29.5	
24.5	25.0	25.0	26.0	26.5	26.5	28.5	29.0	29.0	30.0	30.5	
25.0	26.0	26.5	27.0	27.5	28.0	30.0	30.0	30.0	31.0	32.0	
25.5	26.5	27.5	28.5	29.0	29.0	31.0	31.0	31.0	31.5	33.0	
25.5	27.5	29.0	29.5	30.0	30.0	32.0	32.0	32.0	32.5	34.0	
27.5	29.0	30.0	31.0	31.5	31.5	33.0	33.0	33.0	33.0	35.0	
27.0	29.5	31.5	32.0	32.5	32.5	34.0	34.0	34.0	34.0	36.0	

Table 6.10: Ignition timing ($^{\circ}$ BTDC) for ECU tuning

RPM	0	200	700	1000	1500	2000	2500	3000	3500	4000	4500	5000	5500	6000	6150	6500	7000
	400.0	400.0	400.0	400.0	439.0	329.6	333.8	331.9	339.1	351.3	358.4	361.6	364.7	367.9	368.9	371.1	374.2

Table 6.11: Injection timing ($^{\circ}$ BTDC) for ECU tuning

During this initial tuning two limitations were identified with regard to how the vehicle behaved on the dynamometer. The first was that there were some load points that were simply unachievable in steady state conditions. These fell into two categories, being low RPM/high throttle and high RPM/low throttle. The former produced such erratic behaviour that the steady state was unachievable for the desired lambda values, the latter because the losses within the engine provided too much load to achieve the desired engine speed regardless of the dynamometer setting.

The second limitation involved overheating. Even though a significant airflow was provided to the radiator by means of a very large fan, it was observed that whenever a high load was placed on the engine the temperature would climb very quickly. At its worst extent, being very high RPM and 100% throttle, the engine could only be run at steady state for three or four seconds before significantly overheating. It was believed that this was because the radiator was simply not designed to accommodate this sort of load situation, which is very hard to achieve on the road. Nonetheless, this limitation made tuning in the high RPM ranges difficult because there was only time to make one tuning adjustment at a time, after which the engine had to be idled for a minute or so to return engine temperature back to normal. It was noted that the factory fitted engine temperature gauge was not very useful, always showing a constant value of “normal” until about 100°C where it very quickly climbed to its maximum.

The injection pulse width tuning that was done to determine the few points of injection and ignition advances was deemed too coarse. Since the pulse width is the most important engine parameter for tuning, it was decided that it would be tuned for all load points, therefore ensuring that the desired lambda values were realised, without any additional consideration of engine efficiency. This was a relatively quick and simple procedure, the results of which are shown in Table 6.12 (which also incorporates some extrapolation to the points that could not be tuned).

RPM		0	200	500	700	1000	1500	2000	2250	2500	2750	3000	3250
Effcy %	100.0	66.5	67.6	69.3	70.5	72.5	76.5	76.5	78.0	80.2	81.5	81.2	80.2
	90.0	67.0	67.7	68.8	69.5	70.5	73.0	74.7	75.7	78.0	77.5	77.5	77.6
	80.0	66.0	66.3	66.7	67.0	68.9	70.8	73.5	74.4	75.3	74.6	74.0	74.0
	70.0	63.0	63.6	64.4	65.0	68.2	69.1	71.5	71.4	71.3	70.9	70.6	70.3
	60.0	62.0	63.0	64.5	65.5	67.9	66.5	67.5	67.9	68.3	67.6	66.9	65.9
	50.0	63.5	63.8	64.2	64.5	66.3	62.7	64.7	64.0	63.3	61.1	59.0	58.5
	40.0	62.0	61.9	61.7	61.5	63.0	58.9	58.6	57.3	56.0	52.9	49.8	48.6
	30.0	58.3	58.8	59.5	60.0	63.5	50.9	48.8	45.7	42.6	39.4	36.3	35.0
	20.0	52.1	52.2	52.4	52.5	56.1	41.5	32.4	29.6	26.8	24.2	21.6	20.6
	10.0	38.9	39.3	40.0	40.4	42.3	22.2	19.6	18.6	16.5	14.9	13.1	11.7
	5.0	32.0	31.0	26.8	26.0	26.2	17.0	13.6	13.5	12.4	11.0	9.9	9.8
	0.0	24.6	24.6	16.0	13.1	10.0	10.0	10.0	10.0	10.0	9.5	8.4	8.1

3500	3750	4000	4250	4500	5000	5500	6000	6500	7000	9500
80.7	84.2	85.8	86.5	86.2	86.5	89.9	92.0	87.9	89.0	92.0
78.5	80.0	81.5	83.5	85.2	85.0	86.5	87.0	85.5	86.5	86.5
74.0	76.1	78.1	80.0	82.5	82.0	83.0	83.0	82.5	83.5	83.5
70.0	71.8	73.6	74.9	76.1	77.6	78.0	77.5	75.7	76.5	76.5
65.0	66.7	68.3	68.8	69.2	69.0	69.5	68.0	64.0	65.0	65.0
58.1	58.7	59.3	59.5	59.6	57.1	57.0	53.4	49.5	49.8	49.8
47.5	46.5	45.5	44.7	44.0	40.6	40.0	40.0	38.0	38.4	38.4
33.8	31.3	28.8	27.5	26.2	23.2	23.2	23.2	23.2	23.6	23.6
19.7	17.9	16.1	15.1	14.2	14.0	14.0	14.0	14.0	14.2	14.2
10.5	9.4	9.3	10.3	10.3	10.3	10.3	10.3	10.3	10.5	10.5
8.8	8.2	7.7	7.7	7.7	7.7	7.7	7.7	7.7	7.9	7.9
7.8	7.6	7.5	7.5	7.5	7.5	7.5	7.5	7.5	7.7	7.7

Table 6.12: Injection pulse width (% IJPU, IJPU=13ms) for ECU tuning.

Note: Efficiency % is identical to throttle position % and load % here

6.7.6 Miscellaneous Engine Tuning

The engine map represents only part of the engine tuning process. However, it provides the basis of all subsequent tuning, and any changes to the map may require many other parameters to be reset. While there are many parameters that fall into this category, only the two most noteworthy will be mentioned here. The first is the acceleration enrichment applied to the injection pulse width when the engine is dynamically accelerating through the RPM range. This is required because the engine map only represents steady state values, and a small amount of additional fuel is generally required during acceleration. While MoTeC provided general values for this, it was decided that this too would be tuned while using the dynamometer. The test basically consisted of measuring the lambda value and engine power and torque as the engine was accelerated throughout its RPM range under load. The dynamometer had a special function that allowed this, and allowed acceleration enrichment tuning through experimentation to provide maximum power. This test also highlights the variation of power through the RPM range, which is important in determining drivability. This information is given in Figure 6.13, which shows the maximum power produced by the engine as it accelerates through its rpm range for the factory ECU and for the final MoTeC tuning.

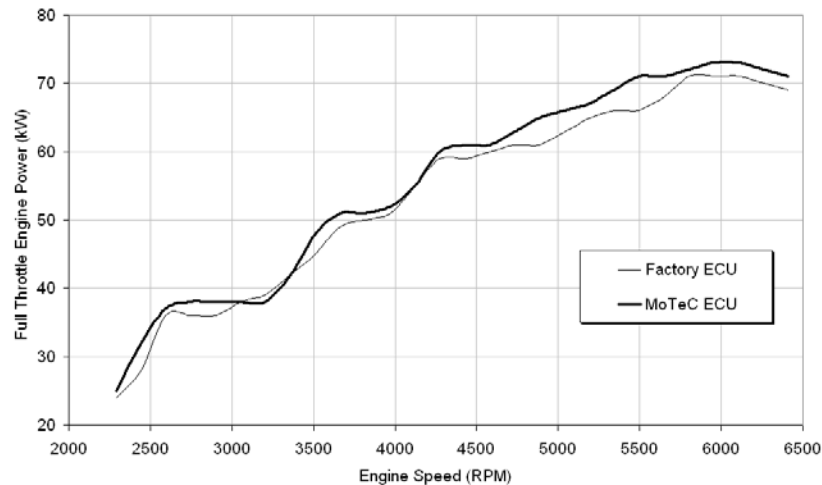


Figure 6.13: Engine power for factory and MoTeC ECUs

The test marked the conclusion of the dynamometer tuning, although not the tuning as a whole. The final feature that needed to be tuned was the engine cold start, which is an important, but difficult parameter to tune. The reason for the difficulty arises on two fronts, the first being that any changes to the map near idle would void all previous work in this area, the second being that an engine can only be “cold” cranked once per day. Nonetheless, the cold start was tuned on the test vehicle over a number of weeks to a point where it would start when cold, although not as easily as when running on the factory ECU.

6.8 Electronic Power Reduction Control

One of the goals for this investigation requires the ability to electronically reduce the power output of the engine for closed-loop intelligent traction control. As stated above, the MoTeC ECU has the functionality to do this, but because it is not a commonly controlled variable it requires more understanding and effort.

Power reduction by means of the intervention in fuel injection and ignition is discussed in [128]. In this paper B. Böning et al describe the means through which engine power can be reduced quantitatively. At its most coarse, power can be reduced on a four-cylinder engine by simply cutting fuel injection cylinder-for-cylinder, which effectively results in five power reduction quantum (although the final stage produces negative power). They also suggest incorporating ignition retard into the system to produce a infinitely more graduation into the control, but point out that this is not practical because the massive ignition retards that would be required would quickly damage an engine and exhaust. Their solution was to use what they called “alternating fuel-injection suppression” in

which they determine a cylinder-for-cylinder cut based on two engine cycles instead of one. In this way they produced nine power reduction quantum by effectively incorporating half cylinder cut which, for example, was done by cutting one cylinder on the first cycle and two on the second, thereby producing a 1.5 cylinder cut.

The MoTeC ECU uses this concept for its RPM limiter and Traction Controller, with two significant differences. The first takes the concept of half cylinder cut further, and introduces very small power reduction quantum. While MoTeC do not provide the information on how this is specifically done, it appears that the ECU cuts cylinders over many more than two engine cycles to provide finer control of engine power. The sequence of the cylinder cut is altered to suit different engines using their “RPM Limit Randomiser” parameter. The second difference is that engine power can be reduced via ignition cut as well as injection cut, or a combination of the two. This helps to overcome the principle flaw of injection cut control, whereby the inlet port walls are prone to drying out during cut and affect the fueling for the next firing stroke. To this end, the engine power limiting technique employed in this investigation incorporated ignition cut as the primary method, followed by injection cut when engine speed exceeded the control range by more than 100 RPM.

Using the MoTeC controller in this respect significantly simplifies the work required on this front, and is one of the many reasons for the ECU selection. Nonetheless, there was still a significant problem in getting a signal from an outside source to the MoTeC ECU to define the quantity of engine power reduction that was desired. MoTeC support were little help in this regard as the problem was a seemingly unique one. The solution appeared to be based in trying to get the MoTeC traction controller to observe a phantom tyre slip. By providing the traction controller with a slip value that could be externally controlled, it could perform its engine power cut as a separate function.

There appeared to be three options in doing this. The first was to “impersonate” at least two wheel speeds via the digital inputs, whereby slip could be defined by creating a difference between the driven and non-driven wheels. The second was to impersonate the MoTeC “Traction Control Multiplexer” module through one digital input and effectively do the same thing. The third, which was finally adopted once its function was identified, was to use the “Slip Voltage” input channel. This method allowed a single analogue voltage input to define the slip used in the traction controller algorithm, but required a

number of unusual settings to be made, the difficulties of which were further compounded by an error in the MoTeC tuning software to display the channel output correctly.

This only formed part of the problem however, as an understanding of how the MoTeC controller used tyre slip to determine the amount of engine cut was necessary. It was particularly important to determine whether the controller incorporated any time dependant functions, as this could significantly alter the control strategy employed and, at the very least, cloud any observation of the controller operation. Unfortunately, MoTeC would not provide this information as they determined it to be their intellectual property. The controller operation, however, could be inferred using two observations. The first was that the traction control tuning function seemed to only tune a proportional gain term, called the “Slip Control Range”, which MoTeC defined as the “additional slip above the aim slip at which full cut will be used”. If the software contained any derivative or integral terms for the controller they are non-tunable and preset, which seemed unlikely. This observation was further strengthened through practical testing and, by varying the slip voltage channel input with the engine running in a “no load” condition, it was possible to observe the traction controller operation. No matter what the slip voltage (and therefore the ECU observed slip) the amount of engine cut did not vary over time. It was therefore determined that the MoTeC traction controller most probably only contained a proportional term. This was a little surprising, given the very high profile of this unit in the racing industry, as it significantly limits the amount of traction control tuning that can take place. It is noted, however, that very few racing teams would have the resources and track time to take traction control tuning to this level, which probably explains the limitation.

With this information it was possible to configure the “slip voltage input” channel directly to a new, but unnamed, “percentage engine cut” channel. This configuration is shown in Table 6.13. In this way, the voltage applied to the slip voltage input is directly proportional to the percent engine cut, where 0V = no cut and 5V = 100% cut as defined in Eqn 6.1. It is important to note here that 100% engine cut does not correspond to full engine cut, as this has the potential of producing engine damage when excessive unburnt fuel ignites in the exhaust. Instead, the “Cut Limit” parameter was set to 75%, meaning that this is the maximum amount of actual cylinder cut that is permissible. Engine cut

percentage is therefore a percentage of this parameter, so 100% engine cut is in fact only 75% of actual cylinder cut as shown in Eqn 6.2.

TC Table (Speed Units)												
TP %	0.0	10.0	20.0	30.0	40.0	50.0	60.0	70.0	80.0	90.0	100.0	
	0.0	0.0	0.0	0.0	0.0	0.0	0.0	0.0	0.0	0.0	0.0	0.0

Traction Control - Slip Control		
Parameter	Value	Slip Ctrl Range
Slip Source	5	Additional Slip above the Aim Slip
Slip Filter	1	at which full cut will be used
Slip Ctrl Range	50	
Cut Limit	75	The Aim Slip is dictated by the
No Cut RPM	0	Traction Control Table
Full Cut RPM	0	
No Cut Throttle	0	Typical : 10 km/hr
Full Cut Throttle	0	
Launch RPM	0	
Launch Ctrl Range	200	
Launch Change Speed	5	
Launch Aim RPM	3000	
Driven Wheel Bal	80	

AV6 Cal (0V = 0V, 5V = 1024)													
Slip V %	0.0	4.0	8.0	12.0	16.0	20.0	24.0	28.0	32.0	36.0	40.0	44.0	48.0
	4	86	168	250	332	414	496	577	659	741	823	905	987

52.0	56.0	60.0	64.0	68.0	72.0	76.0	80.0	84.0	88.0	92.0	96.0	100.0
1069	1151	1233	1315	1397	1479	1560	1642	1724	1806	1888	1970	2052

Table 6.13: Traction control configuration for engine power control

$$\text{Engine Cut} = 0.2 \times \text{Slip Voltage}, \quad 0 \leq \text{Slip Voltage} \leq 5 \quad \text{Eqn 6.1}$$

$$\text{Actual Cylinder Cut} = 0.75 \times \text{Engine Cut} \quad \text{Eqn 6.2}$$

6.9 Narrow Band Lambda Meter

The MoTeC ECU contains the capacity to measure wideband lambda values via an ECU “upgrade” or the purchase of their “Professional Lambda Meter”. Including the cost of the sensor itself, this proved an expense that was not justifiable for this investigation. It will, however, provide a valuable investment for the hydrogen conversion by making significant dynamometer tuning time savings.

Nonetheless, it was deemed important to be able to observe the lambda value of the vehicle to an extent. This was to ensure that the engine was not accidentally made to run lean for an extended period of time, as this would cause damage, and to allow some degree of scope for “on road” engine tuning. To this end, a cheap electronic kit was obtained and built to measure the factory fitted narrow band lambda voltage, and display the result on a LED scale. The final unit, which consists of 10 LEDs, is shown fitted to the vehicle dash above the stereo in Figure 6.14. The red LEDs (left) indicate a lean mixture and the yellow ones (right) a rich mixture, with the six green LEDs (middle) showing the stoichiometric region.



Figure 6.14: Lambda Meter LED display (mounted to vehicle stereo)

6.10 Remarks

The factory ECU was considered inadequate for this investigation and, together with the argument for high levels of engine control in the later hydrogen conversion, a MoTeC M400 ECU was chosen for installation into the test vehicle. This decision was made principally because the MoTeC ECU provided the engine cut capability that was required for this research, and contains a full spectrum of tuning parameters and functions beneficial when attempting to run the engine on hydrogen.

As such, this chapter describes the MoTeC ECU installation and tuning process, including:

- Discussion on sensor features, installation and calibration;
- ECU installation and wiring;
- Derivation of engine tuning goals;
- Dynamometer tuning process;
- Development of the engine cut algorithm; and
- Installation of a lambda meter to avoid the possibility of engine damage.

The installation and tuning provided a highly flexible engine management tool, capabilities of which are barely utilised in this research. In particular, the level of engine tuning completed here represents the minimum needed to produce a smooth and drivable engine. Significantly more work could be completed, especially into cam tuning, to provide better drivability and more power from less fuel and emissions in further investigations. The auxiliary functions of the MoTeC ECU have significantly more capability than the “engine cut” function used in this work and can, for instance, be used for throttle-by-wire, adjustment of engine tuning parameters on-the-fly, running two fuel injectors per cylinder separately and control of auxiliary engine devices. This represents great potential for future research avenues, not only in hydrogen conversion.

CHAPTER

- 7 -

DATA ACQUISITION AND CONTROL SYSTEM INSTALLATION

The MoTeC ECU installation formed an important step in achieving the required functionality to implement the ANN stability controller in an on-line closed-loop manner, but had to be complemented by an upgrade to the data acquisition equipment. In particular, the ADL is only a data logger and, while it was sufficient for the surface identification research, it did not contain the real-time ANN modelling capability required for this investigation. As such, an additional data acquisition device was installed in the test vehicle to complement the ADL and allowed ANN modelling with a full range of inputs, and to implement ANN stability control.

To this end, the following chapter presents the test vehicle installation process used for a PC based data acquisition and control device. This includes the development of additional devices and device communications layouts to obtain the required performances, as well as the installation of a desktop PC and power supply within the vehicle. Finally, this chapter is focused on the hardware installation aspect of the installation, with the development of the software to run it covered in the next chapter.

7.1 Programmable Control

While the data logging capacity of the ADL fulfilled the goals of providing a quickly installed system for off-line ANN investigation, it contained a number of intrinsic limitations. Not the least was the fact that it could not incorporate any level of on-line ANN functionality or control, which was a principle goal of this investigation. This meant that the installation of a programmable controller was necessary. The chosen controller had to meet a number of requirements, which were:

- Must be able to measure all required inputs (in a variety of formats) with reasonable accuracy and high update rates;
- Data inputs must be flexible to accommodate future work;
- Must have at least one analogue output, although additional analogue, digital and serial outputs would be desirable;
- Controller programming must be extremely flexible to enable a variety of ANN controllers to be investigated, and to accommodate future work;
- Controller programming should be in a familiar and simple language, which is easily altered as requirements change. This was particularly important because the author had limited programming experience and training; and
- Cost should be kept as low as reasonably possible.

These requirements made it possible to exclude a number of possible options out of hand, such as the use of programmable micro controllers. Instead, the advice of a number of individuals was sought and two options were identified.

The first, which was eventually adopted, was to obtain a multifunction data acquisition device (DAQ) that could be integrated with a computer. These come in a number of varieties, but all provide input and output functionality to the computer, which in turn can be programmed to perform the desired data acquisition and control in a number of different programming languages. Further, the computer can accept serial inputs, which means that the AHRS sensor accuracy can be significantly improved by using RS232. This would circumnavigate the sensor's digital to analogue conversion and remove the need for the custom amplifier, which would both reduce measurement error and noise.

The second option also required the use of a computer, but in this case would have used the CAN bus to acquire all of the input data. In this way the ADL and ECU would provide all of the inputs to the computer via the CAN bus. This would have had additional benefit because the ECU / ADL / control system would have been totally integrated and enabled the user to use the strengths of each device. This option, although perfectly feasible, was not adopted in this case due to a number of potential problems. One was that the computer would have to incorporate a simple DAQ device of some kind to send the output signal because the MoTeC ECU is not programmed to receive real-time user CAN signals. Further, no one within the School of Engineering had experience with CAN, making support very difficult. Additionally, the CAN bus speed, although comparatively fast, cannot match the sampling speed of DAQ devices. Finally, the CAN bus/computer interface is only via PCI card (making the use of a PC inevitable), and carries a price of approximately twice that of sufficient DAQ devices.

Investigation of appropriate DAQ devices revealed National Instruments Corporation (NI) as the preferred supplier. Although generally more expensive than other companies, their devices are well regarded (and are used almost exclusively with the School of Engineering). Additionally, all of the NI DAQ devices are designed to work effortlessly with NI's graphical programming language "LabVIEW". This was particularly favourable because the author has previous experience with this language. Furthermore, the technical support staff within the School of Engineering were extremely experienced in the use NI DAQ devices and LabVIEW programming, and were willing to provide a significant level of assistance – which was a very valuable asset.



Figure 7.1: DAQ user interface

Nonetheless, there are still a very large variety of appropriate NI devices, and choosing the best one was a difficult task. Particularly, problems were encountered with unforeseen data transfer differences, which saw the initially purchased device replaced with a more acceptable one. The final installation's user interface is pictured in Figure 7.1, and is detailed in the Appendix.

7.2 National Instruments DAQ Pad

The NI DAQ Pad-6015 was originally chosen to perform the data acquisition and control. The device has the particular advantage that it is a USB device, and therefore is very flexible in its use. NI describe the device, which is pictured in Figure 7.2, as:

The National Instruments DAQ Pad-6015, which delivers USB functionality equivalent to PCI and PXI DAQ devices, is designed specifically for mobile or space-constrained applications. Plug-and-play installation minimizes configuration and setup time, while direct screw terminal connectivity helps keep costs down and simplifies signal connections.

The DAQ Pad-6015...is ideal for...applications where portability and accurate measurements are essential, such as in-vehicle data acquisition.

National Instruments Corp. [131]

Further, NI state the specifications of the DAQ Pad in their web based documentation [131], which is exhaustively given as:

- 16x Analogue inputs
- 2x Analogue outputs
- 8x TTL/CMOS digital I/O lines
- 2x Digital counter/timers
- 16-bit analogue input measurement at 200,000 samples/second
- 16-bit analogue output measurement at 300 samples/second
- $\pm 0.5V$ to ± 10 input range



Figure 7.2: NI DAQ Pad-6015 device [131]

Based on this information, and advice supplied by NI and School of Engineering technical staff, the DAQ Pad was purchased with the view to use it to communicate with

a notebook PC. In this way the device would be extremely portable and robust for use in the vehicle, and still be flexible for future research and easy to install. Upon installation technical staff wrote a small LabVIEW data acquisition program to communicate with the device, with extra features that could be added to for investigation of the quality of data. This proved very valuable because a very significant flaw in the USB data transfer was identified.

It was found that, even though the DAQ Pad was capable of sampling the inputs at 200,000 samples/second, it transferred this data to the notebook PC in “batches”. At approximately every 100ms, all of the measured data from the previous 100ms would be sent to the notebook. This was unalterable and was not stated on the NI specification sheet. In addition, it took a number of lengthy phone calls with NI representatives to confirm the problem was due to the device, and not our software. Finally, however, NI admitted error in recommending the product and allowed it to be exchanged. It is noted that this limitation was perfectly adequate for data logging and many forms of control, but in the case of this investigation would have constituted a significant shortcoming.

The problem was identified as a USB limitation, which arose because of its processor’s “interrupts” operation. All of the data that comes through the USB channel must go via the computer processor, which in turn must stop its other operations to process the data. If there is a lot of data coming through the USB this can significantly slow the computer down, since the processor is constantly stopping and starting its other operations. Because the DAQ-Pad transfers data in this way, NI designed it to transfer data in “batches” to reduce the effects on computer performance. This resulted in the problems above.

As such, a DAQ device with different computer communications functionality had to be chosen.

7.3 National Instruments Multifunction DAQ

Attention shifted to NI PCMCIA cards (DAQ Cards) for notebooks, but it was observed that similar problems were likely. This was because the PCMCIA slots also operate via processor “interrupts”. As such, this option was quickly discarded. Unfortunately, the

DAQ-Pad and DAQ-Card devices represented all of the suitable notebook PC devices NI had in production. This meant that their exclusion also corresponded to a decision to use desktop PC devices.

Desktop DAQ devices are in many ways superior to their notebook counterparts, normally providing more inputs and outputs at higher rates, higher accuracies and lower cost. They also communicate to the computer via a PCI slot (shown in Figure 7.3), which means that the data can flow directly into the computer RAM without using processor “interrupts”, greatly increasing transfer speeds. Unfortunately, they must also be installed in a desktop PC, installed into the test vehicle. Nonetheless, many people have installed desktop PCs into vehicles in the past [132, 133], and no insurmountable problems were anticipated – the installation of which will be discussed later.

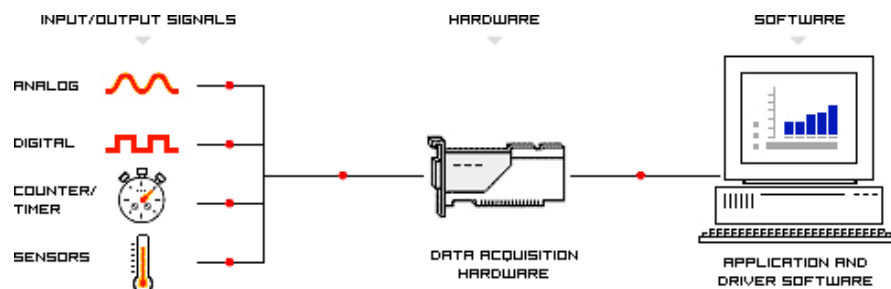


Figure 7.3: Desktop PC based data acquisition [131]

These observations resulted in the purchase of a PCI card from NI’s “Low-Cost M Series Multifunction DAQ” range. This was a new range, and represents far superior operation to previous ones at much lower cost. NI describe this range as:

The M Series is the next generation of multifunction data acquisition (DAQ) device from National Instruments. NI M Series technologies, including the NI-STC 2 system controller, the NI-PGIA 2 amplifier, and NI-MCal calibration technology provide more performance, more accuracy, and more I/O than other data acquisition devices. The new technologies and features of M Series devices make them well suited for a wide range of applications in test, control, and design, including automated test, process control, prototype verification, and sensor measurement.

National Instruments M Series low-cost multifunction DAQ devices provide optimised functionality for cost-sensitive applications... Low-cost M series multifunction DAQ is ideal for applications including data logging, control, and sensor and high-voltage measurements when used in conjunction with NI signal conditioning.

National Instruments Corp. [131]

From this range the “NI 6221-PCI” card was chosen, which is pictured in Figure 7.4 and has the following specifications [131]:

- 16x Analogue inputs
- 2x Analogue outputs
- 24x TTL/CMOS digital I/O lines at up to 1MHz
- 2x 32-bit digital counter/timers at 80MHz
- 6x DMA channels
- 16-bit analogue input measurement at 250,000 samples/second
- 16-bit analogue output measurement at 833,000 samples/second
- ± 10 , ± 5 , ± 1 , ± 0.2 V programmable input ranges



Figure 7.4: NI 6221-PCI DAQ device [131]

This device represents the lowest cost PCI card in the range that includes analog inputs and outputs, digital I/O and digital counter/timers. Nonetheless, it is more than adequate for this research and was very simple to install into a desktop PC and setup in the LabVIEW software by following the NI documentation [131].

Even so, the DAQ device is designed to use a separate connector block for individual input and output wiring, which must be connected to the PC PCI card via a cable. In addition, because automotive interiors are considered electrically “noisy” environments, this connector block and cable had to be shielded. To this end, the NI SCB-68 shielded I/O connector block and the NI SHC68-68-EPM 2m shielded cable were purchased, and represented a significant part of the DAQ expense. These components are both shown in Figure 7.5, which NI describes as:

The SCB-68 is a shielded I/O connector block for interfacing I/O signals to plug-in DAQ devices with 68-pin connectors. Combined with the shielded cables, the SCB-68 provides rugged, very low-noise signal termination.

The SHC68-68-EPM is specially designed to work with M series devices. The cable includes separate digital and analogue sections, individually shielded twisted pairs for analogue inputs, individually shielded analogue outputs, and twisted pairs for critical digital I/O.

National Instruments Corp. [131]



Figure 7.5: NI shielded connector block (left) and shielded cable

The connector block is quite simple in its functionality, and consists of a number of screw terminals for each of the DAQ input, output and digital channels, a number of “jumper” switches to alter some internal functions and a fuse for overload protection. It also contains two “breadboard” areas to allow the user to install additional circuitry for signal conditioning.

The connector block was installed to rest underneath the glove box, to the right of the passenger’s feet. In this position it is highly accessible and reasonably safe from accidental damage. It also results in minimum wiring length for the analogue sensors to reduce noise that, together with the general wiring details, will be discussed later.

7.4 PC Installation

The use of a PCI DAQ device necessitated the use of a desktop PC to control it. This required the installation of a desktop PC into the test vehicle, which by its nature produces a few significant problems. These problems revolved around converting a piece of equipment that is designed to be stationary to being made mobile.

The most obvious problem was that a desktop PC requires AC power, whereas the Corolla produces only DC power. The desktop PC, however, transformed the AC power into DC at a number of different voltages via its “Power Supply” module, so conceptually this was not a significant problem. Unfortunately, devices could not be sourced that would allow the existing AC-DC power supply module to be replaced by a DC-DC module, which would effectively run the computer from the 12V battery supply. It was also considered that building this device “in house” would be significantly difficult, especially when considering the large variation that can be expected in supply voltage from the vehicle battery. Instead, it was decided to perform a DC-AC conversion to power the PC directly. This required the purchase of a “Power Inverter” and, to cope with the extra power demand, an additional battery. This had the added

benefit that AC power would be available in the vehicle for other devices, although it is noted that this also produced some safety concerns. The installation is pictured in Figure 7.6.

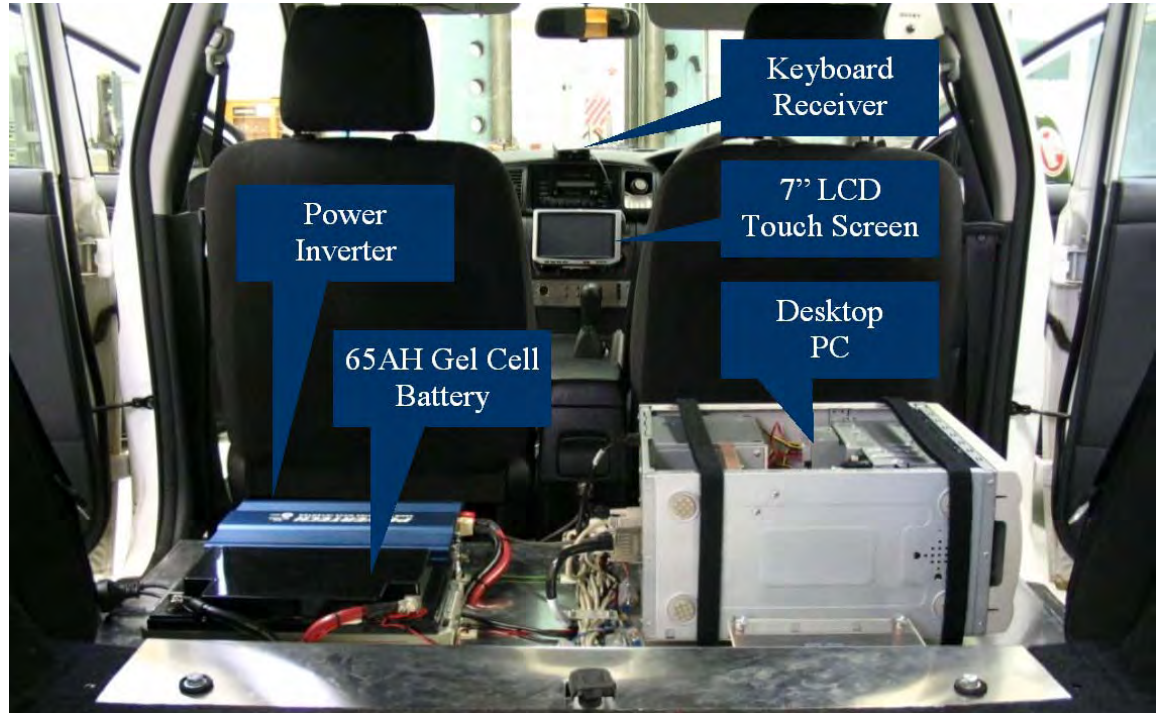


Figure 7.6: Desktop PC installation in test vehicle

Another clear problem in installing a desktop PC into a vehicle was that of vibration. While notebook PCs are designed to cope with a large variety of vibration, due to their stationary nature desktop PCs are not. This means that problems may arise from hard disk crashes, CD drives may fail, and devices and connectors may vibrate free of their electrical contacts. Consultation with a variety of people revealed that hard disk and CD drive problems were unlikely, and that the problem of electrical contacts should be focused on. To this end a number of measures were taken to minimise these effects.

The final significant problem to overcome in the installation was that of an adequate computer interface. Further, there was some concern about mounting AC powered displays on the dash, as there was a potential electrocution risk in case of a crash. In the end a 12V 7" TFT LCD touch screen VGA monitor was chosen, and mounted on the dash below the stereo. This was complimented by an infrared keyboard, with integral trackball for cursor operation.

7.4.1 Battery, Inverter and Charger

The 500W Powertech MI-5085 power inverter was purchased to run the desktop PC. This capacity was chosen to provide a more than adequate supply for the PC and a CRT monitor, and also allow the addition of other low powered items such as laptop PCs, exhaust gas analysers and video cameras, without a need for separate batteries. This added ability was considered important to ensure that any system added to the vehicle would be flexible, portable, reliable and simple to use. The ability to run battery powered items from a common source was also considered important, due to previous experience with items unexpectedly requiring recharging in the field. Further, having the capacity to run a CRT (or large LCD) monitor within the vehicle would allow the possibility of interactive static displays for the public, which was a foreseeable occurrence. The inverter has the following specifications:

- Maximum continuous power 500W
- 20 minutes power 650W
- Max surge capability (peak power) 1000W
- DC Input voltage range 10.7V-15V
- AC Output range 230V +/-3%
- Frequency (may be specified) 50 or 60hz
- Efficiency >85%
- Dimensions (LxWxH) 335x236x83mm
- Net weight 3kg

Many power inverters do not produce perfect AC sine wave outputs. This is not a problem for most AC devices but, in the case of the computer, this type of power inverter was not considered a wise investment. Instead, the purchased inverter was of a “pure sine wave” variety (with a total harmonic distortion of <3%), and produced a power output very similar to the mains supply. This was considered particularly important because the DAQ device and sensors would also be powered through this source, and any step to reduce potential erratic behaviour or noise was considered vital.

Further, it was noted that the vehicle alternator did not have the capacity to run the computer and charge the battery. This meant that simply wiring the inverter to the existing vehicle power supply would constantly drain the battery, which was not good

for the battery and could make the vehicle inoperable. It was observed that installing a second battery would extend the driving time of the vehicle, but this did not solve the fundamental problem that the batteries would be constantly draining. This effect can be minimised by installing a power management system, which among other things, would ensure there was always enough power to start and run the vehicle. It was considered that this system would be expensive, complicated and difficult to install, and was not adopted.

Instead, a decision to power the inverter separately to the vehicle supply was made. This had a two-fold advantage to the other options, in that it was much cheaper and easier to install, and significantly reduced the likelihood of noise within the DAQ system. A battery of sufficient size to power the computer for a day of testing could be installed in the car for day-to-day use, along with a battery charger for overnight charging. This had the added advantage that an approximately constant voltage could be used a supply to the inverter, which was simply not possible when using the vehicle supply, due to erratic loads and noise. This meant that the computer and DAQ system could operate on a totally separate supply to the rest of the vehicle (although commonly grounded to the vehicle battery 0V) and be immune to electrical disturbance within the vehicle supply.

To this end a 65AH 12V battery was selected to run the power inverter. The battery was sized to be able to run the computer and a CRT monitor for a least 4 hours at constant maximum load. In reality, however, the battery was capable of running the computer for well over 8 hours, which was in excess of the requirements of this investigation. The battery was also of a “gel cell” kind, which is essentially a sealed lead acid battery. These kind of batteries, while generally more expensive and larger than wet cell lead acid batteries, do not produce dangerous fumes when charging and are safe to use in enclosed spaces. As such, the battery was safe to be installed into passenger compartments, which was necessary in this case as the engine bay had little room for an extra battery (especially when considering the proposed hydrogen conversion).

Finally, the battery must be charged. Because the system was separate to the vehicle alternator, this was only practically possible via an external power charger from the mains. As such a battery charger was purchased so that when the vehicle was parked it was possible to charge the battery from the mains overnight. Further, gel cell batteries have special charging requirements, and only specifically designed charges should be

used. Unfortunately, previous experience with earlier Intelligent Car projects has shown that this is not well known, with normal chargers often used. Gel cell batteries charged by non gel cell chargers do not last long at all, and chargers within the School of Engineering are frequently “borrowed” and mixed up. As such there was concern that as others used the test vehicle, the battery would be rapidly destroyed. Mounting the battery charger to the test vehicle and permanently wiring it to the battery solved this potential problem. In this way, the battery could be recharged by simply plugging the charger into the mains and turning it on.

The three devices can be seen installed in the test vehicle in Figure 7.7. In addition to that specified above, the battery is also fitted with a number of resistors (mounted at the battery positive terminal) to divide its voltage into the 0-5V range. This was added to allow the DAQ system to monitor the battery voltage and sound a warning if it was too low (as this would also damage the battery and crash the computer).



Figure 7.7: DC-AC power inverter (top left), battery (centre right) and charger (bottom left)

7.4.2 Mounting and Vibration Isolation

The desktop was mounted into the test vehicle to reduce vibration, and therefore to reduce the likelihood of problems with loose internal contacts and hard drive crashes. Initially, the PC was installed into the vehicle onto a 50mm thick piece of high-density foam (which was recommended as the best foam for this purpose) of the same dimensions as the PC base. Two foam lined metal straps held the PC in place. Unfortunately, it was found that when the vehicle performed high acceleration manoeuvres (such as a quick turn) and when the road was very uneven (such as a pot hole) the computer was likely to power off and reboot.

Observation of the mounting showed that, while it was more than capable of damping high frequency/small amplitude oscillations, it particularly could not handle high amplitude disturbances. To correct this it was decided that the mounting would have to allow the PC much more freedom of movement. To this end, the HD foam was reduced to a 150x150x50mm size and the metal straps were replaced with flexible Velcro® straps. In this way, the foam allows the PC a great deal of movement while also providing sufficient dampening. The straps, which are attached directly to the PC, simply hold the PC in place and allow a mechanism for damping adjustment by “preloading” the foam. The system is shown in Figure 7.8 and was found to work very well.

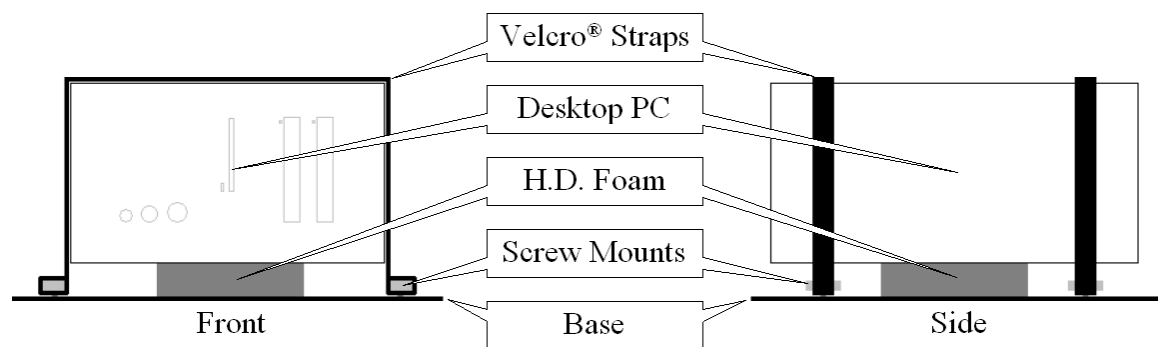


Figure 7.8: Mounting of the desktop PC for vibration isolation

7.4.2.1 Securing PC Internals

Even with the best vibration dampening, a desktop PC installed in an automobile will undoubtedly experience greater forces than it would on a desk. Desktop PCs are not designed to be moved frequently, nor are they designed to be shaken while running. As such, it is foreseeable that the component mountings may not be particularly strong or ridged.

Particularly highlighted as a potentially problematic area were the PCI slot connections, because the cards could vibrate themselves free or be forced free through flex in the PC chassis. As a countermeasure to this, an additional brace was placed within the PC chassis, from which extra support for the PCI cards was installed. The brace made from a bent and drilled aluminum bar, and was bolted between the PC chassis and power supply. A thick plastic sheet was cut to approximately the same profile as the PCI cards and bolted to the mount as a support, with foam also installed to avoid ridged contact between the cards and the support. This installation is shown in Figure 7.9.

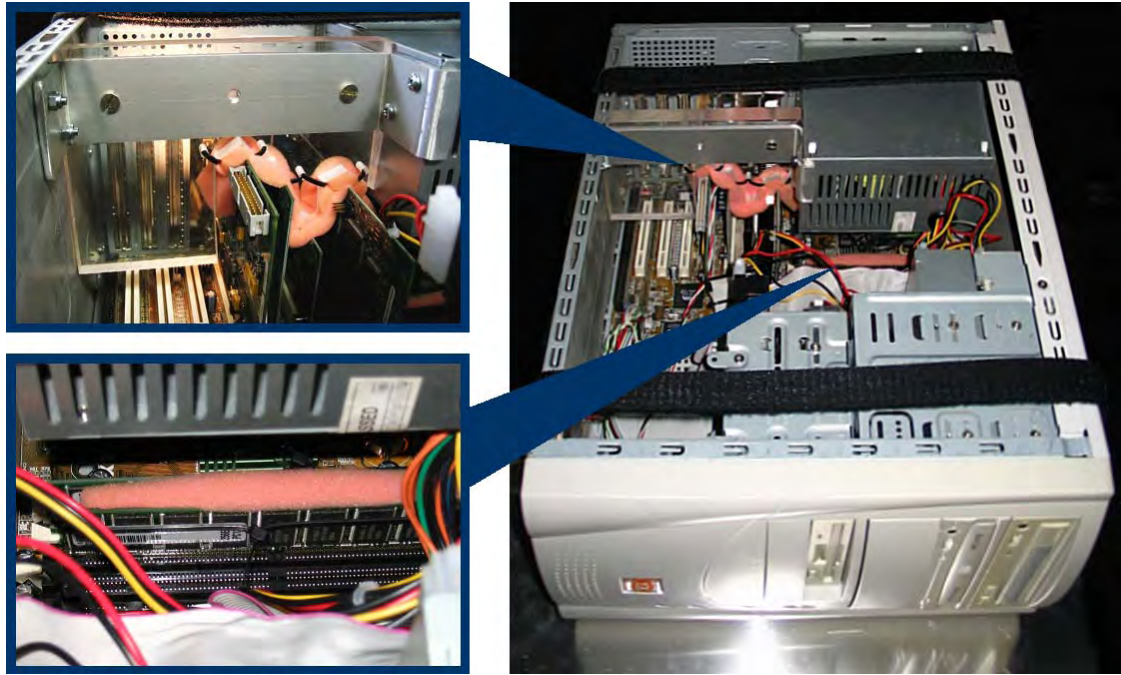


Figure 7.9: Method of securing PC PCI cards (top) RAM (bottom)

Using this installation no PCI connection problems were identified, which suggests that the steps taken were sufficient. Problems were, however, encountered with the computer randomly crashing in a variety of ways. Advice suggested that this was due to poor RAM connections, and so the two RAM cards were also supported. Due to space limitations however, the two cards were not supported from the PC chassis, but instead from each other. This was done by placing some foam between the two cards as a spacer and cable tying the two cards together, the installation of which is also shown in Figure 7.9. Further testing revealed that this remedy had solved the problem.

After lengthy testing an additional problem was identified – with the computer again crashing, but this time with hard drive warnings. Investigation showed that the hard drive was not damaged, and that the problem was a result of connection problems at plug connectors. Simply unplugging and replugging each of the connectors, which was adequate for the remainder of the research, solved this. It is noted, nonetheless, that this is not a permanent solution, and further work should attempt to fix this problem.

7.4.3 Touch Screen Display

The Xenarc 700TS 12V 7” TFT touch screen VGA monitor was purchased as a display for the PC, and is shown in Figure 7.10. This monitor was chosen to provide a safe and useable display that could be positioned somewhere the driver could see it, of adequate size and resolution, and at a reasonable price. Choices were also significantly limited by

University of Tasmania supplier policy, which made it difficult to find retailers for particular products due to warranty concerns.



*Figure 7.10: 12V 7" TFT Touch screen VGA computer monitor
(right: hinge action for dash access)*

Of particular concern in the monitor selection was using a 240V AC power supply in front of the driver. This was because if the monitor was damaged it would most likely expose its internal AC power, which could pose an electrocution risk. To this end only 12V monitors were considered, which significantly reduced the available range.

Secondly, to increase its usefulness, the monitor had to be as large as could reasonably fit into the vehicle dash, and of high resolution. The maximum size that could be used was determined to be 10" at a 4:3 aspect ratio. It was found, however, that monitors in the 8" to 13" inch range were generally not available and very expensive. Conversely 7" monitors are comparatively common (because of their use in automotive applications and ability to fit into dash stereo compartments), have a reasonably high resolution and are relatively low in price.

Further, the 7" monitors often incorporated touch screen functionality at very little cost. Although this was not required, it was observed that incorporating a touch screen into the PC installations would enhance the user interface and improve the overall presentation of the vehicle.

These points culminated in the purchase of the Xenarc 700TS monitor, which has the following specifications:

- 7" (16:9) screen size
- 800(H) x 480(V) WVGA physical resolution (640x480 to 1600x1200 supported)
- 2400 x 480 (1,152,000) dot resolution
- 330 cd/m² display brightness through touch screen
- 7.75"(W) x 4.75"(H) x 1.38"(D)

The monitor was installed onto the test vehicle dash, directly below the stereo so the passenger and driver had equal view. This position placed the monitor in front of the air conditioner controls, and a hinged system was installed to allow the monitor to be raised to allow access to the controls. This can also be seen in Figure 7.10.

7.4.4 Keyboard and Trackball

The Wombat KSI-2105 Wireless Infrared Keyboard was chosen for use with the in car PC, and is pictured in Figure 7.11. The 1.2kg 292x162x27mm PS/2 device is reasonably standard, and incorporates a trackball and mouse buttons. This is particularly helpful because it would be extremely awkward to use a mouse (or any other pointer) within the vehicle. Further, with the IR sender mounted to the top of the vehicle dash, the keyboard and trackball can be used throughout most of the car and externally.



Figure 7.11: Wireless keyboard with integral trackball, and IR receiver

7.5 Wheel Speed PIC

As discussed previously, the wheel speed sensors generate a digital waveform output, which the DAQ device must interpret to generate the wheel speed measurements. It was originally envisaged that the DAQ 1MHz digital I/O lines would be adequate to perform this task, but some investigation of the device specification proved otherwise. This was because it was observed that up to 800 teeth/second might pass the sensor at legal speeds, and it was felt that insufficient counter resolution could be obtained without

computationally intensive filtering. Conversely, it was possible to measure the wheel speeds to high accuracy using the 80MHz counter/timers, but because there were only two inputs for this, it was considered impractical.

School of Engineering technical staff suggested a solution, however, which was eventually adopted. This was to use an external device to measure the wheel speeds and communicate the result to the computer via RS232. While it was observed that the fastest update rate of the inputs would thus be approximately 60Hz due to the serial limitations, it was also noted that the external device could perform all of the counting, filtering and calibration functions and thereby reduce the computational load on the computer processor. To this end the technical staff produced the “PIC Core PCB”, pictured below in Figure 7.12, which was housed behind a Perspex plate as seen in the figure.

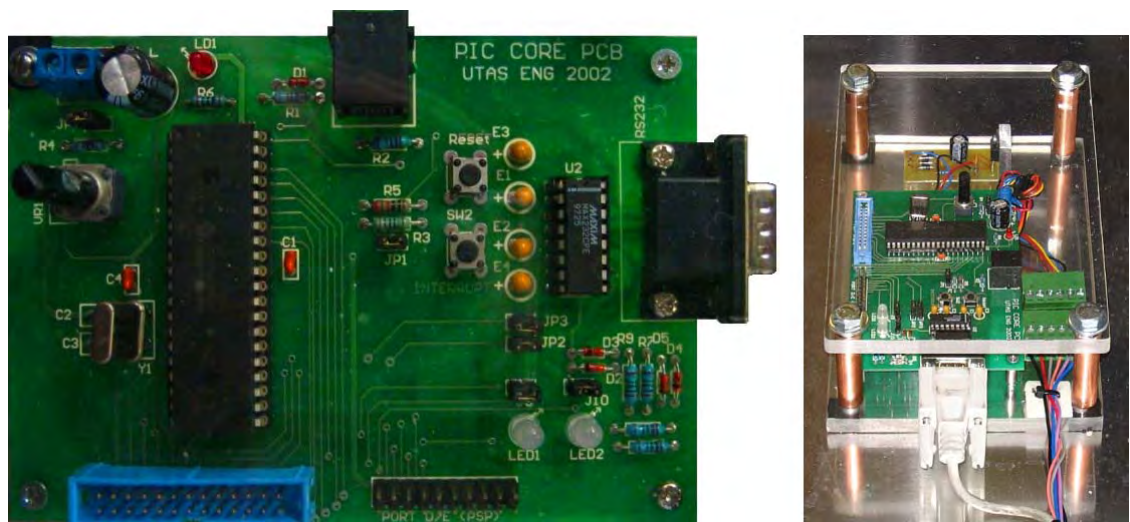


Figure 7.12: Custom PIC core PCB for wheel speed measurement

This device was programmed to give 24 bit pulse durations for each of the four wheels with 1.6 μ s resolution. To reduce noise, each pulse duration is averaged over 10 pulses or 5000 timer counts (8ms total), whichever is shorter. As a result the device's measurement accuracy is in the order of 0.5% of the reading, and the maximum input frequency is approximately 2kHz (which corresponds to about 330km/hr with a 40 toothed disc and wheel 1.830m diameter). The four averaged pulse durations are streamed at 19.2kBaud (with a checksum) to the PC via the devices RS232 serial port. The “PIC Core PCB” provides a high level of signal conditioning, and utilizes the slow nature of RS232 communications to provide time for sufficient filtering to remove the noise that is produced by counter resolution limitations.

7.6 Installation and Wiring

As in many of the figures above and in Figure 7.13, most of the in-car PC installation was mounted to a metal plate, which was in turn mounted where the back seats normally are. While it is noted that the installation could have been placed in the rear of the vehicle, space requirements for the hydrogen conversion and a desire to minimise sensor-wiring lengths made this option impractical.

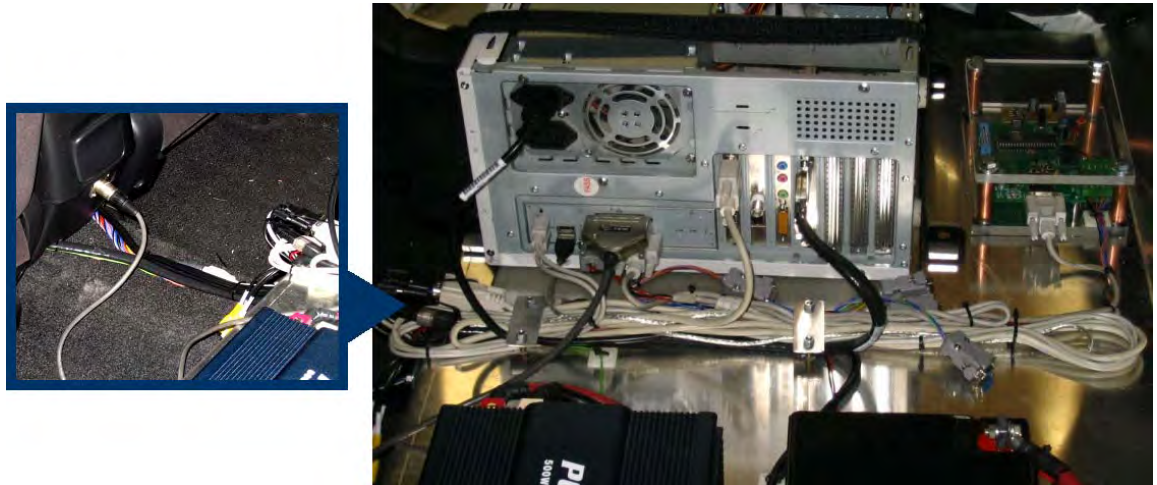


Figure 7.13: In-car computer wiring (right), CAN plug and cables (left)

The rear seats were totally removed and replaced with a carefully bent and shaped aluminium plate. This plate was rubber mounted to the chassis, with care taken to ensure rigidity. Components could then be screwed or double sided taped to the plate to ensure a neat installation, which can also be seen in Figure 7.13. Further, wiring such as the battery charger, battery high current leads and AC cables could be hidden under the plate to avoid damage. This arrangement had the additional benefit that the large 65AH battery could be recessed into the cavity below the plate to further enhance the appearance of the installation. The computer itself is connected to (left to right in Figure 7.13):

- | | |
|-----------------------------------|--------------------------------|
| a. AC Power | f. CAN cable parallel port |
| b. Keyboard PS/2 | g. AHRS serial port |
| c. Mouse PS/2 | h. Wheel speed PIC serial port |
| d. USB touch screen | i. LCD display port |
| e. USB backup external hard drive | j. DAQ device port |

The wiring for the DAQ produced the need to re-wire many of the ADL sensors and connect to a number of the ECU sensors and ECU inputs and outputs. In addition, it was noted that the analogue sensor accuracies would be significantly eroded due to increased noise if they were split between the ADL and DAQ. Further, previous testing had highlighted a need for better wire shielding and reducing wire lengths. With this in mind, most of the sensor wiring was completely re-designed and replaced, and the final arrangement is shown in Figure 7.14.



Figure 7.14: Final wiring arrangement behind glove box

This new installation included moving most of the wiring connectors from the engine bay to behind the glove box. The ADL analogue suspension position and steering angle sensors were also disconnected and instead powered and sensed using the DAQ, although connectors were installed to allow simple conversion back to the ADL arrangement. This is in contrast to the AHRS measurements, where the ADL powers the unit and measures its analogue outputs, while the PC measures its serial ones. Furthermore, the suspension position sensor shield wires were shortened and fitted to ensure as much shielding as possible, and the unshielded steering sensor wires were replaced with shielded ones. Wheel speed sensors readings were split between the MoTeC ECU, ADL and DAQ, and are powered by the MoTeC ECU. Engine sensors were also split between the factory ECU, the MoTeC ECU and the DAQ, although the DAQ RPM measurement was taken as a digital MoTeC ECU output. This was done because the raw crank angle sensor magnetic sensor output was too difficult to configure due to its missing tooth arrangement. Furthermore, an additional CAN plug was installed into the rear of the centre console (Figure 7.13) to allow the in-car PC to be used for MoTeC ECU and ADL tuning. All of this wiring, in conjunction with the ADL and MoTeC ECU wiring diagrams, is explained in Figure 7.15.

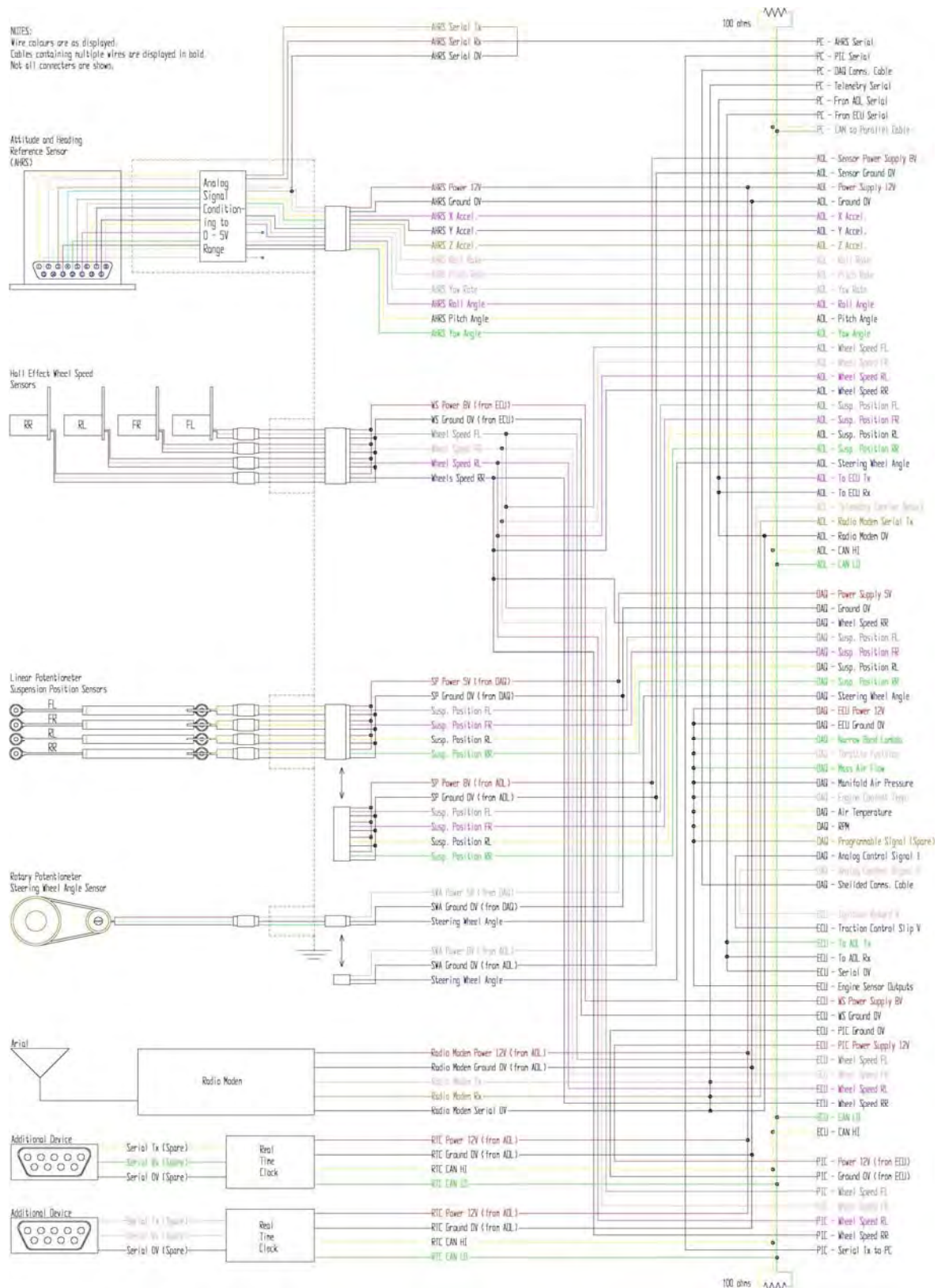


Figure 7.15: System wiring diagram

Finally, each of the DAQ inputs and outputs were wired to the screw terminals of its connector block, as in Figure 7.16. These were all wired with a “single ended” arrangement, whereby each of the voltages are measured against a common ground. This increased the number of available inputs, as explained in detail in NI documentation [131].

One of the counter/timer inputs was connected to the RPM output of the MoTeC ECU, and the other to the rear right wheel speed sensor. The latter was not used in this research, but was incorporated to allow future on-line testing of the road surface identification research presented here. Both of the analogue outputs were wired to the MoTeC ECU inputs. As described above, one of these was for engine power cut control, while the other was spare.



Figure 7.16: DAQ shielded connector block internal wiring

This was a significant and complicated project, and resulted in the removal of a large volume of wires. The new system, however, integrates the MoTeC ECU, the ADL and the DAQ together quite well, plays on the strengths of each device and increases measurement accuracy. Its functionality could be increased, at no extra cost, by adding DAQ to ADL serial communications, which is essentially a programming problem. Furthermore, the addition of a CAN bus to the PC would enable full integration of the three devices and allow huge research potential with minimal set up effort. Additional devices, such as a wide band lambda sensors, GPS and mobile phone modules, could further increase the

functionality of the system. Nonetheless, the installed system is still extremely versatile and powerful, and was more than adequate for this research.

7.7 Remarks

The new data acquisition system provides much more functionality than the ADL. The new system is designed to integrate with the ADL so the benefits of each can be exploited. In particular, the new system provides a means through which many different devices can be used to compliment each other, and is highly flexible to meet future needs. These installed devices include ADL, MoTeC ECU, DAQ, PC, 240V supply, wheel speed PIC, radio modem, AHRS, chassis and engine sensors, engine idle control valve, lambda meter, CAN bus, RS232 comms (ADL to radio model, ADL computer, external device to ADL, external device to computer (two way), AHRS to computer (two way), PIC to computer (two way), and ECU to computer), user displays and user control devices.

As such, the installation is sufficient to meet the needs for the development of the ANN stability controller, and for implementation in an on-line and closed-loop manner (the software that needs to be developed to accomplish this, however, will be presented in the next chapter). The system is highly flexible, and allows wide ranging automotive research to be undertaking in future work with minimal effort. It simplifies the process of attaching additional devices, like GPS and GSM modules, to the system, but this functionality could be further improved by installing a CAN bus PCI card into the PC. Replacing the existing PC with a more current model would significantly enhance system performance.

CHAPTER

- 8 -

INTELLIGENT STABILITY CONTROL

The potential of intelligent stability control is discussed in this chapter, and results in the construction and on-line closed-loop testing of an Intelligent Traction Controller fitted to the test vehicle. In particular, the general control goals are discussed and types of ANN controllers are presented from theory. Test tracks are chosen, and traditional traction control and ANN training data derived initially. The training data was used to construct a number of different ANN models, which were utilised in a range of off-line controllers. The performance of these controllers when compared to the performance of the traditional traction controllers are used to select the most promising model.

The chosen ANN controller underwent additional training and architecture modification to reduce error, and was subject to significant off-line testing. At this point, many of the potential limitations and benefits of ANN stability control were identified. The ANN controller was utilised on a real vehicle and in real driving scenarios to monitor its actual performance. This on-line closed-loop control could be evaluated and compared directly to the performance of the traditional traction control. This comparison, and the information derived through off-line testing, could be used to determine the general potential of ANN stability control, although it is noted that many more resources are needed to produce conclusive evidence of the ANN accuracy.

8.1 Rationale

The benefits of increased stability controller performance have been discussed in depth. There appears little doubt that ever increasing stability controller performance will enhance vehicle performance, and increasingly provide driver support during critical manoeuvres. Whether or not drivers choose to use this performance to increase safety or to increase their average travel speed is another question entirely, the answer of which will vary from driver to driver. A distinguished sea captain once suggested that:

A superior seaman uses his superior judgment to keep out of situations requiring his superior skills.

R. Cahill [2]

This statement makes it clear that good judgment on the driver's behalf is much more important in avoiding an accident than a high level of skill or performance. For example, and averaged over all crashes, the decision to travel faster results in a fatality risk increase to the fourth power of travel speed [2]. Nonetheless, even with the best judgment accidents still happen, and drivers must be able to react in a timely and appropriate manner when these situation arise. Unfortunately, as M. Dilich et al [10] comments, this is often not the case.

When a threatening situation arises which demands hard braking, swerving, or both, most drivers lack experience to predictably and successfully handle their vehicles. The uncertain and potentially dangerous outcome of such aggressive handling may restrain drivers from fully utilizing the capability of their vehicle's control systems...Pyrnne and Martin (1995) found that "this phenomenon tends to affect cautious drivers more severely because the accident situation is even further beyond their normal driving experience.

M. Dilich et al [10]

Further observation shows that by combining Cahill and Dilich's statements a bleak "Catch 22" situation arises. It seems that by utilising superior judgment the driver does not produce any "opportunities" to develop superior skills through experience. Likewise, gaining superior skills on public streets requires the driver to make a number of "poor" judgments, which are wholly unsafe, and when deliberate, often illegal. The solution to this problem seems one of training in a safe environment. This would obviously have some advantage by providing drivers with experience navigating their vehicle at the edge of adhesion. Unfortunately, and as Prynne and Martin state, the emergency nature of automotive accidents and near accidents add another dimension to the problem.

In moments of extreme stress, humans tend to revert to the response they used most often to a particular stimulus so if a new response has been learnt recently the older response

will be used instead. This means training can not be expected to have much, if any, effect on behaviour in emergencies.

Prynne and Martin [10]

Indeed this view is supported by Evans [2], whom provides a volume of evidence to suggest that driver education does not practically increase safety. Part of this evidence was formed by comparing crash rates of racecar drivers and non-racecar drivers through a number of USA states. Surprisingly, racecar drivers were up to twice as likely to be involved in an accident and three times as likely to be caught speeding.

These points produce a serious quandary. Clearly good judgment will reduce crash risk and severity. However, when an imminent accident must be avoided, most drivers do not possess the required skills to conduct effective manoeuvres. Furthermore, even if they have conducted in depth driver education, they are likely to react in an inappropriate way as a result of the human “emergency” mechanisms that tend to produce forceful, rapid and less coordinated movement.

Plainly, any system that will allow the driver to operate the vehicle in a more precise and predictable manner in these emergency situations will be of significant benefit in crash avoidance and mitigation.

The benefits of increased stability controller performance have been discussed previously, and in depth. There appears little doubt that ever increasing stability controller performance will enhance vehicle performance, and increasingly provide driver support during critical manoeuvres. Nonetheless, the problem of maximising tyre grip with the road surface for specific manoeuvres is a difficult one, with many variables and many limitations.

8.1.1 Traditional Stability Controller Limitations

As discussed previously, the focus on stability controllers has been on controlling slip to achieve maximum accelerations in particular directions while maintaining drivability. Determination of the “optimum” slip is an extremely difficult process, as this value varies as a function of a great number of parameters, and controllers generally choose particular values based on a number of significant assumptions. This has the obvious limitation of degraded performance in conditions when these assumptions are false.

Furthermore, stability controllers generally do not measure many parameters that deal with tyre contact patch state. It seems this is partly due to the physical cost of increased sensor arrays, and partly due to the difficulties in incorporating this additional data in a useful way into stability controllers. As such, stability controllers must make further assumptions on the state of vehicle variables, at a further degradation in performance.

Finally, although slip is a very important control parameter to increase vehicle grip between the tyre and the road, it is by no means the only one. Slip regulation can be complimented to a high degree by other controlled variables such as variable wheel camber, variable suspension dampening, variable ride height, and so on for significantly improved performance. These are generally not implemented in passenger vehicles for the same reasons of cost and difficulty in effective incorporation into a stability controller.

In general the implementation of an extra measurable parameter, or the addition of another controlled variable, results in an exponential increase in the programming complexity of the controller. With this in mind, it is likely that controller programming limitations will slow stability controller progress to a greater extent than available hardware. Indeed, this already seems the case with a widespread rejection of suspension position sensors in passenger vehicles despite their comparative low cost (especially if mass produced) and clear ability to evaluate vehicle performance within the racecar industry.

8.1.2 Future Stability Control Trends

Current stability control systems can be improved significantly, in a range of areas. As such, the goals of future intelligent control systems will most likely be to:

- Provide optimum performance in all conditions;
- Evaluate driver requests and alter vehicle parameters to suit;
- Determine operation goals such as performance, safety, fuel economy or comfort;
- Accommodate for physical vehicle alterations, such as weight distribution changes and tyre wear; and
- Alter as many control parameters as possible to provide maximum tyre adhesion levels, including active suspension, real time damping, active camber change, automatic load distribution and rear wheel steering [14, 29].

In short, the future trends in stability control systems will seek to improve the usage of available traction under complex, real road conditions and extend the range of performance [12]. Clearly this means the inclusion of more comprehensive mathematical models and associated sensory data using traditional techniques. The complexity of the system, however, means that the inclusion of increased data would require extensive investigation and algorithm development to model the effects on the vehicle dynamics. This means a significant increase in the size of the necessary control algorithm computations, which exponentially grow in complexity with the inclusion of additional parameters, as illustrated by Bannatyne [28].

An alternative to the extensive algorithm development required to meet these future goals exists in a number of intelligent systems. These systems, which are numerous in and widely varied, offer a huge number of potential benefits. Some are adaptive, some can be programmed using easily understandable heuristic knowledge, some can learn the dynamics of the processes on their own and others can reduce computational complexity. In addition, the ability to replace the complex mathematical models used in current systems with models based on observation can significantly reduce model complexity, allowing for the addition of extra sensory inputs and control outputs. It is this ability to incorporate additional data into the control algorithm with minimal programming and computing resources that makes the use of these non-conventional techniques desirable. The possibilities that these systems offer the automotive industry are great. In fact, many automotive systems are already taking advantage of these unconventional approaches in other areas of research and development, as discussed earlier. [21, 23, 89, 134]

8.1.3 Benefits of ANN

Artificial Neural Networks are an unconventional control method, and are designed to mimic the operation of the brain at a neural level. The potential benefits of ANN models for stability controller design have been discussed in detail in previous sections, with numerous case studies presented as examples.

In addition, past research carried out at the University of Tasmania has shown the use of ANNs as predictive tools for stability control to be extremely satisfactory, with a number of different models showing excellent capability [40, 87, 88]. In this research, data was acquired on straight line and figure of eight courses, using the F-SAE racecar on a near

homogeneous surface, to provide information over a range of simplified driving conditions. This data was used to program a number of ANNs in the interests of predicting vehicle longitudinal and lateral acceleration and yaw angle from 14 measured parameters. The models were tested, displaying results of between 0.2% and 8.3% full scale RMS error. This previous research further strengthens the argument to use ANN models for stability control.

8.1.4 Problem Simplification

Although the argument has been made that ANN models may provide an extremely flexible tool to allow a range of stability control strategies, this will not be fully investigated here. Such a work, even considering the argument that ANN models simplify the controller development process considerably, is beyond the scope of this research. The reasons for this include:

- The state of Tasmania has no suitable test tracks for the thorough investigation needed to evaluate complicated stability controllers;
- There are no automotive manufacturers in Tasmania to be of assistance, and no assistance offered by interstate manufactures;
- The project budget precludes the use of expensive prototype controllers, sensors and actuators other than those already on hand;
- The provided test vehicle does not contain any method of electronic brake control;
- The University of Tasmania has extremely limited automotive engineering resources; and
- The work required to construct the controller hardware and software, and objectively evaluate their eventual performance, is considered beyond the scope of a single PhD investigation.

Instead, the investigation was planned to tackle the problem from another direction. It was observed that one of the principle benefits from the use of ANN models was their adaptability from system to system. With this in mind, it was therefore considered that proving the ANN model applicability and demonstrating controller performance for a simplified case would be sufficient to make a strong case for more complex controllers. Likewise, if no advancement could be made with this simple case, the usefulness of ANN controllers for stability control could be considered partially disproven.

Considering the points above, the use of a system requiring brake pressure control of any kind was considered impractical for this investigation. This was a relatively simple observation because the vehicle was not fitted with any form of electronic brake control and the addition of any such system would be difficult, expensive and raise some safety issues. Of particular concern was the possibility that such a modification would render the vehicle illegal for street use, as this would conflict with the goals of the “Intelligent Car” and hydrogen conversion projects. Unfortunately, this leaves very little room to investigate many different types of stability controllers, as brake control is absolutely necessary for slip regulation in ABS and the more advanced stability controllers. This leaves only traction control as a possible avenue for investigation.

Unlike ABS and the newer stability controllers, many traction controllers do not include electronic brake control as one of their controlled variables. Instead, driven wheel torque is often solely controlled by engine power reduction of some kind. Such systems can handle longer periods of traction control operation (as brakes often overheat very quickly), but suffer performance losses on “spit μ ” and other surfaces. This is because the controlled variable is the torque transmission to both wheels through the differential, rather than torque control at individual wheel. Nonetheless, engine power can be reduced in a number of ways too. MoTeC traction control, for instance, utilizes electronic engine power reduction through injection and ignition control, with no brake control. Other systems incorporate throttle position control (or secondary throttle control) to limit airflow to the engine, and for power reduction control. The best performing systems, however, include both brake and engine power reduction control.

As discussed above, nonetheless, the implementation of brake control was not considered appropriate for this investigation. This, then, reduces the control problem to traction control using engine power reduction – and limited the choice to one between injection/ignition control, electronic throttle control, or a combination of both. This decision was influenced by the knowledge that the vehicle would be converted to hydrogen in the future, and therefore require the addition of a programmable aftermarket engine management system. The MoTeC ECU that was chosen through the course of this investigation had the ability to affect injection/ignition control based on an external signal, and so this was selected as the easier option. This decision was greatly influenced by the fact that the MoTeC ECU contained a traditional traction control function that would allow direct comparison with the ANN controller. In contrast, implementing

throttle control was considered a worse solution, in part because of its reduced response in limiting power. A more important factor in this decision was the difficulties in actually implementing the control as it was not considered wise within the scope of this investigation to directly electronically control the throttle for safety reasons. Likewise, the installation of a secondary throttle was not considered an appropriate course of action due to the possibility of extremely rich fuel mixtures and backfire during engine cut. Choosing to affect engine power reduction using the MoTeC ECU avoids these problems, although it was noted that injection/ignition cut has limitations. These include potential damage to the engine during extended periods of cut and a limitation in the amount of power that can be reduced without causing engine damage. Nonetheless, the MoTeC ECU contains the functionality for electronic throttle control, so the two methods of control could be combined in the future – but only with considerable knowledge of “drive by wire” systems, and at significant cost and effort.

Finally, although slip control forms the basis of the intended ANN controller, there are many other variables that can be controlled for significant benefit with the installation of appropriate hardware. As mentioned above, however, this hardware was not available, and as a result only slip control will be explored here. Nonetheless, the optimisation method that will be explored in this investigation is considered identical to the method required for any other relevant controlled variable.

8.1.5 Problem Goals

Producing and testing a traction controller that only controls the level of engine power reduction through injection/ignition cut instead of producing a complex stability controller alters the investigation goals. While it is noted that traction control is the least “safety oriented” of the stability controllers, it operates along the same principles and any performance benefit that can be derived from ANN controllers in this regard can be broadly applied to stability controllers in general. Furthermore, the construction of an improved traction controller will have a direct benefit to the racecar industry (in the fields where it is allowed), whereas ABS and other stability controllers generally would not. In addition, testing a traction controller is considered a safer proposition than ABS or the more advanced controllers. This is because when testing these other controllers the vehicle must travel at speed and then complete a difficult manoeuvre, which has inherent risks. Conversely, when testing a traction controller the vehicle must start at a

low speed and manoeuvre while it accelerates. In this case, if the vehicle goes out of control, backing off the throttle will most likely solve any problem.

Finally, it should be re-stressed that this research is not aimed at re-engineering an already successful product. When traction controllers are operated within their design conditions they generally produce large performance gains that are near optimal. Instead this research should be seen as proving an innovative approach for future products by first showing that the presented underlying principles work as well, or better, than existing products. With this in mind, massive traction controller performance gains are not expected in this work. Rather, the ability of the controller to exhibit features that will be of benefit in future products is the goal, and will be proven by providing ANN traction control that is comparable in performance to the current control methods.

Indeed, tuning the MoTeC ECU traction controller involves empirically determining the optimum slip for a particular condition and setting the controller appropriately. Since the goal of the ANN controller is to determine what this optimum slip is, no significant performance gains are expected because the two systems should operate at almost identical slip values. Provided the two systems operate in a similar manner, the major difference here will be the way data is collected, analyzed and evaluated. The MoTeC ECU controller requires numerous tests, significant data analysis and eventually qualitative decisions on the “optimum” arrangement. This is further made difficult by the fact that, at least in racecar situations, the “optimum” value varies from driver to driver, and is therefore difficult to quantitatively determine. Conversely, while the ANN controller will also require numerous tests for tuning, the data analysis and evaluation is done within the controller, and the decision on the optimum arrangement is made within the software. Furthermore, because the ANN model will be trained for a specific driver it is possible to incorporate driver style and preference automatically in the ANN decision-making process. These features should enable the ANN controller to make all required decisions on-line, and as such significantly simplify the tuning process and provide the opportunity for adaptable systems. Such a system, coupled with the other potential benefits of ANN control, would provide an exceptional tool in the construction of much more advanced stability controllers in the future, and would be a significant advancement.

8.2 ANN Traction Controller

With the decision to build an ANN traction controller comes the question of what performance aspect of the vehicle should be enhanced. ABS seeks to improve steering control during panic braking, while high-end stability controllers build on this by enhancing drivability and performance during critical steering manoeuvres. Both controllers are built on the premise that under emergency driving scenarios drivers are unlikely to be able control the vehicle as intended. ABS limits longitudinal braking performance for increased available lateral (steering) force if needed. Indeed, when braking in a straight line with tyres fully “locked” at speeds below 50km/hr stopping distance are generally longer with ABS, than without [34]. The principle of ABS is therefore not one of “optimising” acceleration, but rather one of providing adequate steering response without largely affecting braking performance. This in itself is a subjective criterion, as it is difficult to determine to what slip this compromise should be made, even on a constant surface. While it is true that optimising the longitudinal force component of the tyre (into the transition region) will provide more steering control than a fully locked wheel, this may still not provide enough force to change the trajectory of the vehicle as the driver demands. Nonetheless, in a panic braking situation the driver wants to stop the vehicle as quickly as possible AND be able to steer the vehicle as desired – which, according to the slip curves, are for the most part mutually exclusive. Other stability controllers must make the same compromises, although in the interests of yaw control and the like.

8.2.1 Performance Variables

Considering the above, however, the driver still has in mind the desired acceleration direction (longitudinal for braking and lateral for steering), and a view to the yaw rate at which this should be accomplished. Indeed, the entire process of driving a vehicle can be likened to the control of these three parameters, with all other factors determined by the orientation of the pavement. In panic braking, of instance, the driver would have a very clear idea of the direction of acceleration desired for the vehicle generally and simply would want to make this acceleration as large as possible. Ensuring yaw speed variation is predictable (and linear) is an important consideration to enhance drivability and avoid driver confusion. The stability controller’s function is to determine the driver’s desired acceleration direction and optimise the force transmitted at each tyre to accomplish this, while ensuring the vehicle handles in a predictable way. The

acceleration optimisation forms the physical necessity of the controller, while the yaw control ensures that the driver is as familiar with the vehicle control as possible. The latter point is extremely important because the driver must still play the role of the decision maker, and the controller should support them in this.

The problem thus arises of how to determine what the driver desires. This difficulty is compounded because during an emergency, as previously discussed, what the driver is doing and what they desire to be done can be very different. As a driver support tool alone, stability controllers can only enhance the performance of the vehicle as the driver commands it – so little can be done here. It is worthy of note, however, that as collision avoidance systems develop they may be integrated with stability controllers to control the vehicle in critical situations when the driver cannot. In this case desired stability controller performance can be directly gathered from the collision avoidance software.

Nonetheless, as a driver support tool, stability controllers need to understand what the driver wants from what the driver does. ABS treats the sudden depression of the brake pedal with great force not as a desire for maximum straight-line deceleration (as would be normally expected from such an act), but as a desire for very high deceleration with the possibility of steering control. This is an assumption, and is not always correct.

In this example, however, the driver's intent is made quite clear to the ABS controller over a period of time when the driver does or does not move the steering wheel from the straight ahead condition. After such a time the controller should determine that maximum braking is required and appropriately increase slip. Then, in the event that a sudden steering input is applied, slip should be lowered again to provide steering control. The ability of the system to do this is, of course, determined by the quality and control frequency of the hardware.

The same argument could be applied to determination of intended acceleration direction and yaw rate for any case. By assuming an initial conservative desired acceleration direction the system could monitor the driver's actions and determine if the predicted acceleration angle and yaw rate should be changed. In this way, if the driver increases the steering angle after control is initiated, it could be determined that more lateral acceleration is necessary and, with some evaluation, if the yaw rate should be altered. Nonetheless, the problem of determining desired acceleration direction and yaw rate,

although a significant issue, does seem solvable using traditional techniques for the most part. Using an intelligent tool, such as ANN, may form a helpful means to model the driver in this regard, but will not be discussed within this investigation.

8.2.2 Acceleration Optimisation

Assuming that the driver's desired acceleration direction and expected yaw rate can be empirically determined, the only significant problem remaining is that of finding what the maximum acceleration conditions are during critical manoeuvres. At a given vehicle condition, the theory suggests that each tyre will be able to produce a maximum amount of force in the desired direction, as a function of many different parameters. Optimising each of these parameters will therefore produce the maximum force for the tyre, and is the control goal of any stability controller. In an ordinary passenger vehicle, many of these parameters are either fixed (such as static camber) or uncontrollable (such as tyre temperature), and almost all stability controllers seek to control only tyre slip. As discussed in detail previously, slip is a major factor in tyre force transmission, and is relatively easy to control. Slip is the control variable of this investigation.

The general slip curve for longitudinal and lateral acceleration shows that, assuming all else is constant, longitudinal acceleration increases with increased slip to a point, while lateral acceleration generally decreases with increased slip. Increasing slip is therefore a trade off between longitudinal acceleration and lateral acceleration up to the transition region. Once slip passes this region into the unstable zone, total acceleration always decreases. Further, the general slip angle curves show that this is the case for all steering conditions.

Maximum longitudinal acceleration is therefore at the slip curve peak, while maximum lateral acceleration is at 0km/hr slip. One decreases while the other increases between these two extremes. This principle could also be reworded to state that the maximum force at a particular direction of for each tyre is unique and determined by slip, assuming all else is constant. The maximum acceleration of the vehicle will therefore be reached when these maximum force directions for each tyre are parallel to each other and the each tyre is at optimal slip. Likewise, by controlling the slip at each wheel, the maximum acceleration direction can be altered to lie parallel to the assumed driver's desired maximum acceleration direction. If none of the tyres have passed the optimum slip value for the desired acceleration direction, there is no need for control.

Of course, this rationale is limited to a degree when yaw stability is considered. If the front tyres combined produce more lateral force than the rear tyres the vehicle will oversteer. The idealised case of every tyre providing maximum force, assuming this is even achievable, is very unlikely to produce yaw stability because each tyre will produce an unequal force. Even so, the underlying principle still applies. If a single tyre passes its optimal slip value it should be controlled to produce maximum force in the necessary direction, the same can be said if any number of tyres require control. The only difference to the above case is that the yaw controller must also intervene to assure the controller response also produces drivability.

This intervention is mathematically possible using traditional controllers. By utilising feedback control, decisions can be made to ensure the intended yaw rate is followed. This could be incorporated into an intelligent controller, again such as one utilising ANN models. This, however, is beyond the scope of this research.

8.2.3 Longitudinal Slip Peak for Traction Control

Much of the discussion above applies to stability controllers in general. As stated, however, the problem in this investigation has been simplified to one of producing an ANN based traction controller. As such, much of the information presented above is relevant, but often only in a general sense. It has been provided to ensure the arguments used to construct the traction controller are also applicable to stability controllers in general.

In particular, traction control is generally not an “emergency” stability control. Unless the vehicle is very powerful and the driver responds to an imminent accident with excessive throttle, traction control will do little to help in such situations. It is true, however, that traction control can help avoid accidents and enhance vehicle performance. It does this by ensuring that the vehicle behaves predictably and optimally under acceleration. As such, the operation of a traction controller is generally not under emergency circumstances and appropriate and precise driver response can generally be expected to a point.

Such an observation simplifies the traction controller duties. Principally, the driver can be left in charge of maximising lateral acceleration. This is because lateral acceleration always decreases with increased slip, so if the vehicle is not following the intended path,

the driver can back off the throttle until enough lateral grip can be reached. In automotive racing this is termed “steering with the throttle”. In addition, by providing the driver with total lateral acceleration control they also have control over yaw rate.

This leaves only one parameter to optimise, that of tyre longitudinal acceleration. The controller, thus, has the sole goal of ensuring that optimal slip for each driven tyre longitudinal acceleration is not passed. In doing this, the controller also ensures that a reasonably high degree of lateral slip regulation is inherent within the controller, although it is not explicitly controlled.

This is the goal of traditional traction controllers, and has proved an effective method of control. The difference, therefore, between current traction controllers and the intended ANN controller is the method of determining what the optimal slip for each tyre should be. As stated previously, current traction controllers do not model a number of key vehicle dynamics parameters, and the assumptions this requires results in occasional erroneous control. Conversely, if the ANN controller can model the vehicle dynamics to a high level, it should be possible to determine the optimal slip of each tyre for all conditions the ANN has ‘seen’ before.

This is a difficult task, as the research is intending to replace the current rule based method of estimating optimal slip with an ANN model of the vehicle system which, in real time, provides the actual optimal slip of individual tyres for maximum longitudinal acceleration. To do this the ANN model must understand the vehicle condition/vehicle acceleration relationship to a high degree, and produce appropriate decisions as to where on the slip curve the current condition lies. Then, depending whether the measured slip is determined to be in the stable or unstable region, the traction controller can implement an appropriate control strategy.

8.2.4 Stable or Unstable Test

For the ANN model to operate in the intended manner, it must first be made clear what the “optimisation” dynamics entail, and how that can be defined. At a simple level, the ANN model is attempting to determine at which slip an individual tyre will produce its maximum longitudinal force at any given condition. Unfortunately, the vehicle system is not this simple, and a number of important observations must be made. Firstly, with the installed DAQ (and without great expense) it is not possible to measure the longitudinal

force produced by each tyre. These forces must be inferred from the overall vehicle acceleration, as measured by the AHRS. Secondly, because the vehicle is front wheel drive, the longitudinal axis of the driven wheels varies with respect to the vehicle axis. Thirdly, ground speed cannot be measured directly, so some variation in measured slip can be expected depending on the vehicle manoeuvres. It is noted, however, that the rear wheels free roll under acceleration, so zero slip measurements can be used to estimate ground speed in a repeatable manner (as is also done in passenger vehicles). Finally, the driven wheels are arranged with an “open” differential, which means that the torque applied to one wheel is always equal to the other and they will always impart equal longitudinal force to the pavement (excluding dynamic effects). In this way, if one tyre is only capable of producing a very low maximum longitudinal force, the other driven tyre will be limited to that force, regardless of the force it could otherwise produce.

Defining performance, and how it is to be controlled, is a complex issue. The traction controller presented here controls driven wheel torque via engine power control, so the open differential arrangement introduces additional limitations in getting ‘power to the ground’. This introduces only one control variable, so individual tyre control is not possible. In this way, the only driven tyre that can be ‘optimally’ controlled is the one capable of producing the lowest maximum force. With this in mind, it is possible to easily transform the control goal from improving individual tyre acceleration to improving overall vehicle acceleration. In this case, the vehicle acceleration (as measured by the AHRS) becomes the variable that should be maximised. As discussed above, this is one of the main variables the driver is trying to control, so this approach is ‘goal oriented’ and conceptually applicable to all stability controllers.

When one tyre makes the transition from the stable region to the unstable region, or back again, the vehicle dynamics undergoes a transition. In the stable region, more slip of any wheel produces more longitudinal component acceleration for the entire vehicle. Likewise, more slip of one tyre that is in the unstable region will produce less longitudinal component acceleration. In this way, the instability of a single tyre can be translated to instability of the vehicle generally. Any tyre operating in the unstable region denotes an overall reduction in performance of the vehicle.

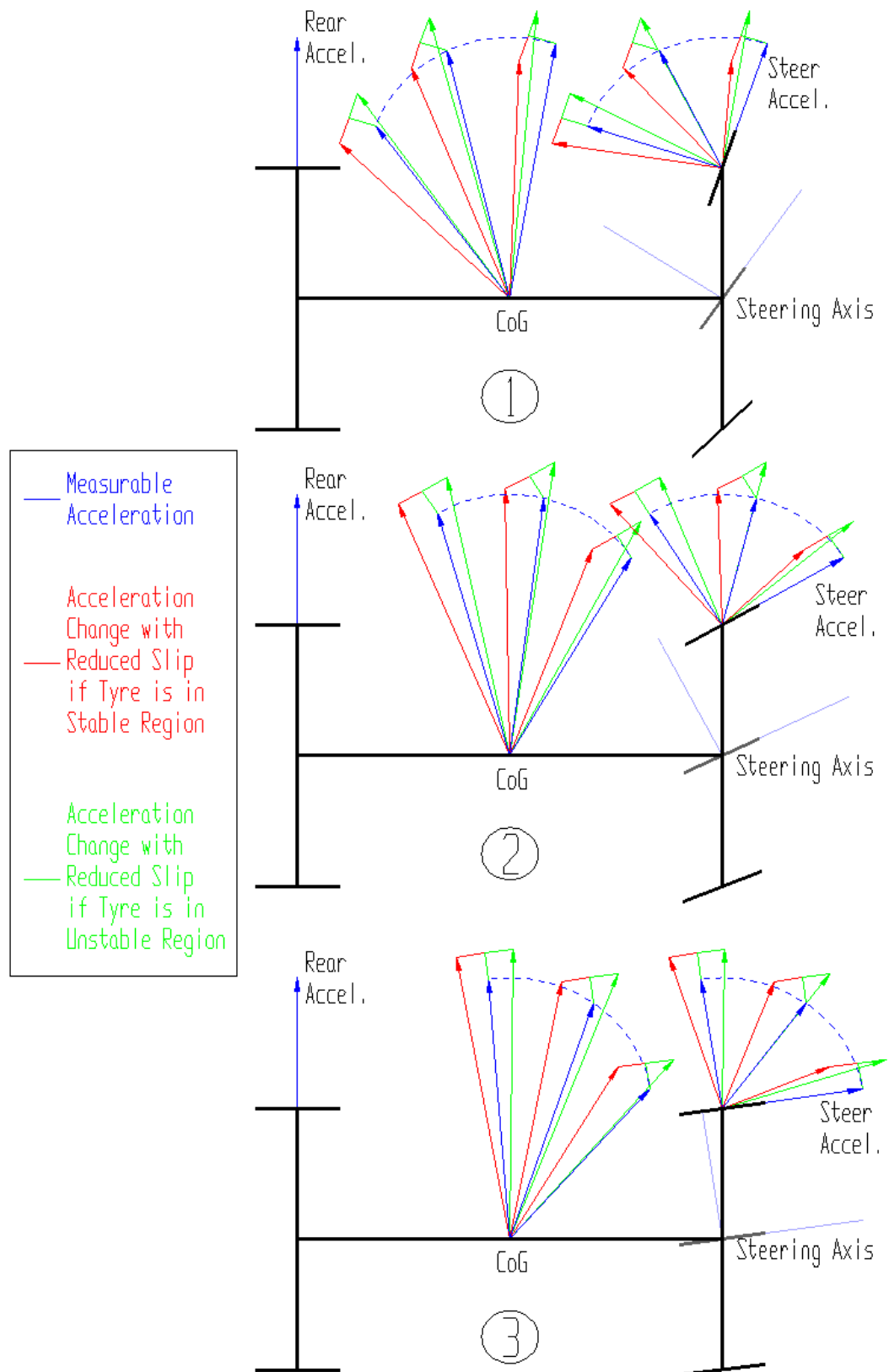


Figure 8.1: Effect of slip reduction to vehicle acceleration

This principle is depicted generally in Figure 8.1, which shows the effect on vehicle acceleration as the inside front tyre slip is reduced. These diagrams (1, 2 and 3) show identical vehicles with varying levels of steered wheel angle. In all diagrams a reduction

of slip always results in an increase of available lateral acceleration at the wheel, whatever the force direction on the tyre. Likewise, a reduction of slip will result in a reduction of wheel longitudinal force if the tyre is stable (red), or an increase in force if the tyre is unstable (green). Furthermore, this relationship exists for each of the vehicle tyres.

This acceleration change must be referenced to the AHRS to enable measurable results. The CoG (Centre of Gravity) referenced accelerations shows how this is done by considering the effect of acceleration change on one tyre at a time. The change in vehicle acceleration from a tyre's slip reduction is referenced to the vehicle by the angle of the tyre. This model neglects yaw acceleration, although it is noted that any increase in front tyre acceleration along the vehicle lateral axis will invariably increase yaw acceleration.

These diagrams now form an important clarification of the dynamics of vehicle stability from a slip point of view. The observations made above for individual tyres can now be transposed to the vehicle generally. Further, by replacing the X and Y coordinate system of the AHRS with a rotating coordinate system referenced to the angle of the tyre with respect to the vehicle, additional observations can be made.

If the tyre is stable, a driven wheel reduction in slip will:

- Decrease acceleration in the tyre longitudinal direction referenced to the vehicle.
- Increase acceleration in the tyre lateral direction referenced to the vehicle.

If the tyre is unstable, a driven wheel reduction in slip will:

- Increase acceleration in the tyre longitudinal direction referenced to the vehicle.
- Increase acceleration in the tyre lateral direction referenced to the vehicle.
- Increase the overall acceleration of the vehicle.
- Increase vehicle yaw acceleration.

Parameters such as yaw acceleration, overall acceleration and change of acceleration direction produced mixed messages on vehicle stability due to the direction of the forces involved. Yaw acceleration, for example, will always increase with reduced slip if the tyre is unstable, but may increase or decrease if the tyre is stable depending on the conditions.

These observations, finally, produce a very simple parameter for comparison. That is, if slip is reduced for a tyre, the acceleration measured by the AHRS in the plane of the wheel (longitudinal to the steering axis) will reduce if the tyre is stable and increase if the tyre is unstable. If the tyre is thus found to be in the unstable region, it should be controlled to reduce slip until stable, or optimally controlled to be at the peak of the slip/acceleration curve. The ANN model can thus be used to evaluate, if all else is constant, whether or not steering referenced AHRS longitudinal acceleration will increase or decrease with reduced slip.

8.3 ANN Control Models

ANN models are generally used in control to replace the linear control parameters normally used with parameters derived from a non-linear model. This often entails replacing a PID controller with an ANN controller, thereby the controller aim value is known and the ANN model is used to determine the best way to get the controlled value equal to the aim value. This is significantly different to the case presented in this research, where the ANN model is principally used to determine the controller aim value. This may be done as an input to an actual PID slip controller or, to incorporate full ANN control, by replacing the PID controller with an ANN controller. Both methods are explored in this research, with the control methods first tested on a simple control device.

8.3.1.1 Aalborg University Investigation

Within the first year of candidature the author traveled to Aalborg University, Denmark for 10 weeks to study ANN control. Aalborg University has a very strong control engineering focus, and this time was used to intensively study different methods of ANN control, including implementation on a simple control system. The university provided a number of their own ANN control references, a great deal of academic support and a single servo control apparatus for testing the theory and programming.

In this time a number of ANN control aspects were investigated specifically for the problem of servo position control, including Process Modeling, Inverse Modeling, Direct Inverse Control, Additive Inverse Control, ANN PID Parameter Estimation and ANN Observer Control. Much of this study was based on the PhD thesis conducted at Aalborg University by Dr Ole Sørensen titled “Neural Networks in Control Applications” [124], and the discussions in the sections below borrow heavily from this work. Nonetheless,

much of the conducted study was eventually deemed either not applicable to the problem of producing a ANN traction controller, or of low likelihood of success. As a result much of the work conducted at Aalborg University has been excluded here, and can be investigated further with the aid of the LabVIEW program that was compiled to test individual models that is provided in the Appendix software.

8.3.2 Inverse Control

One common ANN control method is referred to generally as “Inverse Modeling”. The ANN model is used to predict the required control based on the current system information and the aim system state. The ANN inverse model directly replaces traditional controllers such as PID, as in Figure 8.2.

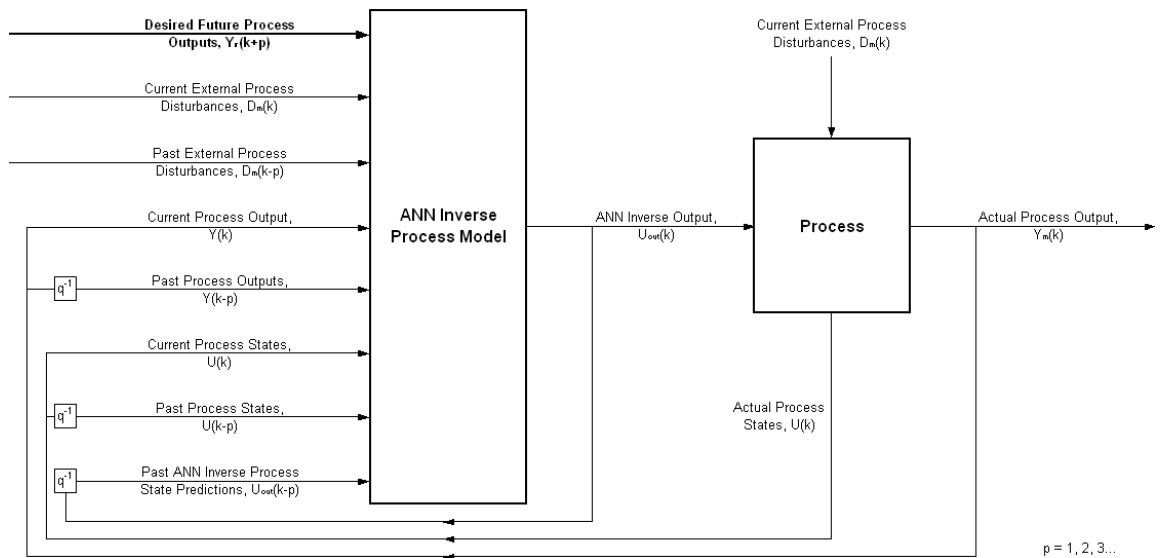


Figure 8.2: Direct inverse control architecture

The diagram shows a generic ANN inverse controller, where “k” indicates the current time step of the controller, “p” indicates additional time steps into the future or past and “q⁻¹” is the time step operator. The ANN inverse model can take as input controller aim values, process external disturbances, process state variables and previous model outputs. It can incorporate past values to determine the dynamics of the system and future controller aim values (where known) to ensure appropriate response. These inputs are similar to traditional controllers, such as PID, and the ANN inverse controller should be viewed in a similar way.

Differences obviously arise in the way the controllers are tuned. Traditional controllers rely on linearising the process and, in the case of PID control in selecting appropriate

proportional, integral and derivative terms based on programmer observation. These values can vary over time, and it is up to the programmer to observe the system, conduct empirical tests and produce tables or functions that define appropriate values. ANN inverse models, on the other hand, can model non-linear systems, are trained by observing the system and simply predict the required signal to control the process in the desired way. The ANN model is thus simply answering the question “if I want this result, what control signal should be used?” This is very different to PID programming, where the programmer must answer the same question.

This difference of replacing manual tuning with model-based solutions produces one obvious problem. The quality of control of the system using ANN inverse control is totally dependant on the quality of the ANN model, and if any divergent behaviour exists the controller may produce highly erroneous solutions. As a result the ANN model must be trained to be of a high quality for all possible operating conditions, and divergent behaviour eliminated.

With this in mind, there are two types of ANN training that are generally described by many researchers applying ANN for control. Each produce different results, and generally are recommended to be used in combination. The two methods are depicted in Figure 8.3, and are referred to as “General Training” and “Specialised Training”.

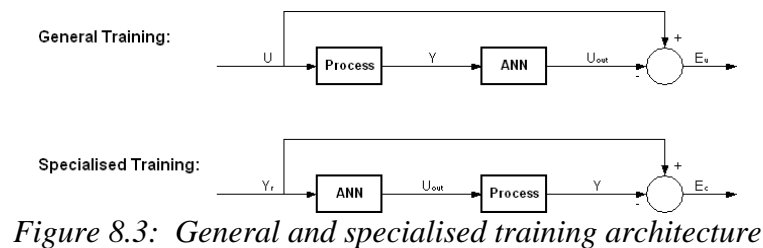


Figure 8.3: General and specialised training architecture

8.3.2.1 General Training

In general training a process input U is first used, and as a result the process control is independent of the ANN model. The process produces an output Y and, along with other relevant ANN inputs, is used to train the ANN model. The ANN model prediction is used to determine the prediction error, and the training process is repeated iteratively for additional U until the error E_u is within an acceptable range.

This method is the easier of the two to implement because the training can be completed using previously logged data, meaning training can be completed “off-line”. The error

term can also be directly used in the ANN training algorithm, making programming simpler. It does, however, have two significant limitations. The first is that the method is not “goal directed”, meaning that it may not be possible to ensure that the full range of Y will be trained into the ANN model by selecting different values of U . As a result, the function of the controller may be limited in extreme control cases. The other limitation is that an incorrect inverse can be obtained if the non-linear process mapping is not one-one. This is of particular concern because in many cases where ANN control may be required a one-one relationship cannot necessarily be determined.

8.3.2.2 Specialised Training

Specialised training, on the other hand, requires the ANN model to control the process and avoids these limitations. The desired process output Y_r , along with other relevant data, is first used as input to ANN inverse model. The resulting ANN prediction of the required control signal U_{out} is then input into the process, and the corresponding process output Y recorded. The training error E_c is determined, and training completed iteratively until E_c is within an acceptable range.

This training process is particularly appealing because the architecture allows ANN training in the full range Y and will produce appropriate inverse models even if the process mapping is not one-one. Unfortunately, however, this training process also has two significant drawbacks. The first is that, because the ANN is functioning as a controller while it is being trained, control of the system will be erratic until the ANN model is significantly trained. This has an associated problem in that different model and control architectures must be evaluated physically, and cannot be simulated. Secondly, the error term E_c has to be transformed into an equivalent error on the input side of the process in order to carry out ANN training. This can be done if the Jacobian of the process can be determined. This is a difficult process, and the suggested method is to obtain the Jacobian from calculating the Gain Matrix from the trained feedforward ANN model of the process. The method requires the process to be first modelled off-line with an additional ANN model, and the Gain Matrix Jacobian calculated for each ANN inverse model training iteration. This can be calculated using:

$$N = F'(X3) W3 F'(X2) W2 F'(X1) W1 \quad [124] \quad \text{Eqn 8.1}$$

Where: $F'(X_n)$ = Neuron function derivative at layer n

W_n = Neuron weights at layer n

In practice, however, this method could not be made to work and was not discussed in-depth in the available literature. The reason for this failure was that the $F'(X_n)$ and W_n matrices are of a shape that precludes multiplication. Instead, in an attempt to enable investigation into specialised training, the author developed a more intuitive approach to determining the Gain Matrix. This consisted of using the ANN process model and testing the effect on the model output by very small changes in each model input individually. The linearised transformation of each input could be determined and used to estimate the conversion of E_c (derived from Y) to E_u (derived from U). E_u could then be used to train the ANN inverse model.

In practice, this aspect of specialised training, which requires the calculation of the Gain Matrix to convert E_c to E_u , produces a significant problem. The requirement of training an additional ANN model of the process to be controlled, is an addition that is philosophically hard to accept. ANN models inherently contain a degree of error, and using two models should clearly have a detrimental effect. At the very least, such a method would introduce a degree of noise into the error term used to train the ANN inverse model. Further, the presented mathematics required to directly calculate the Gain Matrix are either flawed or poorly described and understood. Finally, the author's own method is very computationally intensive and may reduce sampling and control timing to an undesirably low rate depending on the size of the ANN model and speed of the control hardware.

8.3.3 Observer Control

The control methods described here as “Observer Control” falls in the broad category of “Optimal Control” and essentially aims at supplementing the functionality of a traditional controller with data derived from a model that observes what the process is doing. The observer, therefore, is generally a model of an aspect of the controlled process and can be used to derive additional information for the controller, in Figure 8.4.

The observer (in this case an ANN model) is used to determine a state variable $X_{out}(k)$ of the process, which is used as input to the process controller. The controller uses this value to determine the process control signal $U(k)$ and in turn controls the process. This

has particular benefit because it allows extra information to be feed to the process controller that may otherwise not be possible to measure. Further, the observer can be used to determine optimal control parameters as determined by the programmer. For example, in the case of the optimal control implemented in [124], the observer is used to “punish” increments of the control signal to reduce control activity.

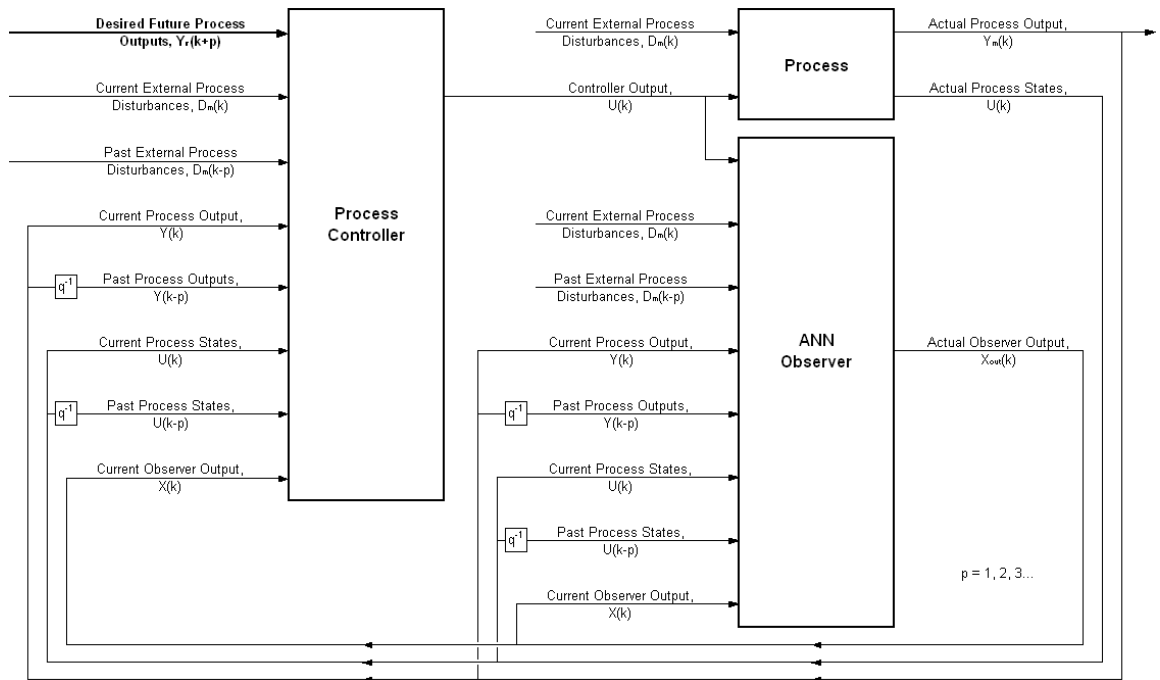


Figure 8.4: Normal process controller with ANN observer architecture

In the case of this investigation, the observer control architecture has particular promise for a number of reasons. Firstly, unlike inverse control, the process controller is separate from the ANN observer model. This provides the ability to focus the ANN model on the determination of relevant vehicle dynamics, and to use a traditional controller to control the process based on the observer findings. Secondly, the ANN observer can be trained off-line, which avoids all the problems of specialised inverse training without many of the drawbacks of general training. Finally, the ANN observer model is extremely flexible, and can be used in a wide variety of ways.

Of particular benefit for this investigation, the observer can be used to determine gain values of the process parameters at discrete operating conditions.

8.3.3.1 Gain Method

The procedure of determining the gain of process parameters was briefly introduced previously for inverse modeling. The goal of this procedure was to determine the

instantaneous amount that a change in a process input would affect a change in the desired process output. The gradient of this relationship is referred to as the input gain, and is the amount that the input must be multiplied by to produce the desired output.

This has the particular benefit in modeling vehicle dynamics because it enables the highly non-linear process to be broken into instantaneous linear relationships. By modeling vehicle dynamics process with ANN models and incorporating this method, it becomes possible to determine the short-term effects of altering any process input parameters. It is then possible to conduct hypothetical tests on the process by answering the question “if I alter this process input value individually, or in combination, what will the affect be on the process output?”

The ability to answer this question whenever it is posed is a very valuable tool. Further, the problem of determining vehicle stability, discussed above, can also be stated in a similar way; “if I reduce wheel slip, will the steering referenced longitudinal acceleration of the vehicle increase or decrease?”

Such a method can thus be used to answer this question. This can be accomplished by, for example, training the ANN observer to predict steering referenced longitudinal acceleration based on driven wheel slip and other state variables. The ANN observer can then be used to predict the current expected acceleration, and twice again for marginally reduced slip at each driven wheel. This entails significantly less computation than the method described for inverse model specialised training. If the acceleration decreases, the vehicle can be considered stable, with a “no control” signal sent to the process controller. Conversely, if the acceleration increases, a “control required” signal can be sent to the controller, as the vehicle can be considered unstable. In the later case the slip/acceleration gain could be supplied to facilitate determination of the control aim slip.

This method essentially can be considered to provide two pieces of information to the process controller, if the vehicle can be considered stable or unstable, and what the instantaneous slope of the slip/acceleration curve is. This is very important information for the controller and, if the model operates as expected, improved performance can be expected. There is a difficulty in this form of control, however, in that the observer does not explicitly define the aim slip. Instead the process control is expected to determine this value based on supplied data. This is a problem without a definite answer, and the

process controller must estimate the aim slip and then implement appropriate control. This requires additional control assumptions and controller tuning, which will be discussed later.

8.3.3.2 Curve Method

A way to avoid this problem was developed using a “curve” technique, which further expands the process of determining process gains. It was hypothesized that by varying a single ANN observer input through its entire range, an estimate of the effect on the process output could be observed. This estimate would be based on the “if all else is constant” principle, and would clearly lose a degree of accuracy when the current condition differed to a large extent from the test condition. Nonetheless, such a test would produce a non-linear estimate of how much changing an input parameter by any extent will affect the process output.

Applying this principle to the slip/acceleration example above would, thus, produce slip/acceleration curves for each driven wheel. As the theory suggests, the slip at the transition region of each graph (corresponding to maximum acceleration) can be used as an estimate of optimum slip. Such a method would provide all of the information to the process controller the gain method provides, as well as an ANN determination of aim slip. If such a method was found to work appropriately it would vastly increase the response of the controller as it would reduce the reliance on “close-loop” controller decisions which can take a long time to converge. It would also promote the controller’s ability to cope with process state changes that may make the aim slip vary to a large degree. It is noted, however, that the method used to produce a curve of the response of process outputs to any process input will require the ANN observer model to run consecutively a number of times (depending on the desired accuracy). This level of computation may slow the controller sample rate to unacceptable levels, or require hardware upgrades.

Many aspects of the investigation of each of these methods can be completed off-line, whereby performance predictions can be compared to actual values. However, it is noted that some of these methods require greater process feedback than others, and as such this would form an unfair comparison. Furthermore, one of the principle goals of this investigation is to actually implement ANN traction control, which requires real-time data acquisition and control at suitably high sample rates. Many aspects of the hardware

that was used have been presented in previous sections, but the investigation specific software that will enable ANN control and analysis is yet to be discussed.

8.4 Data Acquisition and Control Software

The software that was developed for this research had to perform a range of specific roles. Firstly, it had to interface with the range of input sensors to acquire data in a suitable way. This data also had to be capable of being logged, with other programs utilised to perform off-line ANN training and performance analysis as needed. Acquired data was utilised in a number of different controllers, which had to be programmed. Finally, the controller outputs had to be actuated via changes to the DAQ output voltage. Furthermore, “housekeeping” functions also had to be performed such as providing checks and warnings if the programs were not working correctly, and ensuring controller outputs remained in safe bounds.

Most of these functions were integrated into a comprehensive “Intelligent Traction Controller and Data Logger” LabVIEW program (referred to as the DAQ controller), as summarised in Figure 8.5.

LabVIEW VI: Intelligent Traction Controller and Data Logger.vi

Note: Most of program is within the While Loop, which updates the measured data from each device as fast as possible (to ensure most current data is used).
Note: Case Structure is used within the While Loop to activate control and data logging at the requested sample rate.

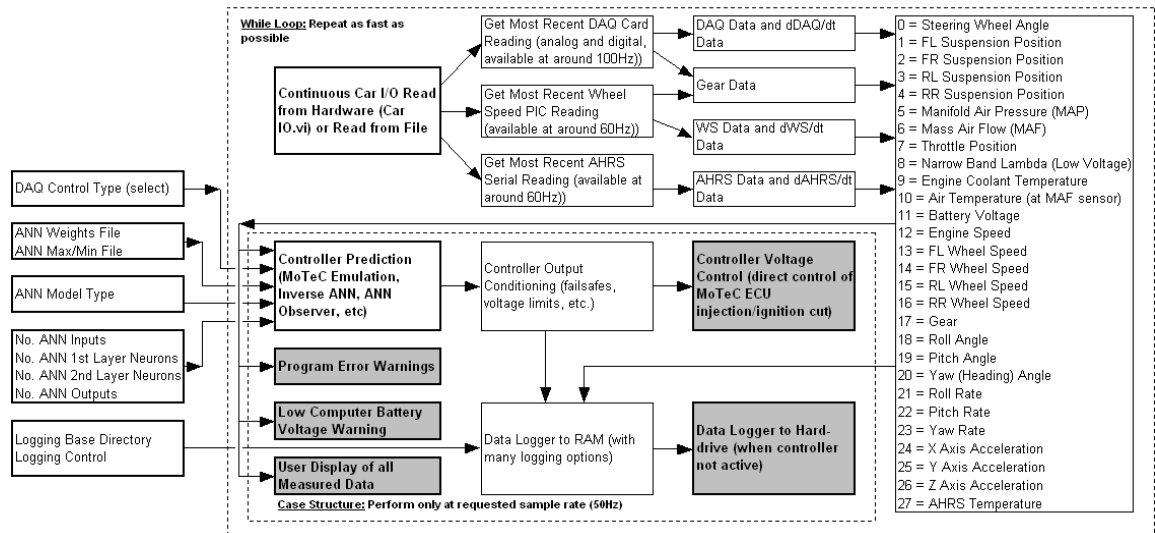


Figure 8.5: “Intelligent Traction Controller and Data Logger.vi” basic functions

Here, it can be seen that the program firstly acquires data from the sensor array, or from file. This ability to utilise pre-measured data from file provides extra program flexibility to evaluate different controller types off-line, and also provides a useful program

debugging tool. Otherwise, however, the principle role of this part of the program is to acquire information from each of the sensors as fast as possible. In the case of the serial inputs, this comprises of acquiring new data as each packet arrives (at around 60Hz for both serial devices). In the case of the DAQ digital and analogue signals from the DAQ, this process involves updating each signal for each while loop iteration. Since the while loop typically iterates at higher rates than 60Hz, this means that the DAQ signals are updated faster than either of the AHRS or wheel speed serial signals, and that the two serial devices are not synchronized (i.e. they do not update at the same rate or at the same time). As such, the data arrives at this point in the program as the “most recent” measurement of each sensor for each while loop iteration. In this fashion, the program utilises the “dead-time” between control iterations (chosen here as 50Hz) to acquire data to be made available when needed. This method is in contrast to the other possibility of trying to acquire all of the data at exactly the same time (synchronized), which would have been significantly more troublesome and provide much slower acquisition.

The process of obtaining a number of serial, digital and analogue signals and integrating them together is a significant problem, nonetheless, and investigation of the “Car IO.vi” subVI shows much complexity. For instance, the serial devices cannot transmit data to the computer without receiving sensor control data first. To ensure error free serial communication these two sensors must first be “initialised”, and the AHRS must receive a signal to ensure it operates in the desired “scaled angle” mode. Transmitted data must be continuously read to identify “packets” of data, and these packets must be converted into signals that can be used within the rest of the program. The DAQ digital and analogue inputs must be initialised, and read in the correct fashion. In the case of the digital measurements, this includes a test to see if the current buffer has already been read, and obtaining the most current measurement values as required. The analogue signals are acquired using a similar process, although the readings are filtered in an attempt to reduce noise by averaging the samples that were obtained since the last “read” command (and are contained in the buffer). All of these functions are contained within the “Car IO.vi”, and provide the complex but simple to use data acquisition required for this research.

As data is acquired, for each while loop iteration, the next stage of the program is to condition the raw signals and provide 1st derivatives of the data. The derivatives are calculated by observing the change in the current data measurement from the previous

one, and dividing this by the time between measurements. The current gear is calculated at this stage by comparing engine speed to average front wheel speeds and applying the known gear ratios. This data is compiled into an array, as shown in the diagram. The values and the differentials for each of the 28 parameters are assembled into the array, forming a total of 56 inputs.

The input data array, like the raw measured values, is updated for each while loop iteration and provides the most recent measurement/calculation of the input parameters. There is no timing control in this loop, however, as the function of acquiring data requires the fastest update rate available. As such, it would not be appropriate to embed the controllers into this loop. This is because a fair comparison of each of the controllers can only be made if they operate at the same sampling rate, which must be constant. As an example of this concept, consider a PID controller that is well tuned for a current testing condition (such as the MoTeC traction control), and a complex ANN model that is tuned generally. PID control requires significantly less computation here than many ANN controllers, and as such is capable of much higher sampling rates. Since higher sampling rates within feedback control can significantly improve control accuracy, this would not provide a fair comparison. This is particularly the case when it is observed that an ANN model utilised in purpose built parallel processing unit (unlike the serial processing of a computer, as is the case here) may be faster than a PID controller.

To this end, a case structure is embedded into the while loop to perform all of the program functions. The case structure is designed to activate every 0.02 seconds (50Hz), and then utilises the 56 values of the input array. In this way, correct timing is assured and the most recent sensor measurements are used for all functions within the case structure.

Data logging, for instance is housed within this structure, and observes all of the measured and differentiated values, as well as the controller output signal and other controller performance values. Furthermore, while in use, this controller logs to RAM only to avoid excessive slowing of the program during hard drive accessing. When the controller is inactive, or when high sampling rates are not necessary, the information in the RAM is dumped to the hard drive as a new file, thereby avoiding this problem. In addition, the data logging component of this program is capable of many different

logging functions, such as logging only when certain trigger values are met and recording pre-trigger events.

Warning systems are used within the case structure to highlight potential and existing problems as they occur. This essentially includes two types of warning, the first being that if the computer battery voltage goes below a critical value, the user will be notified of an imminent system crash and advised to turn the computer off. The second type of warning concerns failure of sensors. Here, the sensor signals are monitored, and if a value is found to be static when it should not be, the user is warned. In practice this was found to be particularly useful with regard to the AHRS serial communications, which would occasionally produce an error that required the sensor to be reset. Similar problems were found with the engine speed digital sensor, and in these rare cases the testing would be halted while the system was reset and returned to normal.

A user display of all of the measured parameters is included in the program, in which the LabVIEW graphical display of dials and gauges is utilised to show the user all of the information concerning the measured vehicle dynamics. This was included as a presentation tool, to enable visual evaluation of sensor performance and required program debugging. It is also included within the program as a separate SubVi that must be opened for viewing, thereby avoiding the processing requirements for the graphics when they are not needed.

The final function of the program is to complete the various types of traction control for investigation. This functionality is embedded within the aforementioned case structure to ensure consistent control timing and useful data logging. Each of the control functions are placed in an additional case structure, so that the desired control model can be simply chosen by the user within the one program. Each model has the ability to individually accept the vehicle sensor data, to then process the control result, and then provide any information pertaining to this result to the data logger. Models that require ANN information (such as weights, normalisation data and number of hidden neurons) are supplied this data from pre-selected files and user inputs.

Of significant benefit from utilising this type of arrangement is that process controllers of any sort can be easily placed within the control program, and are independent of other systems that may have been previously utilised. As such, many control models can be

attempted with little programming complexity. It would be a tedious process to discuss them all here, however, and instead they will be summarised and their control philosophy discussed as needed in the following sections.

The final function of the program is, thus, to implement the control signal that the selected controller has evaluated. This has two stages, where the first is to ensure that the generic control limitations are maintained (such as ensuring that the output voltage does not exceed the hardware limitations of -5 to 5 volts). The second is then to implement the desired control voltage at the DAQ hardware analogue output. This in turn operates one of the MoTeC ECU input pins, which has the function of “slip voltage” as discussed in a previous section. Here, an output signal of $0V$ corresponds to no engine cut and $5V$ to maximum allowable engine cut, with a linear scale between these two values. Furthermore, since it is possible for some noise to exist within this signal wire due to the electrical interference that is inherent within normal vehicles, it was observed that this might produce long running low levels of engine cut. This is clearly undesirable, and the program was also modified to whenever a “ $0V$ ” signal was sent by the selected controller, a $-0.5V$ signal would actually be sent by the DAQ output to offset any noise. If the signal was greater than $0V$, however, that same 0 - $5V$ sliding scale would still be used.

The “Intelligent Traction Controller and Data Logger” program is capable of a range of functions, which are all highly applicable for research conducted on the test track and in simulation. Furthermore, the “Car IO.vi” program is generic to the DAQ and serial communications used in the vehicle, and can be easily modified to accept other sensors or acquire data at different rates and quality. In particular, there are many other types of serial communications with potential within the car that could be connected to the PC for use in future research, such as ADL, GPS, GSM and telemetry communications. The “Car IO.vi” program will simplify this installation process.

8.4.1 ANN Training Programs

Although the “Intelligent Traction Controller and Data Logger” program is a flexible data logger and control program, it is not capable of training the ANN programs (but it is noted that future research may look at altering the program for real-time ANN training for adaptive control). As all ANN training for this research will be completed off-line, the program does not require this functionality. Instead, the “ANN Training from File”

program presented previously, is used with no modification for ANN training, and simply requires properly formatted files containing model input and output data. As well as highlighting the generic qualities of the development of this program, this simplifies the effort required to train ANN models for this investigation.

The main practical problem in ANN training and testing, is obtaining the required data files, and ensuring they contain only the data required for particular models. Different models require different inputs and outputs, and so require different formatting. Furthermore, some models may want to include aggressive driving data only, to ensure accuracy in critical manoeuvres. This means that files must be formatted to correct input/output combinations and relevant data acquisition cases. This is clearly outside the scope of manual data manipulation, especially when considering the number of files the “Intelligent Traction Controller and Data Logger” is capable of producing and the Excel and memory limitations in dealing with large amounts of data. As such, a number of programs were produced to manipulate the logging files to create ANN training and testing files automatically. While this required a significant amount of programming complexity, this will not be presented here. This is because the function of these programs are very easy to conceptualise, and are basically to move and exclude data to correctly format ANN files within the scope of training.

A number of other programs, which will not be discussed in detail either, were also developed to perform specialised data analysis. These essentially were used to manipulate existing data to highlight various performance features, where manual data manipulation was not practical. For example, one program produced slip/acceleration curves of measured data at different speeds by simply braking the data into slip and acceleration “bins” and averaging the result. This program essentially answers the question “at this speed and this slip, what acceleration is the vehicle likely to experience based on statistical histories, and assuming no other variables affect the result?” The information that this produced, while subjective, was valuable for the simple and repeated tests used in much of this investigation, and provided a very useful performance analysis tool.

Another program was designed to look at repeated straight-line acceleration tests, and to determine which run produced the greatest acceleration, and which aspects of each run produced the best performance. In this way, empirical evidence could be developed on

what the optimal performance parameters were and, by combining elements of each run that produced the best performance, the performance limit of the vehicle. A similar program was developed for tests that saw the vehicle completing constant radius circles at different speeds.

8.5 Test Track Selection

The straight line and circular tests form some of the experimentation carried out for the research, which will be discussed further here. Of particular importance is that, unlike the surface identification investigation detailed earlier, the testing required in this research cannot be legally completed on the open road. This is because, by its nature, traction control testing required the driven wheels to be spun excessively and for severe manoeuvres to be completed. Furthermore, to conduct a thorough performance investigation, many similar manoeuvres had to be completed with as little surface variation as possible. Lastly, testing on dry roads entailed very fast wear on tyres and the vehicle, and as such most of the testing was better performed on a wet road. This could not be completed on the street, as relying on rainfall was difficult.

To these ends, most of the testing for the Intelligent Traction Controller was performed at the Hobart Police Academy skidpan, as pictured in Figure 8.6.



Figure 8.6: Police Academy testing grounds

This skidpan is constructed of cement, has an oval perimeter and forms a bowl shape. It is irrigated by a number of water outlets around its perimeter, with a drain in the centre

of the pan to avoid pooling. Vegetable oil is regularly applied to the surface to further reduce its coefficient of friction. In normal use, the skidpan is used for police and public driver training for limit driving, and the low friction surface allows this to happen at low speeds with a high degree of safety. As such, it was considered ideal for the bulk of these tests.

Close observation of the photos, however, shows that the track was not uniformly wet. In particular, there were large areas that remained dry due to movement of the cement slabs as the track has aged. These areas, nonetheless, form only a small part of the useable area, and by careful selection of test areas it was possible to avoid them entirely, and to focus on the uniform areas. These areas also formed the most used sections of the track and were almost level, meaning that the distribution of the vegetable oil and tyre rubber could be assumed almost constant. Furthermore, areas that were found to have high variations in friction coefficient were identified at an early stage and removed from any test manoeuvres. In a very similar method to the test track selection used in previous “Intelligent Car” investigation [40], three test tracks were chosen, and are shown in Figure 8.7.

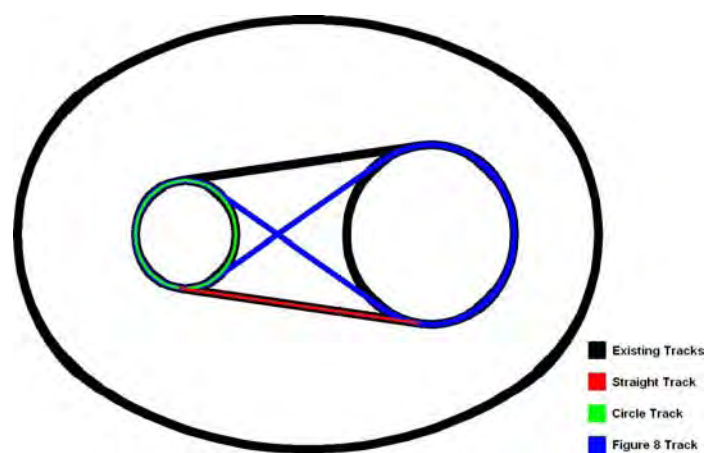


Figure 8.7: Police Academy testing tracks

The existing driver training track was used to construct three research tracks, and that the perimeter of the skidpan was avoided because of irregularities of water coverage. The existing track basically consisted of two circles of different diameters connected by straight sections, and appeared to be the area of highest traffic. However, there was a patch of the course that has a glazed appearance that had no practical grip, and the test track selection was made to avoid this. As such, three test tracks exist, with a fourth categorised as “miscellaneous” where random paths were chosen within these tracks.

The three tracks include the straight-line, the constant circle and the figure eight. The first two were chosen to provide simplified performance tests that could be compared, and performance differences directly evaluated. The third and fourth tracks provide an approximation of “normal” conditions, where the chassis controllers had to be robust enough to handle a range of conditions. As such, these four tracks provided sufficient data to compare specific performance features in simplified cases and to also gain more general observations of performance in real driving conditions.

Nonetheless, it is noted that attempting to utilise this controller on just one surface would limit the scope of this research to a degree. It has been argued previously that the generic nature of ANN controllers is one of their principle benefits, and as such it would be a suitable test to attempt to use the developed controllers on another surface. In particular, even though surface identification does not form one of the goals of these ANN controllers, they should be easily re-trained or augmented to operate well on any given surface.

This presented a problem, however, because there are no other suitable private test tracks in the area that would provide this level of investigation in unstable conditions. Instead it was noted that on unsealed surfaces quite high slips are common in normal driving. Furthermore, these high slips do not correspond to a loss of control of the vehicle, as might be the case on other surfaces. In this fashion, the vehicle can be driven at low speeds on unsealed public roads to safely and legally gain relatively high slip measurements. While it is noted that this removes some of the scope for investigation because the full slip range cannot be investigated, it should be sufficient to prove in principle that ANN models can be used generically on a number of surfaces. This would add further strength to any argument in future work for adaptive ANN control.

To this end, the unsealed Fern Tree test track was selected for ANN traction control testing, as described earlier. In particular, the uphill section of the track, which was about 1km long, offers additional benefits because high slips can be safely realised with little change in vehicle speed. This not only enhanced the range of possible slips to be observed, but meant that the vehicle did not have to be constantly slowed to a safe testing speed.

Once these tracks were selected, testing preceded over a wide period of time. In particular, testing at the Police Academy was first used to ensure the “Intelligent Traction Controller and Data Logger” operated reliably, and to obtain data for off-line analysis of the traction control programs that were developed. Subsequent testing was used to compile comprehensive data for MoTeC traction control tuning and ANN training, and to monitor the performance of specific controllers. Once the best ANN controller was chosen, the test was completed on the unsealed track. The testing goals and types of testing for each day are covered in more detail below. The full results of these test is covered in the Appendix.

8.5.1.1 First Day – Police Academy (Wet)

Preceding work had been carried out before this testing was started to ensure “Intelligent Traction Controller and Data Logger” debugging, and that the test track was suitable for this investigation. Nonetheless, the first day of testing comprised of work to determine the possible test tracks to be used, and to ensure all problems with the control software were identified and addressed. This comprised of completing a number of short tests to ensure that data was recorded properly, that appropriate test tracks were selected for reliable results and minimal variation in coefficient of friction, that the vehicle behaved in a safe manner and to log data for later off-line development of ANN control models and program improvements. Particular software errors that were highlighted at this stage included occasional computer crashes under high acceleration and vibration, and sporadic variations in sampling speed.

8.5.1.2 Second Day – Police Academy (Wet)

A significant amount of ANN controller and program development was completed preceding this day of testing to overcome the observed problems and to facilitate controller evaluation. As such, one of the main goals of this testing was to provide closed-loop evaluation of the large number of ANN controllers that had been developed and trained using previous data.

Empirical testing was conducted to tune the traction control function of the MoTeC ECU for maximum performance on the wet surface, and also to tune a controller within the “Intelligent Traction Controller and Data Logger” that emulates the MoTeC control. Additional data for as many driving conditions as possible was also logged to provide all of the off-line ANN training data for later model.

8.5.1.3 Third Day – Police Academy (Wet)

The results from the second day of testing were evaluated before this testing occurred, and a specific ANN controller was selected. As such, the day of testing focused on evaluating this model and attempting to make program alterations to improve its performance. As such, some tuning was conducted at an early stage in the day, with the remainder devoted to gaining enough data to evaluate the performance of the controller in a range of conditions. Nonetheless, this proved a time consuming task, and sufficient data was only acquired for straight-line tests.

8.5.1.4 Fourth Day – Police Academy (Wet)

The testing was continued through to the fourth day, with more straight-line, circle, figure of eight and miscellaneous data acquired for ANN performance analysis. It was observed, however, that more data needed to be acquired for the performance on the traditional (MoTeC) traction control, so much of these tests were repeated using this type of controller. Furthermore, some additional data was acquired for driving the vehicle with no traction control to enable a greater degree of comparison. This represented the last day of testing and evaluating the various traction controllers in the wet.

8.5.1.5 Fifth Day – Police Academy (Dry)

To provide some surface variation in the results, as discussed above, it was first hypothesized that using the same test track in the dry would be sufficient. This had the added benefit that the only variation would be how damp the surface was, and provide good capability to directly compare results. However, in practice this proved to be more problematic than envisaged. In particular, two problems were observed. The first was that the forces involved were very harsh on the vehicle, and prolonged testing would cause significant damage due to massive vibrations. The second was that the tyres were simply not capable of any sustained high slip. Within a couple of minutes of testing, the tyres became far too worn to make any subsequent testing valid, and any more would make the vehicle unroadworthy. As it was, one tyre had to be replaced because it became worn to its carcass, as shown in Figure 8.8.



Figure 8.8: Tyre wear on dry surface

This meant that testing had to be abandoned until new tyres could be obtained, and the decision was made to avoid any other attempt to obtain control data on dry pavements.

8.5.1.6 Sixth Day – Fern Tree (Dry Unsealed)

Due to this outcome, and as discussed above, it was decided to attempt to test the robustness of the model on the unsealed surface at Fern Tree. Here, the vehicle was driven along the road once to obtain ANN training data, the ANN model was then trained on the side of the road for 25 minutes and the newly tuned controller utilised on the unsealed road. This was a relatively quick test, with the aim of emulating the process that may happen if ANN control of this nature was implemented in a racecar application. It also marked the conclusion of closed-loop testing of the ANN controller within this investigation.

8.6 Non-ANN Controller Performance

The testing data that was gathered on the second day was obtained with a view to provide results for non-ANN controllers, which could be used for ANN performance comparisons. Furthermore, the data gathered during traditional traction control operation could be utilised for ANN training in some cases. This data was built on with data acquired during the fourth day.

Two types of non-ANN control are utilised for comparison in this investigation. The first utilised the inbuilt MoTeC ECU traction controller, which was tuned to produce the best possible performance. The second method, however, attempted to emulate the MoTeC traction controller within the ANN control software to allow direct comparison between traditional and ANN control performances.

8.6.1 MoTeC ECU Traction Control (METC)

The MoTeC ECU traction controller provides an important comparison tool, and determines engine cut based on the four measured wheel speeds and any relevant engine data within the ECU. Its operational algorithm is not explicitly stated within its documentation, nor were MoTeC support willing to divulge this “commercial in confidence” material. However, and as discussed previously, the control algorithm seems to be based on a linear relationship between the amount of slip above a predetermined level to the percentage of engine cut, with a few other parameters used to provide additional “trims”. For any given track, this means that many parameters need

to be tuned repetitively for efficient operation. This is in contrast to controllers used in typical passenger vehicles because it is not generally robust across different surface conditions, but rather is tuned for maximum performance in specific conditions. In this regard, and if the MoTeC traction controller can be tuned to a high level, the MoTeC traction control can be considered to provide better performance than passenger vehicle controllers. Furthermore, because the controller can be tuned for specific conditions, it is not unreasonable to assume that it would provide near-optimal performance.

Finally, because all of the control logic and sensor inputs are housed within a purpose built and highly refined unit, the sample rate for control can be expected to be much higher than the 50Hz used for the ANN models (although this actual rate is not clear). This would increase the performance of the MoTeC traction controller further and, since all other models are limited to 50Hz, would not provide a fair performance comparison. Nonetheless, the results of MoTeC traction control tuning provide useful information with regards to optimum traction conditions and maximum achievable accelerations, and are shown in Table 8.1 (cumulative slips are calculated from the average of preceding slips), Figure 8.9 and Figure 8.10.

Aim Slip (km/hr)	Aim Slip (m/s)	MoTeC Slip Control Range (km/h)	Controller Gain (for equivalent cut voltage - V/s/m)	Speed at 25m (m/s)	Average Accel. 0m to 25m (m/s/s)	Average Slip 0m to 25m (m/s)	Average Slip 0m to 25m (km/hr)	Cumulative Average Slip 0m to 25m (m/s)	Cumulative Average Slip 0m to 25m (km/hr)	Average Slip 5m to 25m (m/s)	Average Slip 5m to 25m (km/hr)	Cumulative Average Slip 5m to 25m (m/s)	Cumulative Average Slip 5m to 25m (km/hr)
3	0.83	5	3.60	13.03	3.03	1.90	6.84	1.90	6.84	0.65	2.34	0.65	2.34
10	2.78	5	3.60	12.97	2.70	1.88	6.77	1.89	6.80	1.93	6.95	1.29	4.64
10	2.78	5	3.60	12.90	3.27	2.12	7.63	1.97	7.08	1.91	6.88	1.50	5.39
5	1.39	5	3.60	12.86	3.03	1.10	3.96	1.75	6.30	1.02	3.67	1.38	4.96
5	1.39	5	3.60	12.84	3.21	1.69	6.08	1.74	6.26	1.05	3.78	1.31	4.72
3	0.83	5	3.60	12.84	3.24	1.47	5.29	1.69	6.10	0.98	3.53	1.26	4.52
10	2.78	5	3.60	12.83	4.04	1.84	6.62	1.71	6.17	2.46	8.86	1.43	5.14
5	1.39	5	3.60	12.83	3.43	2.04	7.34	1.76	6.32	0.84	3.02	1.36	4.88
0.5	0.14	5	3.60	12.83	3.08	1.02	3.67	1.67	6.02	0.48	1.73	1.26	4.53
5	1.39	5	3.60	12.82	3.26	1.19	4.28	1.63	5.85	0.46	1.66	1.18	4.24
0.5	0.14	5	3.60	12.79	2.85	0.66	2.38	1.54	5.53	0.60	2.16	1.13	4.05
3	0.83	5	3.60	12.75	3.11	1.00	3.60	1.49	5.37	0.64	2.30	1.09	3.91
5	1.39	5	3.60	12.73	3.31	2.38	8.57	1.56	5.62	1.57	5.65	1.12	4.04
0.5	0.14	5	3.60	12.69	2.85	0.58	2.09	1.49	5.37	0.46	1.66	1.08	3.87
3	0.83	5	3.60	12.66	2.80	1.90	6.84	1.52	5.46	1.60	5.76	1.11	4.00
10	2.78	5	3.60	12.65	2.87	2.78	10.01	1.60	5.75	2.87	10.33	1.22	4.39
10	2.78	5	3.60	12.57	2.09	3.11	11.20	1.69	6.07	2.27	8.17	1.28	4.61
1	0.28	5	3.60	12.49	-	0.76	2.74	1.63	5.88	0.47	1.69	1.24	4.45
20	5.56	5	3.60	12.46	2.70	3.43	12.35	1.73	6.22	3.10	11.16	1.33	4.81
20	5.56	5	3.60	12.41	3.40	2.79	10.04	1.78	6.42	3.48	12.53	1.44	5.19
3	0.83	5	3.60	12.39	2.73	2.03	7.31	1.79	6.46	1.10	3.96	1.43	5.13
20	5.56	5	3.60	12.32	3.32	4.14	14.90	1.90	6.84	3.02	10.87	1.50	5.39
0.5	0.14	5	3.60	12.16	2.76	1.07	3.85	1.86	6.71	0.26	0.94	1.44	5.20
1	0.28	5	3.60	12.11	-	1.84	6.62	1.86	6.71	0.34	1.22	1.40	5.03
1	0.28	5	3.60	12.00	2.61	0.59	2.12	1.81	6.52	0.67	2.41	1.37	4.93
1	0.28	5	3.60	11.98	-	0.47	1.69	1.76	6.34	0.43	1.55	1.33	4.80
2	0.56	5	3.60	11.94	2.62	2.20	7.92	1.78	6.40	0.77	2.77	1.31	4.72
20	5.56	5	3.60	11.93	1.36	4.58	16.49	1.88	6.76	2.99	10.76	1.37	4.94
1	0.28	5	3.60	11.90	-	2.81	10.12	1.91	6.87	0.70	2.52	1.35	4.86
2	0.56	5	3.60	11.81	2.65	1.51	5.44	1.90	6.83	0.69	2.48	1.33	4.78
20	5.56	5	3.60	11.80	2.86	3.95	14.22	1.96	7.06	4.29	15.44	1.42	5.12
2	0.56	5	3.60	11.80	2.62	1.81	6.52	1.96	7.05	1.00	3.60	1.41	5.07
2	0.56	5	3.60	11.75	2.61	1.44	5.18	1.94	6.99	0.86	3.10	1.39	5.01
2	0.56	5	3.60	11.74	2.82	1.06	3.82	1.92	6.90	0.72	2.59	1.37	4.94
0.5	0.14	5	3.60	11.66	2.65	1.30	4.68	1.90	6.83	0.60	2.16	1.35	4.86

Table 8.1: Summary of top five METC straight-line accelerations for different aim slips

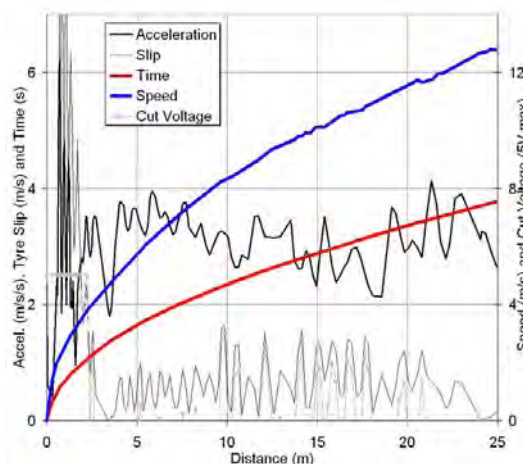


Figure 8.9: Vehicle acceleration, slip and speed for best straight-line acceleration for 3km/hr (0.83m/s) METC

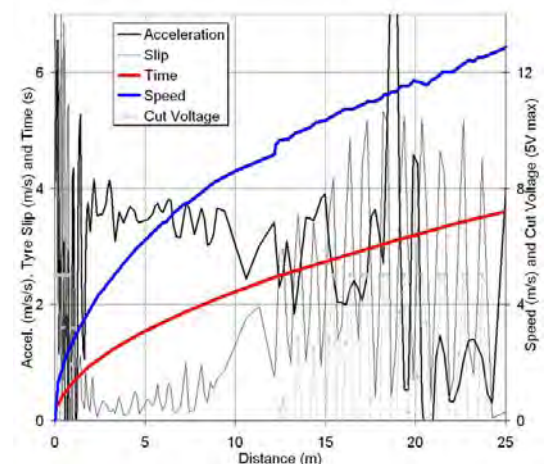


Figure 8.10: Vehicle acceleration, slip and speed for best straight-line acceleration for 10km/hr (2.8m/s) METC

These results were obtained after many traction control tests, which sought to determine three control variables. The first two were concerned with the proportional gains of the controller, and were tuned to give smooth traction control operation. The Slip Control Range = 5km/hr and the Controller Gain = 3.6Vs/m defined the gain and engine full cut limits, and once determined were used throughout subsequent testing. Aim Slip was varied within the traction controller, and the resultant performance evaluated based on repeated runs. To simplify this analysis, testing was only conducted in straight-line tests.

Surprisingly, however, it can be seen that the aim slip seems to have little effect on the performance of the METC. In particular, both low and high slips are present in the maximum accelerations, and it is hypothesized that this is due to two reasons. The first concerns the dynamics of the vehicle at “launch”, and the second is the in observation of the oscillatory nature of the high slip control.

When the vehicle starts off at launch, maximum acceleration is not found by controlling the driven wheels to obtain optimum coefficient of friction. Instead, the limitations of the engine come into play, and it is important to keep the engine within an rpm range that produces sufficient power. Considering what happens as the vehicle first starts moving best highlights this. If the optimum coefficient of friction is at, say, 2m/s and the vehicle is at rest, then the engine must turn very slowly (without ‘dragging’ the clutch) to achieve this slip value. This would probably result in the engine stalling, or a severe drop in power at the very least. If the engine does not stall, the car will accelerate very

slowly at much less than the optimum slip until the engine speed increases to a point where sufficient power may be delivered to the wheels. Only then will “optimum” performance be realised. In contrast, spinning the wheels excessively at launch may produce similar problems. Here, the optimum slip is greatly exceeded and the acceleration is much lower than otherwise possible. In this case the vehicle will slowly accelerate until its speed increases enough to reduce the magnitude of the slip, and therefore gain additional acceleration. This type of problem falls outside of the scope of traction controllers, and is termed “Launch Control”. In fact, operating traditional traction control at very low speeds has the capacity to significantly reduce achievable accelerations. Furthermore, there is a very fine line between good and bad performance at launch, and this has large impacts on the overall acceleration of the vehicle through the straight-line acceleration test. To try and overcome this problem, a large number of tests were completed, where each one attempted to gain the maximum acceleration possible with the current traction control aim slip. However, this effect could not be removed entirely, and has affected the results to a degree.

The second potential source of variation maybe from the controller oscillation at high slips, which is highlighted in Figure 8.10. The vehicle slip oscillates around the aim slip with a large degree of variation, and results in complex vehicle dynamics. This is due to limitations within the METC tuning software that allows only a fixed gain to be tuned, even though the amount of throttle used instantaneously would have a large effect on the optimum magnitude of this value. Furthermore, the lack of integral and differential gain control makes controller oscillation very hard to avoid. Combined with the high sampling rate of the controller, this produces a very high and active control load, and ensured the tyres were constantly experiencing significant transient conditions. This made comparison to the low aim slip control difficult.

Nonetheless, when comparing Figure 8.9 and Figure 8.10, it can readily be seen which type of vehicle dynamics would be desired for smooth and efficient operation while delivering maximum performance. Furthermore the 10km/hr case has launched much better than the 3km/hr case (at lower slip), and then shown reduced acceleration during high oscillation. In contrast, the 3km/hr aim slip case exhibits better acceleration, that the controller is not very active at all, and the average slip exhibited by the car is 0.65m/s (excluding the first 5m due to “launch” effects). By averaging the top ten results together, however, the average optimum slip is 1.18m/s excluding the first 5m (from the

cumulative average slip 5m to 25m column). As such, the best average slip value is in the 0.65 to 1.93m/s range, or on an average basis to be 1.18m/s.

Lastly, the precise control of wheel slip can be used to ensure vehicle dynamics data is acquired for the full scope driving conditions. This is particularly important because, without any traction control, intermediate slips are very hard to realise on the slippery surface. As such, data can be logged for the many different slip values and utilised within ANN controller training sets. It is noted, however, that this type of data acquisition is only appropriate for ANN models that are concerned with vehicle dynamics, and if any engine data is used within the model, this method cannot be used.

8.6.2 DAQ Emulation of MoTeC Traction Control (DEMTC)

To obtain ANN training data that contains engine information at a range of slips the engine cut voltage must also be logged. With the existing setup, this was not possible with the MoTeC traction controller, but could be completed if the DAQ controller was used. As such, the best estimate of the MoTeC traction controller algorithm was programmed into the DAQ controller to provide this data. Furthermore, by emulating the MoTeC control within the DAQ controller direct performance analysis could be made between developed models. This provides the baseline for the impending evaluation of ANN performance, and significant effort was expended to ensure a large amount of testing data was acquired. Some of this data is given in Table 8.2, Table 8.3, Figure 8.11 and Figure 8.12.

Aim Slip (km/hr)	Aim Slip (m/s)	MoTeC Slip Control Range (equivalent - km/h)	Controller Gain (Vs/m)	Speed at 25m (m/s)	AHRS Average Accel. 0m to 25m (m/s/s)	Average Slip 0m to 25m (m/s)	Average Slip 0m to 25m (km/hr)	Cumulative Average Slip 0m to 25m (m/s)	Cumulative Average Slip 0m to 25m (km/hr)	Average Slip 5m to 25m (m/s)	Average Slip 5m to 25m (km/hr)	Cumulative Average Slip 5m to 25m (m/s)	Cumulative Average Slip 5m to 25m (km/hr)
2	0.56	5	3.60	13.34	3.28	0.21	0.76	0.21	0.76	0.25	0.90	0.25	0.90
2	0.56	5	3.60	13.13	3.06	0.42	1.51	0.32	1.13	0.26	0.94	0.26	0.92
5	1.39	5	3.60	13.08	2.97	1.12	4.03	0.58	2.10	0.46	1.66	0.32	1.16
2	0.56	5	3.60	13.07	3.07	0.19	0.69	0.49	1.75	0.26	0.94	0.31	1.11
0.5	0.14	5	3.60	13.04	3.26	0.29	1.04	0.45	1.61	0.16	0.58	0.28	1.00
1	0.28	5	3.60	13.02	3.06	0.71	2.56	0.49	1.77	0.38	1.37	0.30	1.06
0.5	0.14	5	3.60	13.02	2.97	0.00	0.00	0.42	1.51	0.15	0.54	0.27	0.99
1	0.28	5	3.60	12.99	3.35	0.42	1.51	0.42	1.51	0.31	1.12	0.28	1.00
1	0.28	5	3.60	12.97	2.94	0.03	0.11	0.38	1.36	0.16	0.58	0.27	0.96
1	0.28	5	3.60	12.96	3.34	1.99	7.16	0.54	1.94	0.35	1.26	0.27	0.99
0.5	0.14	5	3.60	12.92	2.75	0.44	1.58	0.53	1.91	0.35	1.26	0.28	1.01
2	0.56	5	3.60	12.91	3.33	0.23	0.83	0.50	1.82	0.27	0.97	0.28	1.01
5	1.39	5	3.60	12.83	3.08	1.02	3.67	0.54	1.96	0.48	1.73	0.30	1.06
5	1.39	5	3.60	12.79	2.85	0.66	2.38	0.55	1.99	0.60	2.16	0.32	1.14
0.5	0.14	5	3.60	12.77	2.92	0.60	2.16	0.56	2.00	0.31	1.12	0.32	1.14
1	0.28	5	3.60	12.72	2.87	0.27	0.97	0.54	1.94	0.16	0.58	0.31	1.10
0.5	0.14	5	3.60	12.71	2.96	0.12	0.43	0.51	1.85	0.15	0.54	0.30	1.07
5	1.39	5	3.60	12.70	3.05	0.80	2.88	0.53	1.90	0.36	1.30	0.30	1.08
5	1.39	5	3.60	12.69	2.85	0.58	2.09	0.53	1.91	0.46	1.66	0.31	1.11
2	0.56	5	3.60	12.38	2.92	0.72	2.59	0.54	1.95	0.24	0.86	0.31	1.10

Table 8.2: Summary of top five DEMTC straight-line accelerations for different aim slips

Aim Slip (km/hr)	Aim Slip (m/s)	MoTeC Slip Control Range (equivalent - km/h)	Controller Gain (Vs/m)	Average Speed (m/s)	Average Steered Tyre Long. Accel. (m/s/s)	Average Steering (°)	Average Slip (m/s)	Average Slip (km/hr)	Cumulative Average Slip (m/s)	Cumulative Average Slip (km/hr)
1	0.28	5	3.60	7.25	2.68	-27.7	1.11	4.00	1.11	4.00
2	0.56	5	3.60	7.40	2.58	-28.9	1.08	3.89	1.10	3.94
1	0.28	5	3.60	6.71	2.52	-30.2	1.01	3.64	1.07	3.84
2	0.56	5	3.60	7.72	2.48	-25.6	0.91	3.28	1.03	3.70
1	0.28	5	3.60	7.06	2.44	-28.0	0.92	3.31	1.01	3.62
2	0.56	5	3.60	6.91	2.36	-27.6	0.82	2.95	0.98	3.51
1	0.28	5	3.60	6.83	2.32	-29.1	0.79	2.84	0.95	3.41
2	0.56	5	3.60	7.57	2.28	-25.9	0.91	3.28	0.94	3.40
2	0.56	5	3.60	7.60	2.11	-26.4	1.01	3.64	0.95	3.42
2	0.56	5	3.60	7.70	2.03	-26.3	0.66	2.38	0.92	3.32
1	0.28	5	3.60	6.71	2.02	-26.8	0.58	2.09	0.89	3.21
1	0.28	5	3.60	8.44	1.95	-28.9	1.21	4.36	0.92	3.30

Table 8.3: Summary of top six DEMTC constant circle accelerations for different aim slips

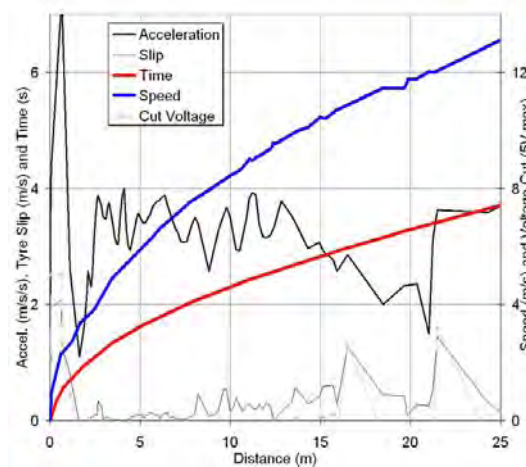


Figure 8.11: Vehicle acceleration, slip and speed for best straight-line acceleration for 2km/hr (0.56m/s) DEMTC

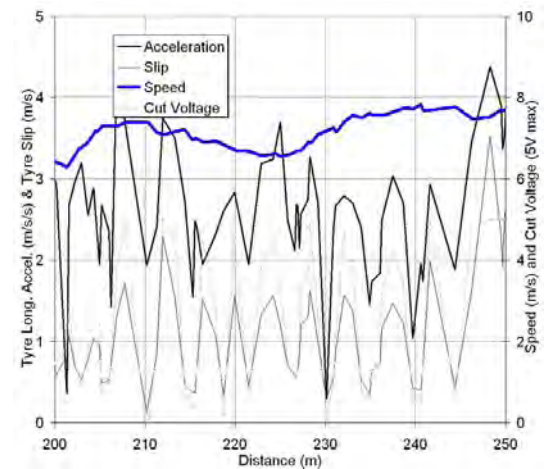


Figure 8.12: Vehicle acceleration, slip and speed for best constant circle acceleration for 1km/hr (0.28m/s) DEMTC

Straight-line acceleration results are complemented by constant circle results. In this way, two simple performance comparisons can be made. Firstly, the acceleration from a stationary start over around 25m in a straight line provides a good indication of the traction control performance. Secondly, the speed at which a constant circle radius can be maintained provides a good indication of the ability of the controller to conduct stability control type operation. This information is derived from driving the car in a constant circle and slowly increasing the throttle. The logged data is decimated into 50m segments (approximately one complete circle) and the fastest segments evaluated. The DEMTC results clearly show that the required slips for the straight-line and circle cases are different. For instance, when completing the circle manoeuvre that the optimum slip is in the 0.58 to 1.21m/s range, with the best at about 1.11m/s. In addition, the slower sampling rate of DEMTC has significantly impeded the controller's ability to achieve the aim slip.

It appears that the best straight-line average slip for DEMTC is obtained at aim slips of 0.56m/s, with average slips in the 0.25 to 0.31m/s range consistently producing best acceleration. This is in contrast to METC, which shows values that are consistently higher. Furthermore, the ultimate speeds that are obtained with METC are lower than DEMTC. This highlights a potential problem in comparing the two results, and is based on software limitations. The METC data was acquired by using the DAQ control software in data logging mode only, and was logged at a faster rate than the DEMTC case, which had to complete control functions and was thus limited to 50Hz. As such, the integration of speed to obtain distances (and thus the speed at 25m) contains different levels of error. As discussed earlier, this problem was identified at an early stage, and subsequent tests do not contain this problem. Even so, the ranking process of determining the fastest arrangements is still valid.

Nonetheless, the control sampling speeds between METC and DEMTC clearly show a problem in directly comparing the control results. The METC clearly controls the wheel slips at much faster rates, and better performance is gained. In contrast the DEMTC controller exhibits slow control, and is relatively inactive. As such, it is possible for high levels of engine cut to effectively brake the vehicle (as can be seen at 0m in Figure 8.11) and cause other undesirable operations. Unlike the METC, any high slips will result in severe engine cut and significantly reduce performance within a short period of time. The same is true in the opposite sense as well, with a delay in reducing engine power when high slips are encountered, resulting in large deviations from the aim slip.

While this method of simply presenting the best testing runs provides a useful analysis tool, it is limited in application. This has particularly been shown to be the case for determination of what the optimal slip for a given surface should be. As such, a second method for data analysis is presented.

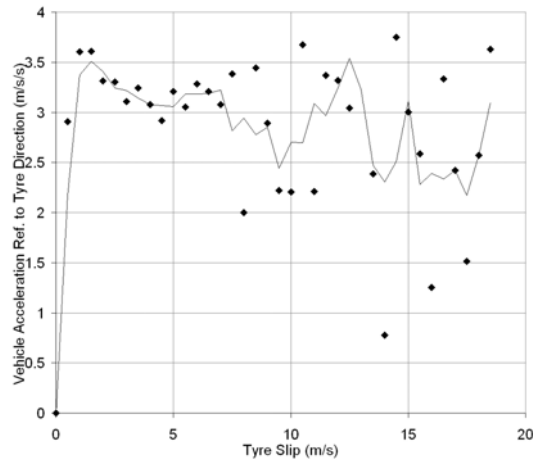


Figure 8.13: Average slip and vehicle straight-line acceleration relationship for 0 to 2.5m/s speed DEMTC

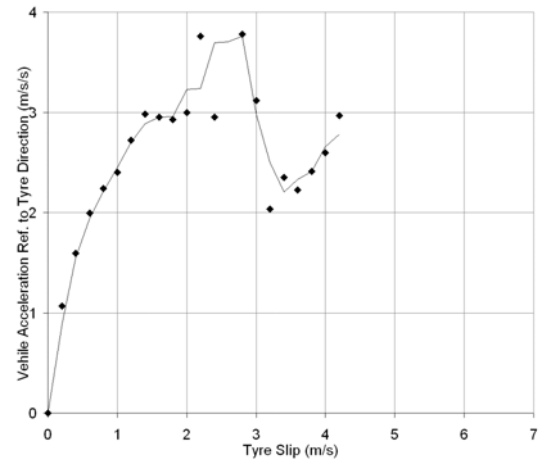


Figure 8.16: Average slip and tyre long. accel. relationship during circle manoeuvre 6.5 to 7.5m/s speed DEMTC

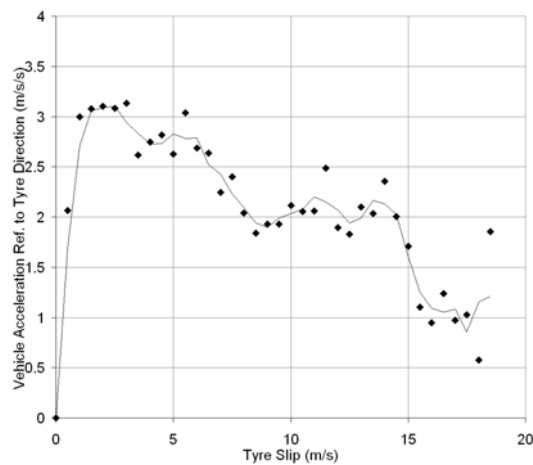


Figure 8.14: Average slip and vehicle straight-line acceleration relationship for 2.5 to 7.5m/s speed DEMTC

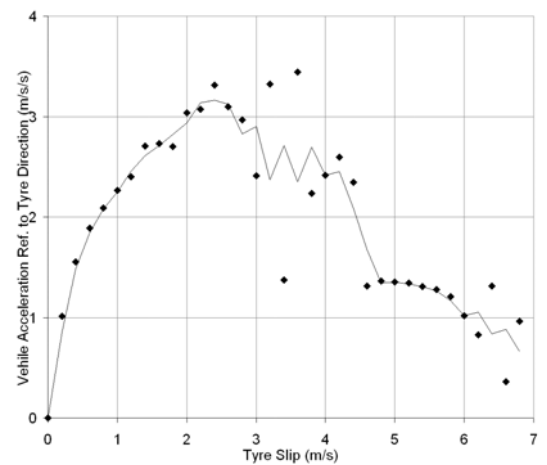


Figure 8.17: Average slip and tyre long. accel. relationship during circle manoeuvre 7.5 to 8.5m/s speed DEMTC

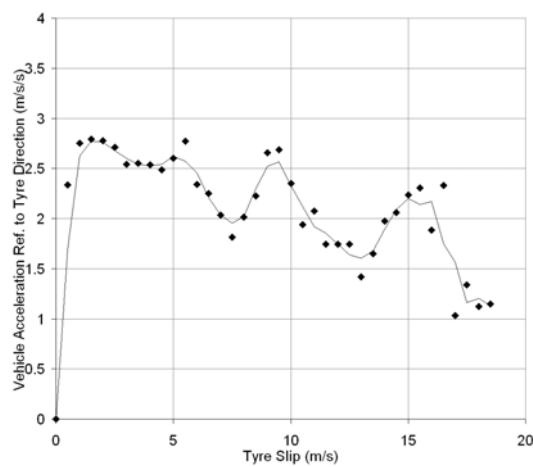


Figure 8.15: Average slip and vehicle straight-line acceleration relationship for 7.5 to 12.5m/s speed DEMTC

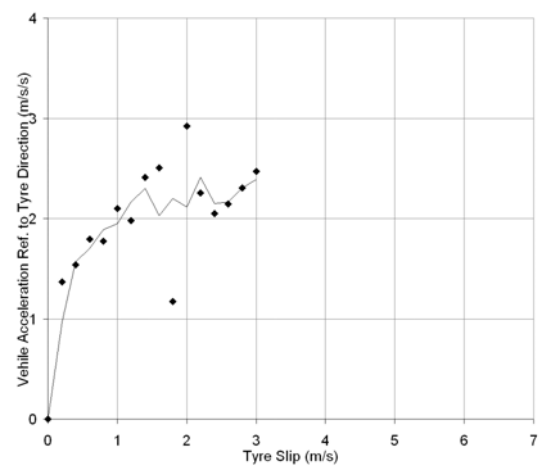


Figure 8.18: Average slip and tyre long. accel. relationship during circle manoeuvre 8.5 to 9.5m/s speed DEMTC

This method is based on the desire to construct slip/longitudinal acceleration curves for given conditions. In this way, driven wheel slip can be related to the acceleration of the vehicle to obtain optimal slip data. Nonetheless, these curves are functions of many parameters, and the testing data is insufficient to cover all of these conditions. Instead, it is observed that the general slip curve for a surface can be constructed by simply comparing wheel slip to measured acceleration in the longitudinal direction for every measurement sample. All of the measured data can be decimated into “bins”, where each bin comprises of specific slip and acceleration combinations. For instance, a single bin may consist of all acceleration values that were measured within a specific slip range. The acceleration values could be averaged together within each bin, and average slip/acceleration curves obtained. Furthermore, it is possible to add additional bin conditions to gain slip/acceleration curves as functions of additional parameters, such as vehicle speed or suspension position. Curves can be derived that show the general coefficient of friction nature of the surface, and to highlight general optimal slip values. The results of this process are given in Figure 8.13 to Figure 8.18, where the individual curves represent the filtered points.

There is some variation in the curve shapes from the ideal. In particular, there is often a significant amount of scatter where the curve condition is not well represented in the logged data (such as very high slip at very low speed), and curves are not complete at the limits of operation (such as at high circle speeds). It can be seen that the straight-line and circle curves are quite different. This is because the longitudinal acceleration is based on the acceleration of the vehicle in the direction of the steered wheels, and as such the cornering process augments the result. In general, however, the optimal average slips are:

- 1.4m/s for straight-line at 0-2.5m/s
- 2.0m/s for straight-line at 2.5-7.5m/s
- 1.8m/s for straight-line at 7.5-12.5m/s
- 2.6m/s for circle at 6.5-7.5m/s
- 2.4m/s for circle at 7.5-8.5m/s
- >3m/s for circle at 8.5- 9.5m/s

8.7 ANN Controller Development

The ANN models were developed over a number of steps to obtain the most appropriate control model. This included a preliminary investigation to ensure the ANN models would perform with that kind of accuracy and characteristics for ANN control, training

and evaluation of a number of different ANN models to investigate their potential and developing and testing actual ANN controllers utilising these models. In all cases the ANN training data comprised of data obtained on the straight-line, circle, figure eight and miscellaneous test tracks.

As discussed, the data gathered on the first day was used to conduct a baseline investigation into ANN traction control possibilities. From previous discussion and observation of earlier “Intelligent Car” project results, it can be seen that much of this possibility revolves around the abilities of ANN models to predict various vehicle performance parameters.

This preliminary investigation, thus, seeks to repeat this work on the new test vehicle to provide a starting point for further work. In particular, previous “Intelligent Car” research [40, 71] used FFBP and General Regression ANNs to predict vehicle acceleration and yaw. It yielded the observation the FFBP models provided significantly more accuracy than GR models, which is the principle reason this investigation focuses on the feedforward family of ANNs.

To this end, the data from the first day of testing was used to construct an FFBP ANN model that attempted to predict vehicle longitudinal, lateral and yaw acceleration, and yielded comparable results. These predictive results can be seen in Figure 8.19, Figure 8.20 and Figure 8.21 for an 31 input, 10 1st layer, 5 second layer 3 output ANN model. The 10x5 internal architecture was determined through investigation producing the lowest error.

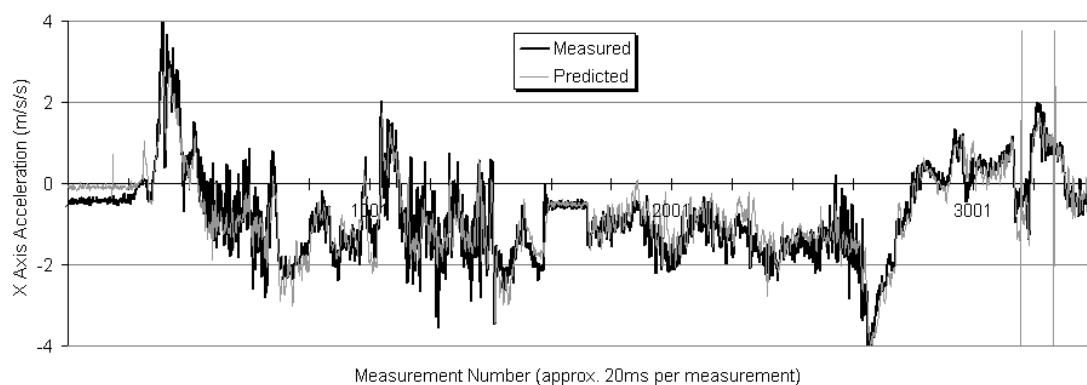


Figure 8.19: Model X axis acceleration output comparison for testing data with 10x5 BP ANN preliminary model (RMS error=2.6% full scale)

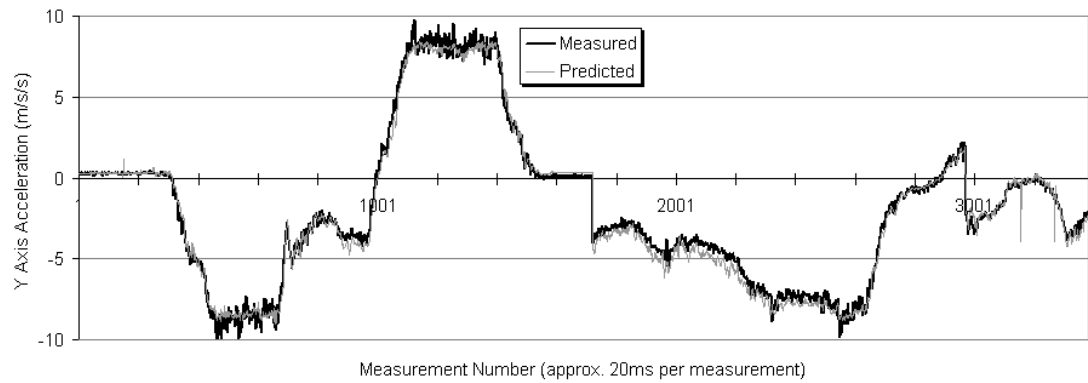


Figure 8.20: Model Y axis acceleration output comparison for testing data with 10x5 BP ANN preliminary model (RMS error=2.3% full scale)

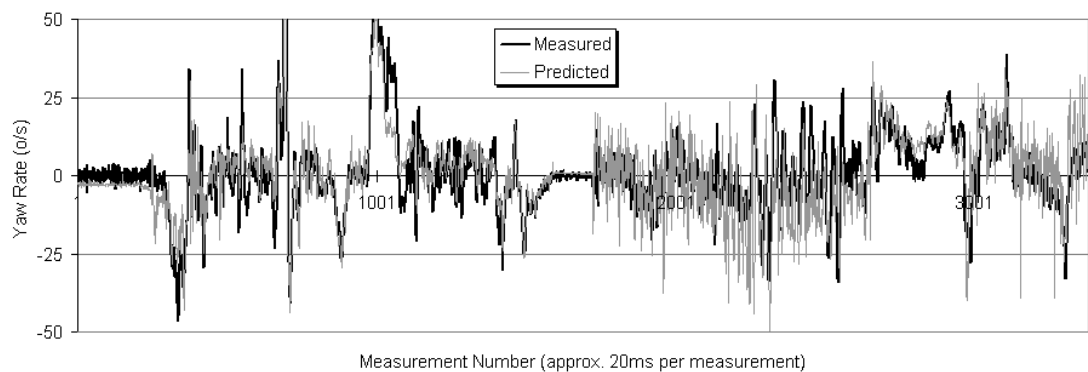


Figure 8.21: Model yaw acceleration output comparison for testing data with 10x5 BP ANN preliminary model (RMS error=5.1% full scale)

The ability of the ANN model to predict vehicle states is quite good, with the testing data producing RMS errors of around 2-5%. This provides some compelling evidence that the ANN models may have application in the regard. However, this type of modelling must be implemented in a thoughtful way. For example, the ANN model above can predict longitudinal vehicle acceleration with only 2.6% RMS error, but utilises the rear wheel accelerations as ANN inputs. It would be fair to comment that longitudinal acceleration is proportional to vehicle acceleration for the most part, and that the ANN may have not learnt the dynamics of the process, but rather has simply learnt the simple relationship. This possibility is also evident in an input importance analysis carried out on the ANN model, as shown in Figure 8.22. As discussed earlier, this table shows the relative increase in model error as each input is set to a constant value to recreate input “failures”. Inputs that correspond to a high increase in error are, therefore, considered more important to the model accuracy.

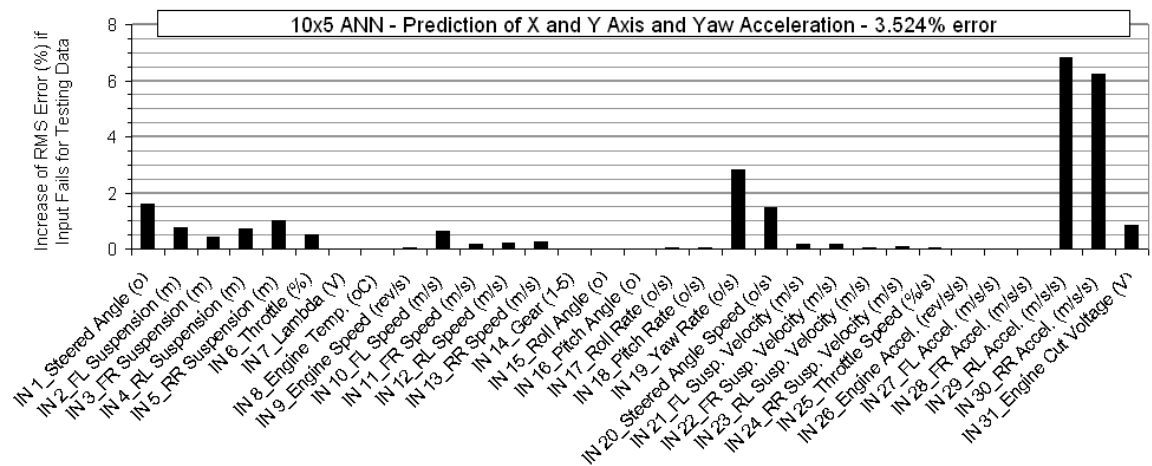


Figure 8.22: Input importance analysis for ANN preliminary model

Rear wheel acceleration, yaw rate, steering angle and steering speed represent the most significant input parameters. These are also the parameters one may expect to have simple relationships to the vehicle longitudinal, lateral and yaw accelerations. This is true, at least, when the vehicle is used within the linear region of its tyres, as in normal driving conditions. The problem is, therefore, will the ANN model be able to identify when the vehicle is unstable, so it can deviate from these linear relationships?

This highlights a conceptual problem with this type of ANN modelling, because a model that has only learnt the linear relationship will exhibit similar levels of error as a model that has comprehensively learnt the dynamics of the system. Furthermore, because the ANN models are contained within a “black box” it is very difficult to determine which of these two cases is true. In addition the ANN models cannot be influenced in their training to exhibit a particular modelling characteristic. Instead, appropriate input parameters and condition ranges must be selected to ensure that the ANN model behaves as desired. In particular, this means highlighting and removing parameters that are over-represented, or directly related to other input parameters, as well as ensuring training data is only acquired for relevant conditions. Once this is done, the performance of the ANN model must be evaluated to ensure it operates as desired, or modified iteratively to obtain the desired response. Returning to the ANN model that is presented, this translated into determining if the transition and unstable regions of the vehicle operation have been modelled adequately. This is an important aspect of research yet to be presented, because the ANN response is directly related to the performance of the ANN controller.

8.7.1 ANN Training and Optimisation

The ANN control methods discussed above require inverse or direct ANN models to be developed. As stated, however, these models must also exhibit the correct vehicle dynamics relationships within the scope of the controller if they have any hope of working correctly. Furthermore, the actual type of controller utilised has a direct bearing on what the predicted output of the ANN model should be.

In particular, an inverse ANN model must predict a control variable, which instantly suggests using the engine cut voltage as an output. Such an output places the dynamics of the engine and the MoTeC ignition/injection cut within the ANN model in addition to the vehicle dynamics. This may significantly increase the modeling burden on the ANN model, and result in degraded performance. Furthermore, generalised training of this type of model requires a large amount of data derived from DEMTC testing to gain cut voltages, and may require cut voltages to be used that would potentially damage the engine.

The scope of the inverse controller can, thus, be reduced by considering throttle position as model output. The MoTeC engine cut algorithm can be removed from the ANN modeling process, and the ANN can then to “recommend” a throttle position to the driver. This recommendation could be used in a simple controller to reduced engine power appropriately. Such a model has the added advantage that it can be trained without having to implement any form of traction control to acquire the data.

This principle can be taken even further, with the inverse ANN model used to simply model the vehicle dynamics to the exclusion of any engine effects. The inverse model could be used to predict the desired wheel slip (either at each wheel or as a driven wheel average), and then leave a traditional controller to ensure this aim slip is realised. This provides a number of potential benefits. Firstly, the modeling scope of the ANN is reduced to the dynamics of the vehicle only. Secondly, the ANN output provides the optimum wheel slip for the given condition, which is a generic output. Thirdly, the output can be used in other controllers, which may be easier to use or more effective at actually ensuring that this aim slip is obtained in practice. Finally, the ANN training data can wholly exclude the engine data and can be completed with or without traction control active.

Significant research was carried out to develop each of these ANN models for use within ANN controllers later in this investigation. In particular, the effects of removing or adding ANN input was covered in depth, and the resultant effects in ANN input parameter importance noted. In this case, the goal was to produce ANN models that appeared to rely on relevant generalisations, which were determined by evaluating the philosophy behind each model. The final ANN model results for generalised training are shown in Figure 8.23, Figure 8.24, and Figure 8.25 where “Tyre Long. Accel” is equal to the acceleration of the vehicle in the direction that is longitudinal to the steered wheels.

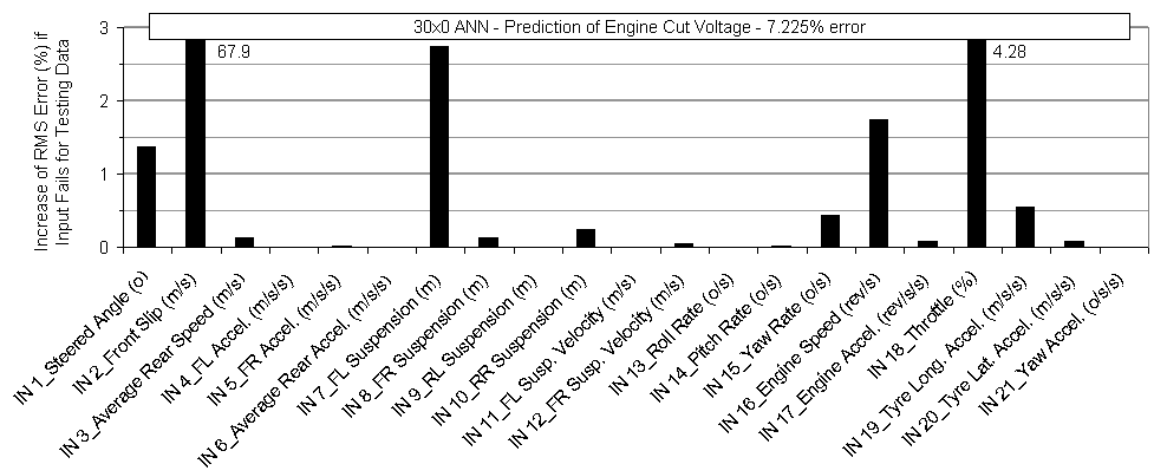


Figure 8.23: Input importance analysis for engine cut voltage output of the 21 input ANN inverse model

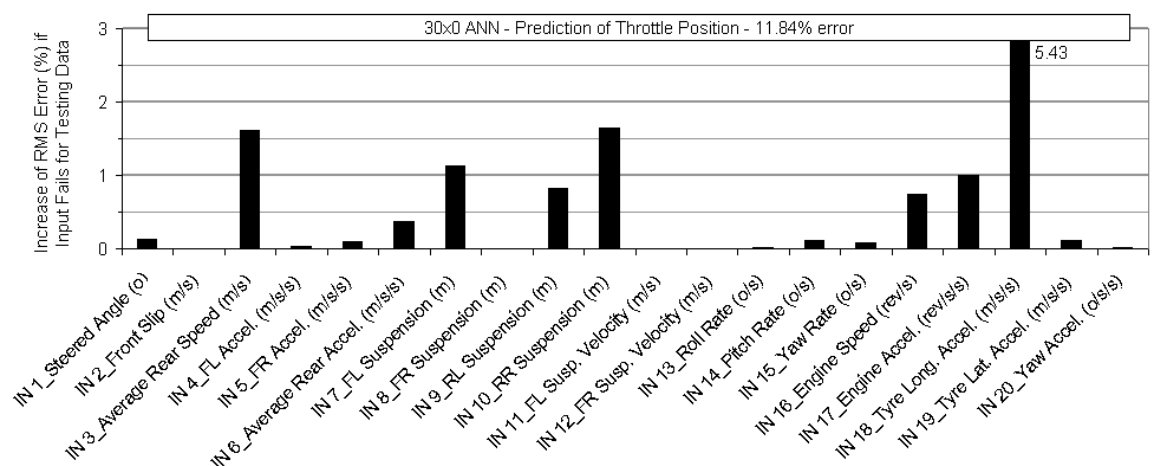


Figure 8.24: Input importance analysis for throttle output of the 20 input ANN inverse model

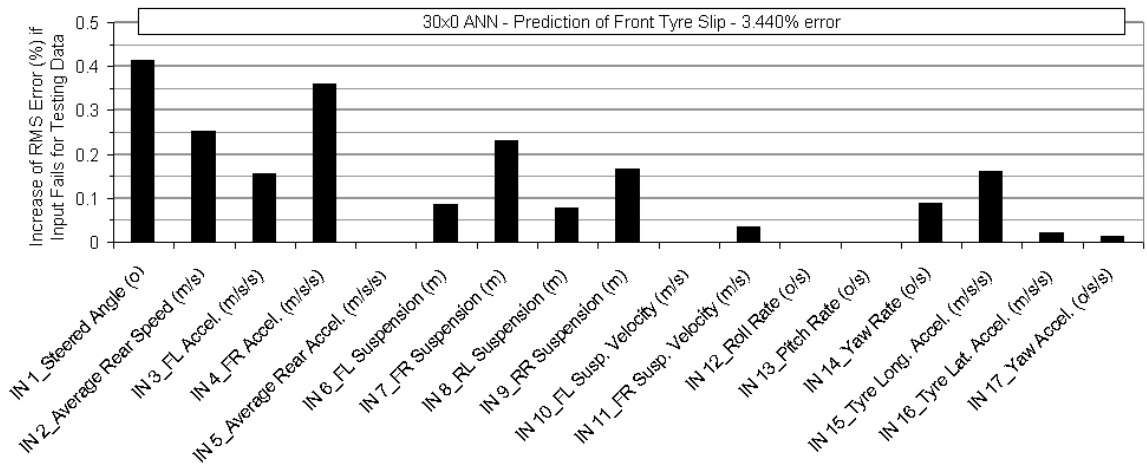


Figure 8.25: Input importance analysis for average front tyre slip output of the 17 input ANN inverse model

The observer controller, in contrast, does not rely on inverse control. Instead, ANN models must be developed to model the system as it is observed, which is referred to here as direct ANN modeling. The process that is being observed is the entire vehicle system, and the performance variable is the longitudinal acceleration of the driven wheels. As such, the measured vehicle parameters form the ANN inputs, and the longitudinal acceleration the ANN output. As stated previously, however, tyre longitudinal acceleration is considered to have similar properties as the entire vehicle acceleration (in the component direction of the driven wheels), and this can be used for ANN training instead.

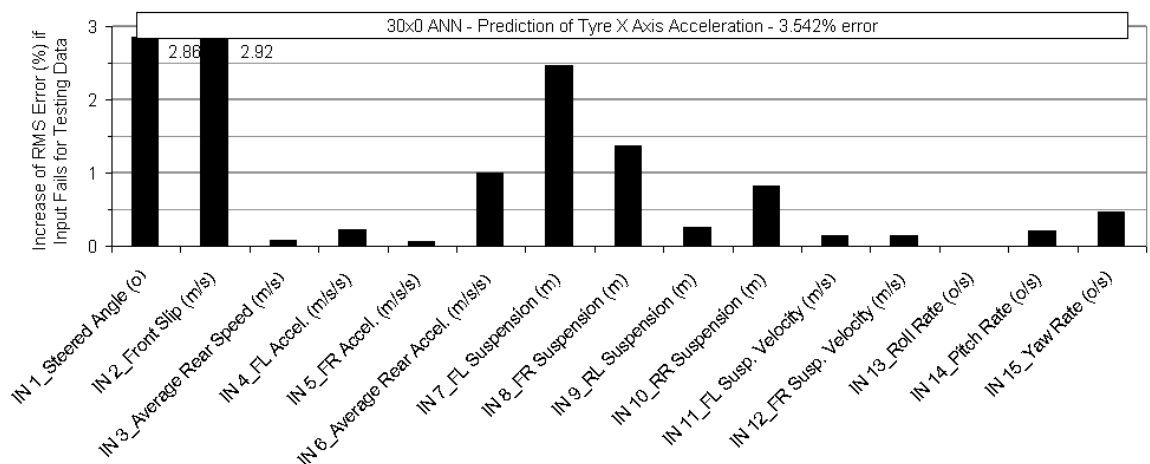


Figure 8.26: Input importance analysis for tyre long. accel. output of the 15 input ANN direct model

Like the investigation for the inverse ANN models, a large investigation was carried out to determine appropriate direct ANN model inputs, with the results shown in Figure 8.26 for one of these cases.

8.7.2 ANN Controller Construction

Once the basic ANN structures were determined, it was possible to construct ANN controllers based on these findings. The controllers could be evaluated off-line using the data from the first day of testing, and on-line during the second day (although the on-line testing was found to provide limited evaluation assistance at this stage).

A number of ANN controllers were developed and implemented in the DAQ controller LabVIEW program for simple and consistent comparison. Each of the tested controllers represented a range of possible control applications, and were developed either as intermediate control steps (such as simply evaluating if control was required) or as complete controllers. Each of these controllers will be discussed below, with the controller analysis excluded for cases that showed little potential.

8.7.2.1 Inverse ANN Cut Voltage Comparison (IANNVCV)

The IANNVCV controller utilises the first inverse ANN model to predict engine cut voltage from measured vehicle conditions. Such a controller, if implemented well, should be able to determine the required engine cut voltage to realise desired amounts of acceleration, and has the potential of being a very valuable tool. Nonetheless, there are a number of issues that make investigation of this controller difficult. This first is that only generalised training can be completed within the scope of this investigation, meaning that the ANN models may exhibit more error than would otherwise be the case.

Another problem is that the inverse model requires an “aim” value to be known. By being supplied with an aim value, the role of the ANN model is to determine an appropriate output signal to produce this value within the controlled system. This is not possible with the current investigation goals, as the “aim” of the controller is simply to deliver maximum longitudinal acceleration, which is a value that is not known.

To this end a simplified preliminary investigation was proposed, whereby two inverse models are utilised in parallel. The one model predicts the cut voltage for the current condition, and the other the cut voltage if the tyre longitudinal acceleration “aim” is slightly increased. One model can be compared to the other to determine whether or not a higher cut voltage is needed to produce an increase in acceleration. If engine cut is needed to improve acceleration, then the vehicle can be considered unstable, and control implemented.

It is observed, however, that this logic can be applied to a single ANN model, and does not require two. This is because the ANN prediction of current state should exactly correlate to the actual state of the vehicle. As a result, the second ANN prediction could be compared to the vehicle condition rather than the ANN prediction of the vehicle condition. In practice, however, it is believed that ANN error would make such a method highly inaccurate. ANN error is a “fact of life”, and this error would probably be greater than the output difference between the two models. As such, comparing the actual result to the increased acceleration ANN result would be highly erroneous. On the other hand, comparing the two ANN models together negates this effect entirely. In fact, by comparing the two ANN results, the effects of model error are totally removed from the comparison, and the strengths of ANN modelling are highlighted. Of particular interest is the ability of the ANN models to generalise the process, which means that for small variations for specific input parameters, the model should be able to accurately predict the corresponding changes to the output. While it is true that ANN model training inaccuracy will affect the quality of these comparisons, this method negates the absolute model errors that often produce control problems.

Such a method produces a very simple signal of whether control is needed or not. However, this is very important information, which traditional controllers cannot determine. In fact, the ability to determine if the vehicle is stable or unstable is the one of the goals that underpins this research, and is an important avenue worth investigating. If the controller can be proven in the binary application it will be possible to build on its functionality in later research within this investigation. For instance, the concept of linearising the ANN gains that was developed in the Aalborg investigation could be utilised to determine appropriate controller outputs. As such, this initial investigation attempts to only investigate the binary ability of this control method, with some of the controller outputs given in Figure 8.27 to Figure 8.30.

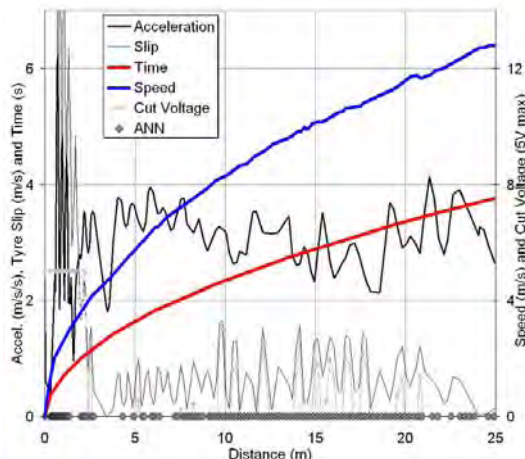


Figure 8.27: IANNCVC prediction of if traction control is needed for best straight-line acceleration for 3km/hr METC

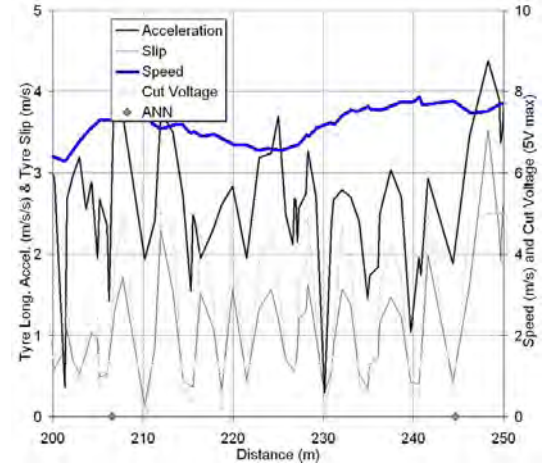


Figure 8.29: IANNCVC prediction of if traction control is needed for best constant circle acceleration for 1km/hr DEMTC

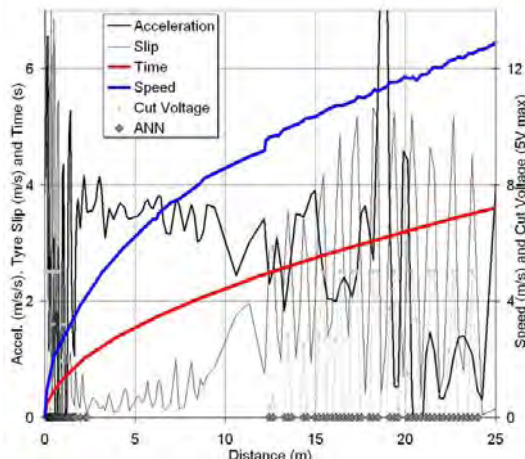


Figure 8.28: IANNCVC prediction of if traction control is needed for best straight-line acceleration for 10km/hr METC

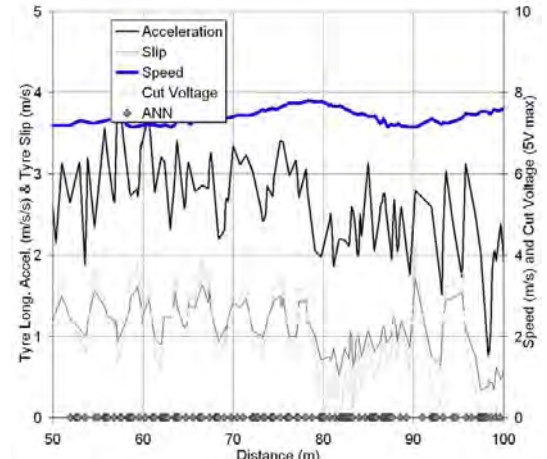


Figure 8.30: IANNCVC prediction of if traction control is needed for best constant circle acceleration for 2km/hr DEMTC

These graphs show the off-line performance of the binary inverse engine cut voltage ANN controller, based on the METC and DEMTC data presented above. The ANN controller is active when the ANN point (grey diamond) appears on the distance axis, and not active when it is absent. As such, the controller seems sporadically active, especially in the circle cases. This is not a good sign for control, and does not correspond to the optimal slip values determined previously.

As a final test to understand the generalisation of the ANN, it is useful to see how it generalises data. In particular, if the ANN has modelled the process well, it should have a clear understanding of the engine cut that is needed to increase acceleration by a specific amount. For a given condition, this will translate to no cut below the optimal

slip and some cut (determined by the control dynamics of the system) above it. This curve can be constructed in a similar manner as for the ANN comparison method, except by applying more comparisons through the range of a single input variable. While it is observed that the resulting curve will have questionable accuracy at its extremes, it is considered that this method provides a useful evaluation tool. The results for the engine cut inverse ANN model are shown in Figure 8.31.

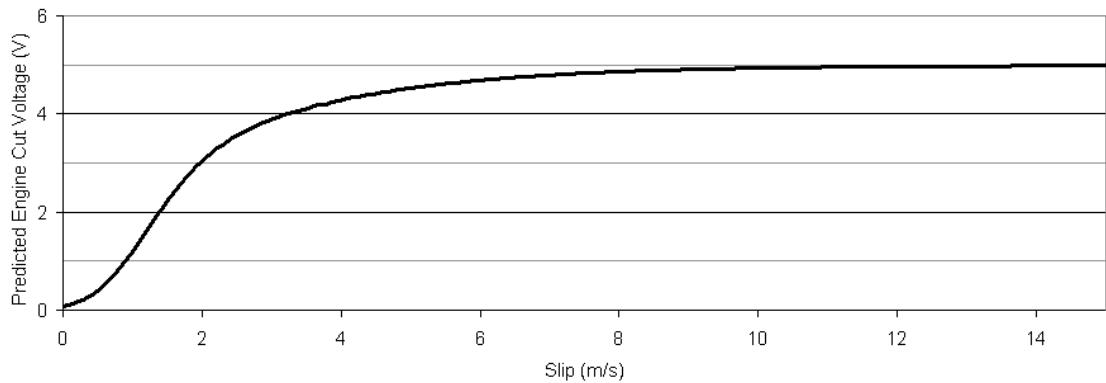


Figure 8.31: Typical IANNCVC prediction of tyre long. acceleration for varying slip

This result shows that the ANN model is not generally behaving as it should be, as it essentially predicts that optimal slip is at, or below, 0m/s. As such, while this ANN control method appears promising in theory, in practice it cannot be easily achieved and will not be explored further in this research.

8.7.2.2 Inverse ANN Throttle Comparison (IANNTC)

Similar logic can be applied to the inverse throttle ANN, presented earlier, by simply considering the throttle position in place of the engine cut voltage. In this case, the inverse ANN predicts the throttle position that the driver should implement to regain vehicle stability. This output could be either implemented by the driver (with limited success), operate a “throttle by wire” system or be utilised in a secondary controller for engine ignition/injection cut. Furthermore, by removing the MoTeC engine cut algorithm from the modeling process, the ANN model can be expected to improve in accuracy.

Nonetheless, the method of simply comparing two ANN predictions based on slightly increased acceleration was found to provide no useful result. In particular, when applied to the off-line simulation, the controller produced no control signals at all, even in cases

where the vehicle was clearly unstable. As such, these results are not provided, and this type of control was abandoned in further investigation.

8.7.2.3 Inverse ANN Slip Comparison (IANNSC)

As previously discussed, the inverse ANN model can be constructed to predict the amount of front wheel slip required to produce the desired longitudinal acceleration in an attempt to remove engine dynamics from the modeled vehicle dynamics. Nonetheless, this controller works in a very similar manner to the two other inverse models presented earlier, that were utilised to predict the current vehicle state and the vehicle state with slightly increased longitudinal acceleration. If the model displays greater slip with increased acceleration then no control is needed. Conversely, if the acceleration increase requires a reduction in slip, then the vehicle is considered unstable. Unfortunately, however, this method was found to produce no useful results either.

8.7.2.4 Inverse ANN Front Left and Right Slip Comparison (IANNFLRSC)

Even though the IANNSC model has limited research potential, the concept does have one particular advantage that was worth exploring further. This is in regards to its prediction of vehicle slip, which it should be able to optimise. Whilst vehicle slip was calculated here as the average driven wheel slips, there is no reason why the ANN model cannot be used to predict individual vehicle slips instead. In this way, the controller could determine optimum slips for each wheel, which would have obvious benefit in all stability controllers where individual wheel speeds can be controlled. While this is not the case in this research it is a useful avenue worth exploring, although it is noted that the increase in the modeling burden on the ANN models will probably reduce prediction accuracy and increase required computations.

To this end, the ANN model that was used in the IANNSC controller was altered (and re-trained) to provide predictions of left and right driven wheel slips. It was implemented in the much the same way as the IANNSC controller, except three ANN predictions were made to determine tyre stability. These included the ANN prediction of vehicle state slip, ANN prediction of left wheel slip and ANN prediction of right slip at greater acceleration. Two comparisons could be made to determine if the individual wheels were stable or not.

Not surprisingly, however, this method produced similar control prediction results as the IANNSC model.

8.7.2.5 Direct ANN Cut Voltage Curve Optimisation (DANNCVCO)

As has been shown, the inverse ANN models were not found to provide satisfactory results. This was because the inability to determine “goal” control values reduces the usefulness of inverse control, and because inverse ANNs are difficult to train effectively. In fact, in an attempt to overcome some of these limitations, the inverse ANN models had been implemented in an “observer” application. While this was done purely as an initial investigation step, it highlights the fact that inverse ANN modelling has limited application in “optimal” control. This is also supported in literature [124]. Instead, direct ANN modelling has greater potential application in this regard, although it is noted that many possible avenues of study exist. As discussed, the ANN prediction of the acceleration of the vehicle in the steered direction is a particularly appealing option, and allows a control observer to “test” the effects of various input changes on the acceleration of the vehicle. In this way, individual model inputs can be varied to determine the resultant changes in instantaneous longitudinal acceleration direction and magnitude. This is also the same method that was used in the Aalborg work to determine the linear gains of the ANN models, and as such, can also be used to estimate the magnitude of control signals. Furthermore, by altering an input value through its entire range and assuming all other values are constant, a curve can be constructed that shows the ANN model’s understanding of the process. As the aim value moves further away from the current value, the accuracy of this method will decline, but nonetheless this provides an important conceptual tool.

With reference to the problem at hand, different amounts of engine cut voltage, throttle position and slip should produce an ANN prediction curve with a peak at the optimal acceleration value. This would provide an approximation of the maximum achievable instantaneous acceleration value, and the required change to a specific vehicle parameter to realise this value (assuming all else is constant). This information is exactly what is required from an observer model to ensure that the “aim” values of the entire control system are appropriately determined and then realised.

In the case of DANNCVCO control, this method requires an ANN model that can accurately predict the dynamics of the vehicle, the engine and the MoTeC engine cut

algorithm. To this end, a model was trained that is similar to the direct ANN model presented earlier, and includes engine cut voltage, throttle, engine speed and engine acceleration inputs. The ANN model was embedded into the DAQ controller and used to construct instantaneous curves of the engine cut voltage/longitudinal acceleration relationship. An example is shown in Figure 8.32.

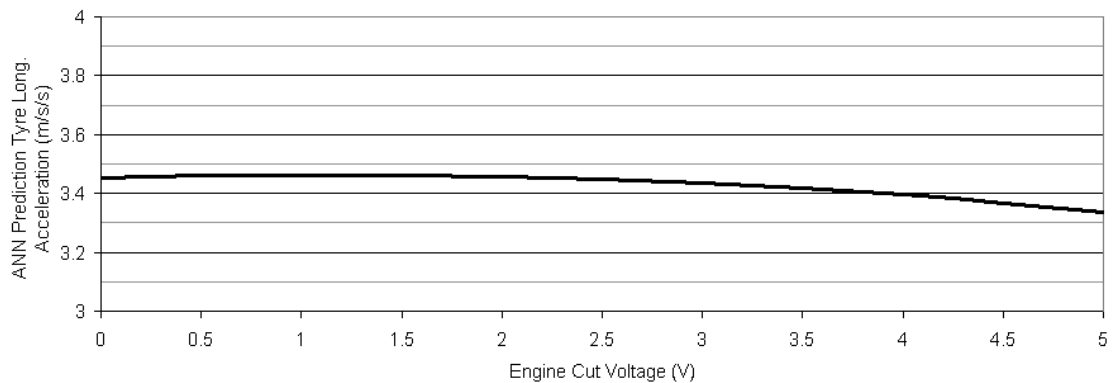


Figure 8.32: Typical DANNCVCO prediction of tyre long. acceleration for varying engine cut voltage

The maximum longitudinal acceleration of 3.48m/s^2 is achieved at an engine cut voltage of 1.1V. As such, it would be expected that the controller would implement a cut voltage of 1.1V for this sample and optimum acceleration would result. This is a particularly useful tool, as it means the instantaneous optimum control value can always be determined. In addition, this optimal value is based on the ANN prediction of the full dynamics of the system, so it takes into account parameters such as tyre transients. It is noted, however, that the further away the current condition is from the optimal, this curve method will lose accuracy. This is because the “assuming everything else is constant” method used to create the curve becomes less accurate near the extremes. Nonetheless, it is expected that if good control were maintained, this condition should only arise when no control is needed, which would produce no control problems.

Finally, this type of controller increases the computational complexity and may reduce sampling rates when used in practice. This is because the ANN model must be altered a number of times within each control sample. In the controller presented, for instance, 12 ANN models are evaluated at each iteration, which increases the controller load significantly. This computational time problem could be overcome if the parallel computing abilities of ANN models were implemented into commercial ECU design. As such this is not considered a significant problem for future work, although it was a

concern that it may provide some control difficulties later in this investigation. Nevertheless, the DANNCVCO controller off-line results are presented in Figure 8.33 to Figure 8.36.

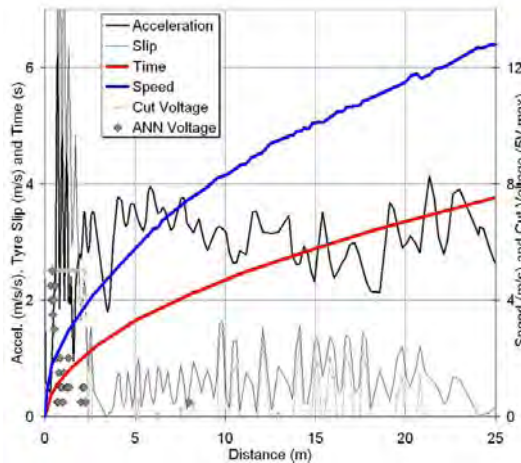


Figure 8.33: DANNCVCO prediction of traction controller voltage for best straight-line acceleration for 3km/hr METC

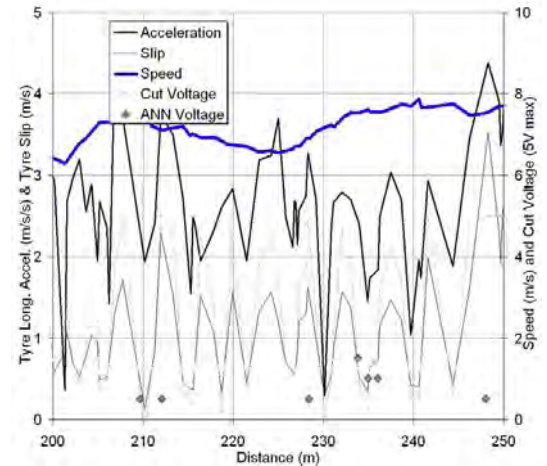


Figure 8.35: DANNCVCO prediction of traction controller voltage for best constant circle acceleration for 1km/hr DEMTC

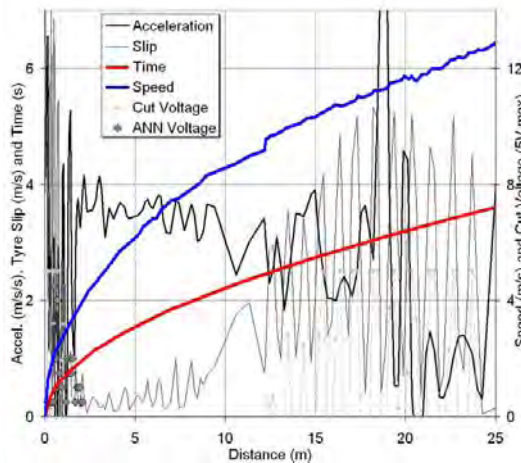


Figure 8.34: DANNCVCO prediction of traction controller voltage for best straight-line acceleration for 10km/hr METC

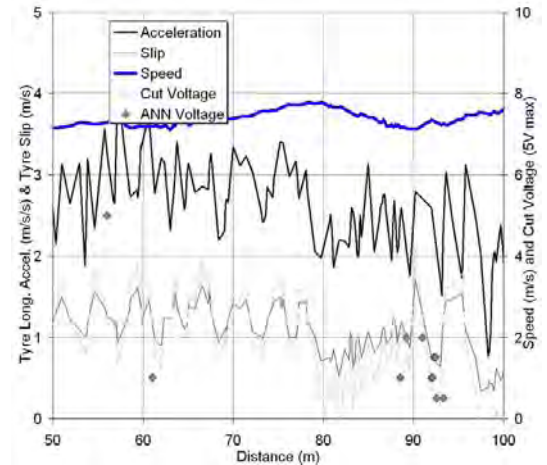


Figure 8.36: DANNCVCO prediction of traction controller voltage for best constant circle acceleration for 2km/hr DEMTC

This model allows the ANN control voltage to be determined, in addition to the simple binary control signal shown for the inverse controllers. Furthermore, the controller seems to operate reasonably well, although it is noted it is erroneous in a number of cases, and is not as active as may be expected. It does, however, provide the general basis for control that appears to be robust and in keeping with the goals of this investigation. With further ANN development and evaluation in closed-loop control, this method shows some potential.

8.7.2.6 Direct ANN Throttle Curve Optimisation (DANNTCO)

A similar investigation used for the DANNCVCO controller was applied to throttle position optimisation. Here, the best throttle position is determined by iteratively modifying its value within an ANN model to find the greatest acceleration. Furthermore, the ANN model is different to the DANNCVCO because it excludes engine cut inputs, and is trained using METC data. In practice, however, this method proved to be much less reliable than the DANNCVCO controller, and no attempt was made to investigate this type of controller further. The reason for the failure is considered to be a result of the ANN model becoming confused between whether throttle or tyre slip cause vehicle acceleration.

8.7.2.7 Direct ANN Slip Curve Optimisation (DANNSCO)

The DANNCVCO concept was again repeated for slip optimisation, in an attempt to remove engine dynamics from the ANN models and increase performance. In this case, slip/longitudinal acceleration curves are produced, and the instantaneous maximum acceleration and optimum slip determined. This has a number of conceptual benefits, including the ability to directly relate the ANN curves with theory, the fact that the chassis becomes a generic controlled element, that the “aim slip” output is easy to comprehend, and that separate (and possibly better) controllers can be used to ensure the aim slip is achieved at the wheels. It also provides the possibility of additional types of control, such as active dampening, to be easily incorporated into the control scheme for future research.

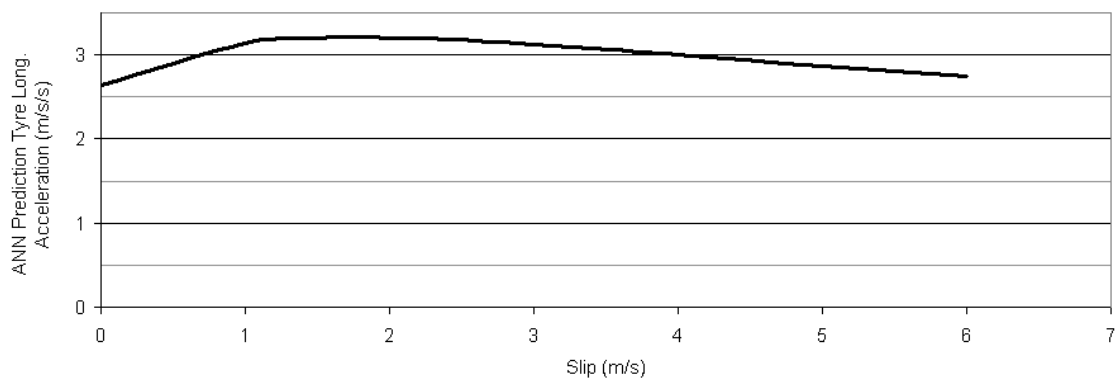


Figure 8.37: Typical DANNSCO prediction of tyre long. acceleration for varying slip

The results from this controller are show promise. Figure 8.37 shows a typical ANN prediction of the slip/longitudinal acceleration curve. It resembles the curves provided

within the theory, although the prediction in the linear range is poor. This is to be expected to some degree, because the linear region represents an “extreme” in the curve, and the ANN generalisation abilities cannot be expected to extend this far. It is the shape of the curve in the transition region that are of most interest, and this appears approximately correct. In fact, the prediction of 1.8m/s optimum slip correlates to the observed DEMTC optimum slips for the straight-line case used in this example.

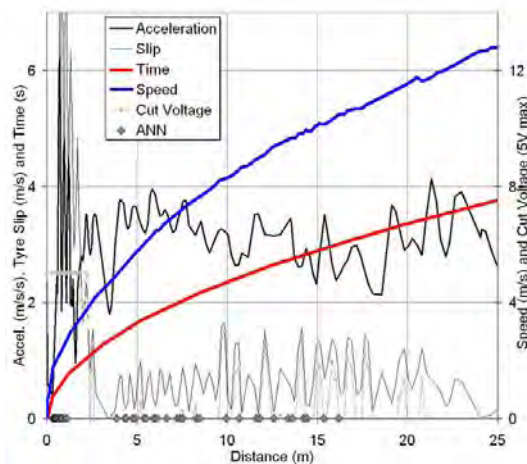


Figure 8.38: DANNSCO prediction of if traction control is needed for best straight-line acceleration for 3km/hr METC

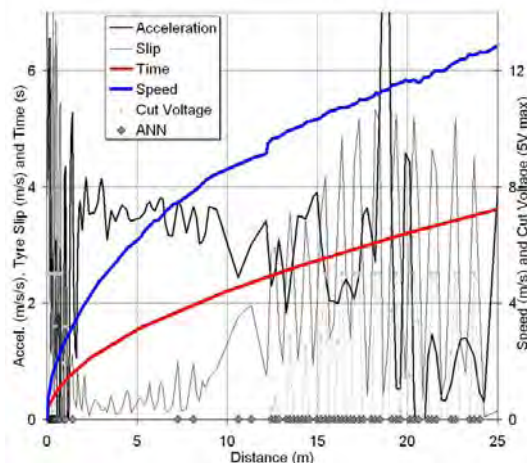


Figure 8.39: DANNSCO prediction of if traction control is needed for best straight-line acceleration for 10km/hr METC

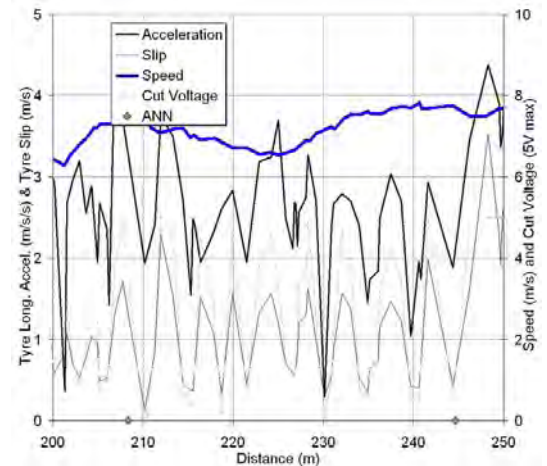


Figure 8.40: DANNSCO prediction of if traction control is needed for best constant circle acceleration for 1km/hr DEMTC

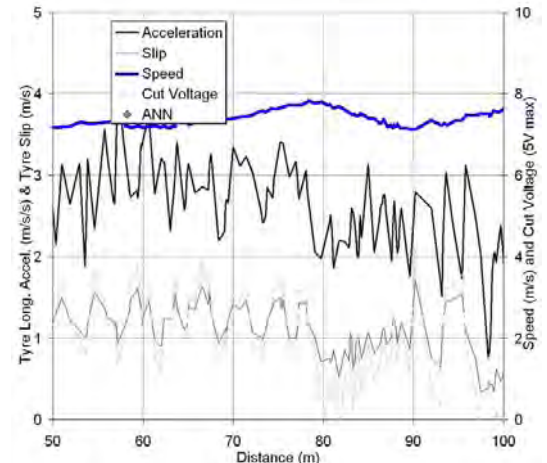


Figure 8.41: DANNSCO prediction of if traction control is needed for best constant circle acceleration for 2km/hr DEMTC

The off-line testing results are provided in Figure 8.38 to Figure 8.41, although simple binary ANN control is presented instead of the ANN control voltage shown previously. This is a result of the type of information that can be derived from this manner of control, with the engine cut voltage needing to be determined from the aim slip value

elsewhere. It can be seen, however, that the controller appears to operate well in some cases and erroneously in others. As such, it is clear that this controller has potential in this application, and could provide the required performance with additional investigation.

8.7.2.8 Direct ANN Front Left and Right Slip Curve Optimisation (DANNFLRSCO)

In an attempt to build on the positive findings of the DANNSCO controller, a modification was attempted to determine optimum slip at each driven wheel. In this way, a new ANN model was developed that used left and right driven wheel slips as input (instead of just average driven slip) and was used to create a slip/longitudinal acceleration curve for each driven wheel. While the concept is the same for the DANNSCO controller, this model would provide control signals that could be implemented with active brake control for improved performance.

As expected the results were worse than the DANNSCO prediction. Furthermore, the results would not provide any additional benefit in this traction control research, so was abandoned.

8.7.2.9 Direct ANN Slip Prediction Comparison (DANNSPC)

As covered in the IANNCVC, IANNTC and IANNSC controllers, simple comparison of to ANN models can provide enough data to determine if the vehicle is stable or unstable. Here one model predicts the current acceleration of the vehicle, and another predicts the acceleration of the vehicle at slightly reduced slip. If the acceleration is equal to or greater in the second model, then the vehicle is unstable. If it is lower, then the vehicle is stable.

It is noted, however, that while this information is useful, it cannot be easily implemented into a control algorithm. Instead, a method was tested that increased the engine cut based on a preset gain for each control sample. For example, when the vehicle was first considered unstable, an engine voltage cut of 0.5V was used. If the vehicle remained unstable at the next control iteration this value would increase to 1.0V, then 1.5V, and so on. Once vehicle stability was returned, the output would return to 0V. Unfortunately, however, this type of control was not very effective.

8.7.2.10 Direct ANN Slip Prediction Comparison – MoTeC Emulation (DANNSCP-ME)

Combining the DANNSPC and DEMTC controllers produce another control option, in which the ANN predictions are used to program the control constants for traditional traction control. The ANN can be trained to model the dynamics of the vehicle, and as the vehicle drives around the test track and specific conditions are met, the MoTeC traction control parameters are programmed automatically. The performance of the ANN predictions could be directly compared to the MoTeC parameters that were determined through prior investigation, enabling simple performance evaluation. In practice, however, this method proved to be difficult to implement, and did not produce the levels of performance required to warrant further work.

8.7.3 Final Direct ANN Slip Curve Optimisation Development

The DANNCVCO and DANNSCO models both show greater stability control performance possibilities than the other models. However, both of these controllers have the same underpinning operation philosophy, and proving one will show significant promise in the other. As such, a decision was made to pursue only one model for the remainder of the research. This would allow resources to be devoted to developing and analysing a specific model, instead of developing two in parallel with significantly more effort for little gain.

To this end the DANNSCO model was selected for further analysis, based on a number of observations. Firstly, the DANNSCO controller models the vehicle dynamics only, and engine data is not required. Conceptually this reduces the modelling load of the ANN models, and intuitively should result in greater accuracy. The DANNSCO controller is also less of a “black box” than the DANNCVCO, because it shows the intermediate step of determining optimal slip. This has the benefit of allowing non-ANN controllers to control the actual wheel torque based on ANN predicted aim values, which may further improve performance in these specialised control circumstances. Thirdly, the derivation of optimum slip is a value that is easy to conceptualise, and will allow additional types of performance comparisons to be made. Finally, the DANNSCO model is more generic in structure than DANNCVCO because it deals with slip rather than specific control inputs, such as engine cut voltage. This has the added benefit that this model can be simply modified to perform other types of wheel control to produce

maximum acceleration, such as brake control, active damping, active ride height, active anti-roll and active camber.

While the DANNSCO controller appears to work reasonably well, there is still significant room for improvement. This is to be expected, however, because the ANN model development had only proceeded through one stage. Appropriate ANN inputs have been determined to try and ensure the ANN produces relevant process generalisations. However, different internal architectures were not pursued, nor were different ANN model types. These different options can significantly improve model accuracy, and should be explored. Furthermore, the ANN training data set could be improved further by providing more testing conditions, including those that cover the “Figure of Eight” and “Miscellaneous” testing tracks. These improvements are explored in this section and thoroughly analysed for off-line performance.

8.7.3.1 Architecture

As in the surface identification chapter, the effect of different internal architectures on ANN model accuracy can be investigated by training many ANN models. Figure 8.42 shows the results of training 46 ANN models, each with different internal architectures. Each of these models take up to 12hr to train, and as a result this represents a significant investigation.

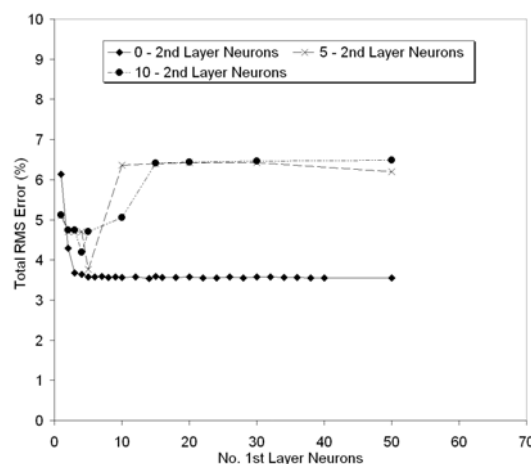


Figure 8.42: Effect of model architecture for DANNSCO testing data (15 input, tyre long. accel. output)

Single hidden layer (0nd Layer) architectures produce better testing results, and 1st layer neurons above around 5 have little effect on model accuracy. Close observation however, shows that the 22 1st layer, 0nd layer (22x0) architecture results in the lowest

error overall. As such, this architecture is used in all subsequent investigations. The histogram of the error that this ANN produces is also given in Figure 8.43.

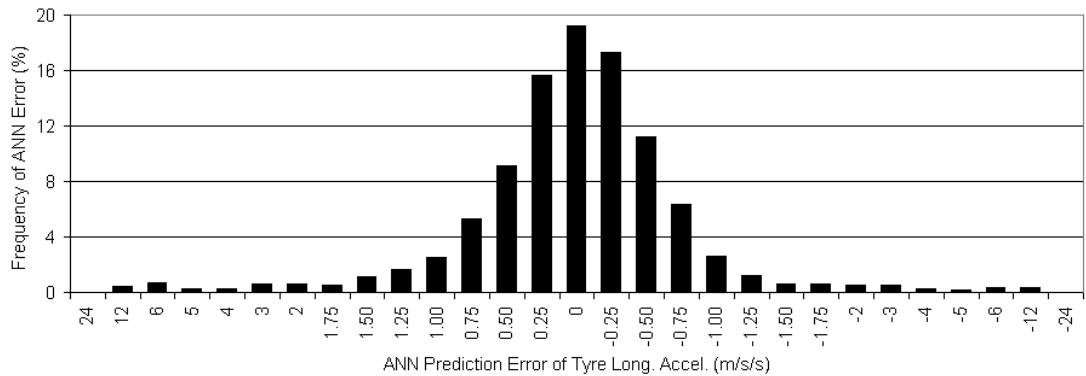


Figure 8.43: Testing prediction error histogram for long. accel. output 15 input 22x0 DANNSCO model

The error in this case fits a “Bell” curve quite well, and indicates good ANN training. In particular, the ANN model is not “biased” towards an extreme, which is a common ANN training problem. It is noted, however, that errors of up to 1m/s^2 are relatively common within the model, and care should be taken to ensure that these absolute errors are not propagated through the control logic. Instead, the ANN model should be used to highlight general relationship trends, which would negate much of this error.

8.7.3.2 Models

The ANN used to date in this stability controller investigation is of the feedforward backpropagation (FFBP) type. The input and output parameters used within the ANN model are normalised into the 0 to 1 range. This forms the most common form of ANN modelling, and has been proven in many applications over a long period of time.

This type of model is known to have a number of limitations in modelling some systems, and as such it is a worthwhile pursuit to investigate other ANN possibilities. The type of normalisations, for instance, can have a significant influence on how inputs are represented within an ANN model. For example, consider the steering wheel angle with a range of -540 to 540° . The usual normalising method would make $-540^\circ=0$ and $540^\circ=1$, drastically shifting the zero value. In this case a -1 to 1 normalisation method may be more appropriate because the zero value would not move. To this end, three normalisation types are presented and include the 0 to 1 and -1 to 1 method discussed here. The third method simply divides each input and output magnitude by a number that will ensure it operates within the -1 to 1 range, but does not explicitly normalise the

data. These results are shown in Figure 8.44, Figure 8.45 and Figure 8.46, and were derived from suitably modifying the ANN training program that was developed in LabVIEW.

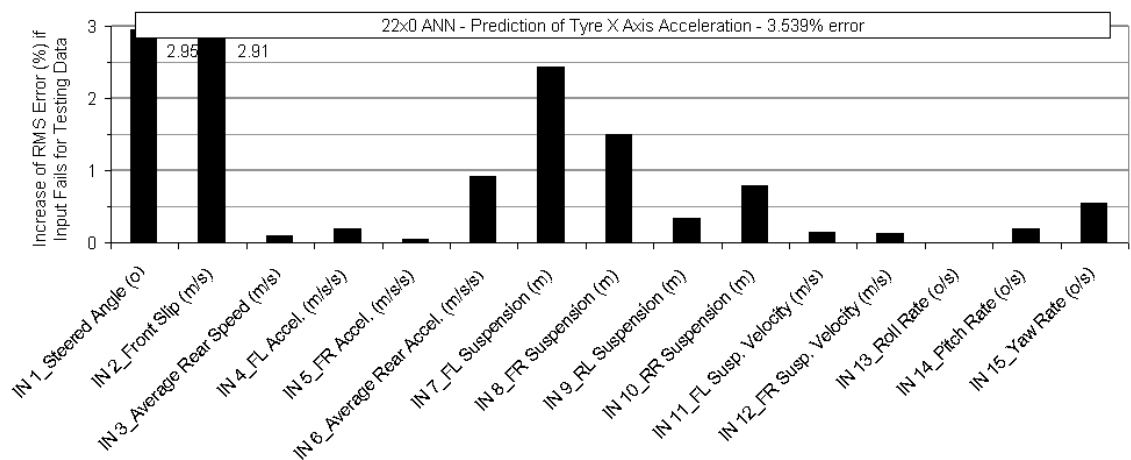


Figure 8.44: Input importance analysis for long. accel. output of 15 input FFBP 0 to 1 normalisation DANNSCO model

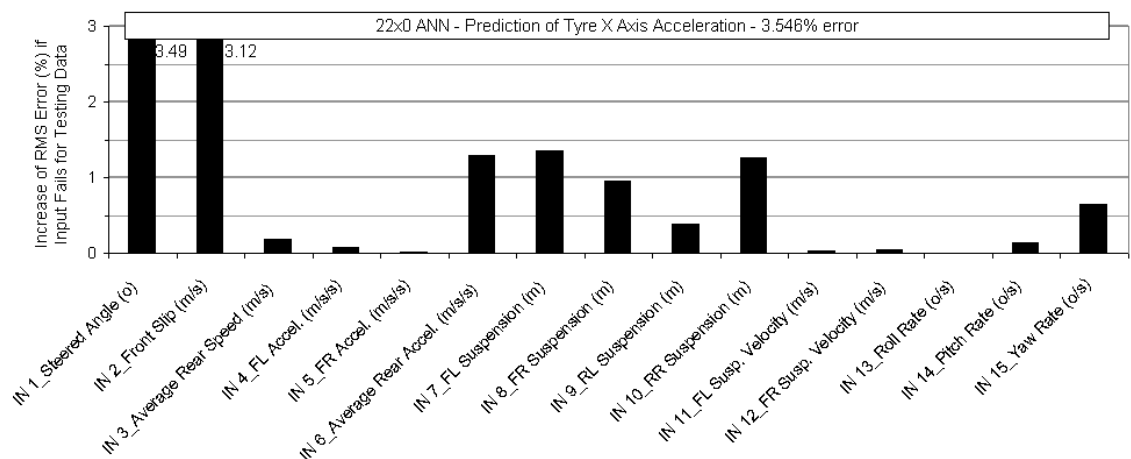


Figure 8.45: Input importance analysis for long. accel. output of 15 input FFBP -1 to 1 normalisation DANNSCO model

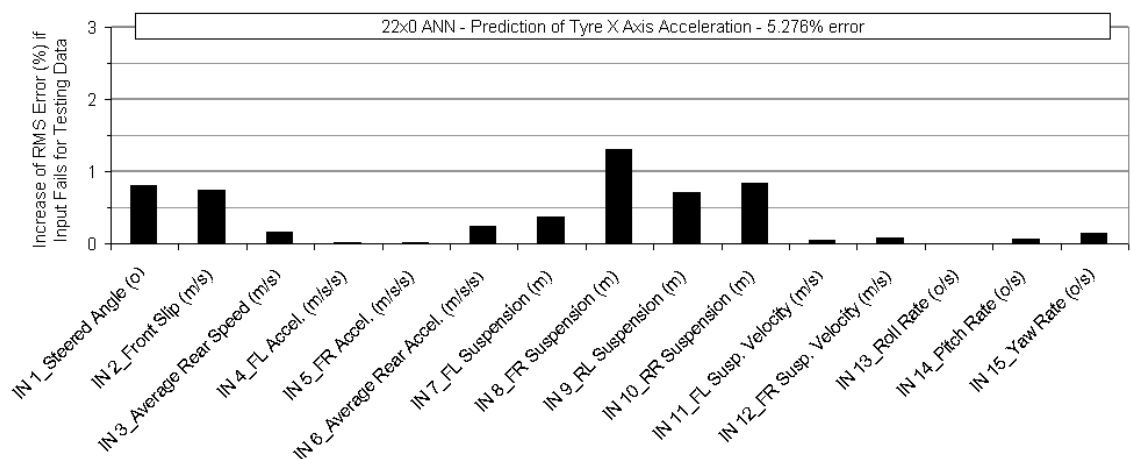


Figure 8.46: Input importance analysis for long. accel. output of 15 input FFBP magnitude scaled DANNSCO model

The 0 to 1 normalisation process is the most effective here, although the -1 to 0 method shows similar performance. As a result it is concluded that the normalisation method does not have a large impact on the quality of the prediction, and the 0 to 1 method is used for the rest of the work.

Further model improvements can be found by altering the structure of the neurons within the feedforward model. In particular, adding extra neurons at the input and hidden layers that produce constant outputs has been shown to avoid ANN bias problems. The outputs of these neurons provide a constant value to each of the neurons in subsequent layers, and the interconnection weight is updated in the same manner as other neurons. In this fashion individual neurons can call on this bias value as needed to complete their error minimisation problem. As such, these neurons are called “bias neurons”. The result of this method is given in Figure 8.47.

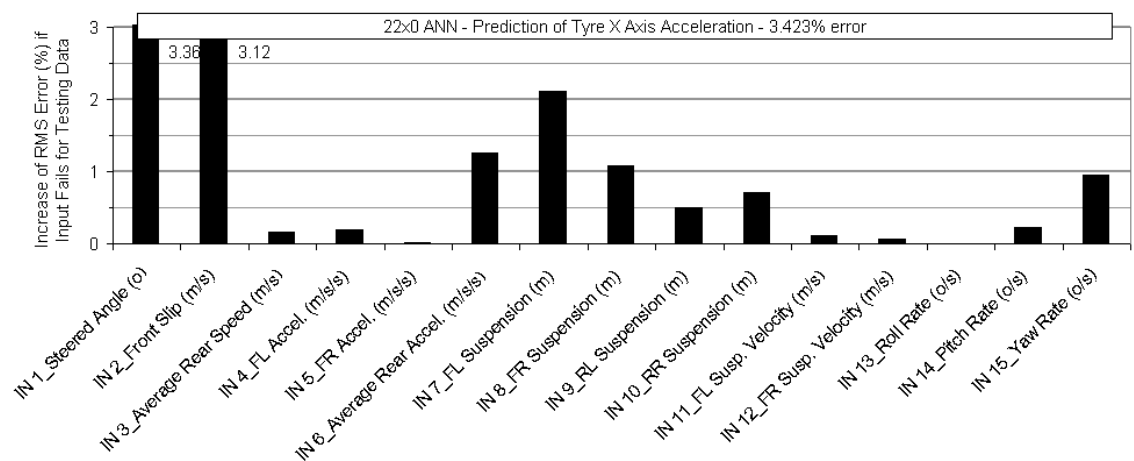


Figure 8.47: Input importance analysis for long. accel. output of 15 input FFBP bias neuron inputs DANNSCO model

FFBP accuracy can be improved by replacing some of the neuron sigmoid activation functions with linear activation functions. Specifically, by replacing the activation function of a single neuron within each of the hidden layers with a linear function, a “linear modelling path” can be established. In this way, the non-linear modelling capability of the ANN model can be complemented with a linear modelling ability, with greatly improved performance in some applications. Combined with bias neurons, this represents potential in improving ANN performance in this application, with the results shown in Figure 8.48.

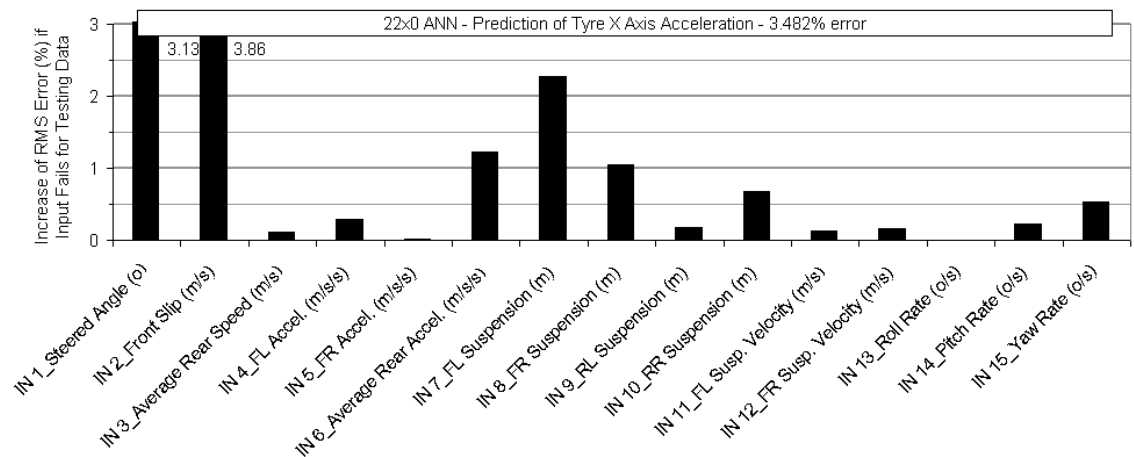


Figure 8.48: Input importance analysis for long. accel. output of 15 input FFBP bias neuron inputs and linear neurons DANNSCO model

Finally, the “Optimised Layer by Layer (OLL)” model offers potential in this application also. In particular, the rapid learning rate that this method is known has capacity for significant training improvement, especially if adaptive control is to be implemented in future work. The structure of this model is no different to the standard feedforward single layer ANN, although the training process is vastly different. Instead of iteratively backpropagation error to update weights, the training process actually mathematically determines the correct weights after seeing the response of the ANN to the entire training set. It does this first for the output layer, and then based on its response alters the entire hidden layer weights. This process is repeated a small number of times until error is low. The training results are given in Figure 8.49.

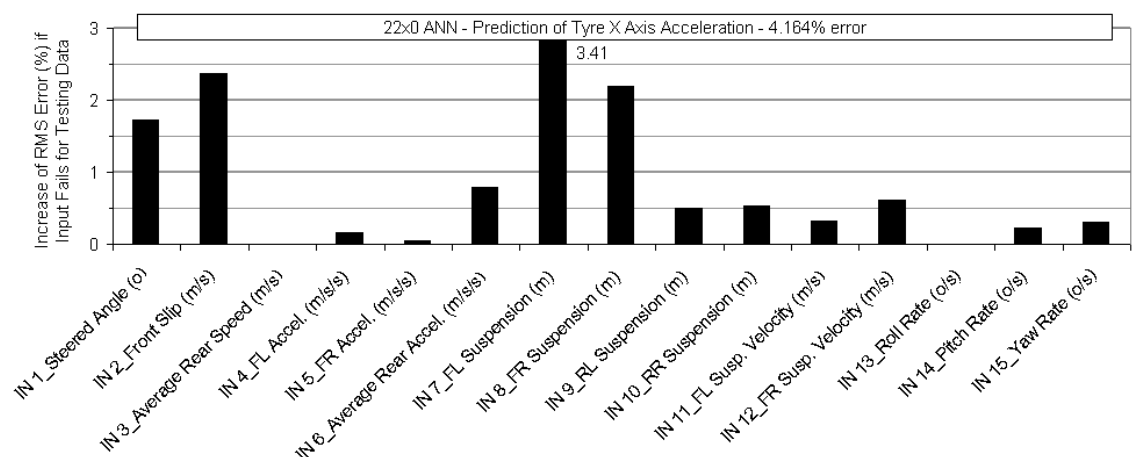


Figure 8.49: Input importance analysis for long. accel. output of 15 input OLL DANNSCO model

Clearly the OLL model contains greater error in this case. Furthermore, the OLL training actually took significantly longer than FFBP. It is believed that this is the case

because the OLL model was developed for small training sets, whereas this one is very large. In particular, the number of ANN inputs and the sheer size of the training files required very large matrices to be produced. These matrices could not be contained in the computer RAM, and required constant hard drive access. This slowed the train process immensely, and meant that even after a massive amount of training time the ANN still exhibited higher error than expected.

The bias neuron ANN exhibits the least error overall. However, the DAQ control program was developed initially to only accept normal FFBP networks, and the incorporation of bias neuron ANN models into it would have required additional complexity. To this end, and considering that the bias neuron ANN is only 0.12% better than the 0 to 1 FFBP, it was decided to use the FFBP ANN in all further research.

8.8 Performance Appraisal of ANN Control

The performance of traction controllers is difficult to evaluate. Intuitively, the best controller can be determined by observing the effects of altering various parameters, and then choosing the best configuration. This is, in fact, the method that tradition traction controllers and the MoTeC traction controller use to determine appropriate settings. It does produce a number of problems, however.

The MoTeC traction controller, for instance, can be tuned relatively easily by setting aim slips for different throttle positions and adjusting two controller gain parameters. This reduces the scope of the traction controller tuning, and makes selection of the settings that produce better performance easier. As traction control systems become more complex this becomes a much harder task, and determination of optimal tuning ceases to be intuitive. In particular, the ANN controller is capable of adjusting aim slip prediction as a function of vehicle speed, wheel load, camber angle, slip angle, transient tyre effects, etc., which all form part of the “black box” ANN model. This massively increases the scope of traction control, and produces many condition combinations that are not possible to explore in any meaningful way.

This problem can be highlighted through the following example. The DEMTC tuning shows that the general optimal wheel slip for the test surface in a straight line is around 1.4 to 2.0m/s, depending on the speed the vehicle is traveling. This data was acquired by

simply averaging the vehicle acceleration to slip relationship within different speed ranges, and as such this “optimum” slip is average in nature. In fact, it is entirely possible that the optimal slip actually varied wildly during the acceleration manoeuvre based on complex vehicle/tyre/pavement relationships, which is not reflected in the average optimal slip figure. In short, the METC and DEMTC tradition controller methods must make large compromises in the control of the system, whereas the ANN model attempts to control all aspects of the dynamic process. As such, they cannot be easily compared.

Furthermore, the actual concept of optimal slip is difficult to prove when more than one or two parameters are involved. It is easy to look at a slip/longitudinal acceleration curve to determine optimal slip, even though such a graph can be difficult to obtain. When another parameter is introduced, such as vertical load however, the three dimensional relationship is harder to observe and optimal slip is harder to find. When there are many more parameters this process becomes extremely difficult. As such, when the ANN model derives an optimal slip value, it is incredibly challenging to evaluate its accuracy by comparing it to a known quantity.

These problems mean that the ANN controller cannot be fully evaluated without access to high quality tyre testing machines, and without exhaustive practical testing on the track. Without these forms of evaluation, it will not be totally clear if the optimal aim slip predictions are accurate.

This does not mean that this investigation cannot provide any evidence to support or rebut ANN control, however. By applying general traction controller evaluation methods it can be shown whether the aim slips are approximately correct, and if the ANN controller has performance that exceeds traditional control. This would prove the concept and application of ANN stability control, although it is noted that a full understanding of its dynamics will only come with an increased level of facilities and expense that is beyond the scope of this research.

8.8.1.1 Off-Line Verification of Aim Slip Prediction

The first step of controller evaluation is to identify if the ANN predictions of optimum slip appear to be in the correct range. This was done with the off-line METC and DEMTC data that has been used above.

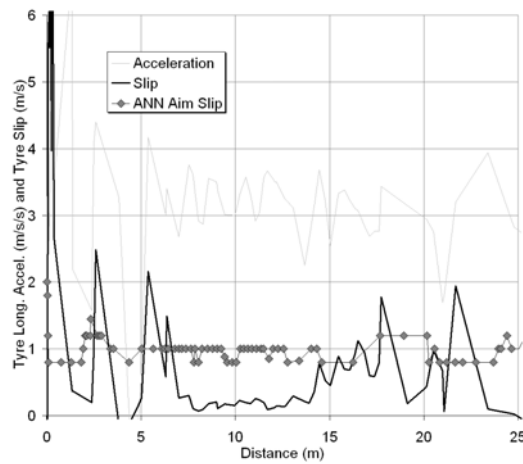


Figure 8.50: DANNSCO prediction of aim slip for best straight-line acceleration for 0.5km/hr METC

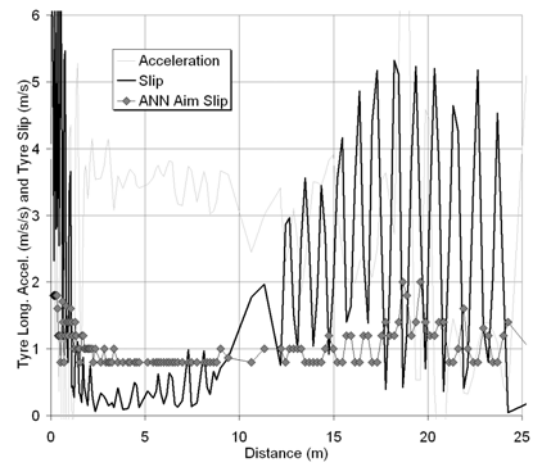


Figure 8.53: DANNSCO prediction of aim slip for best straight-line acceleration for 10km/hr METC

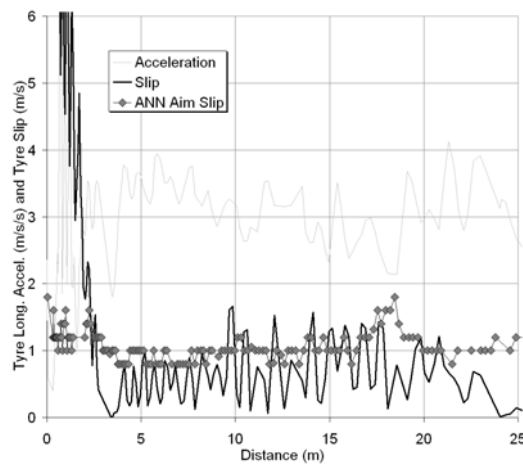


Figure 8.51: DANNSCO prediction of aim slip for best straight-line acceleration for 3km/hr METC

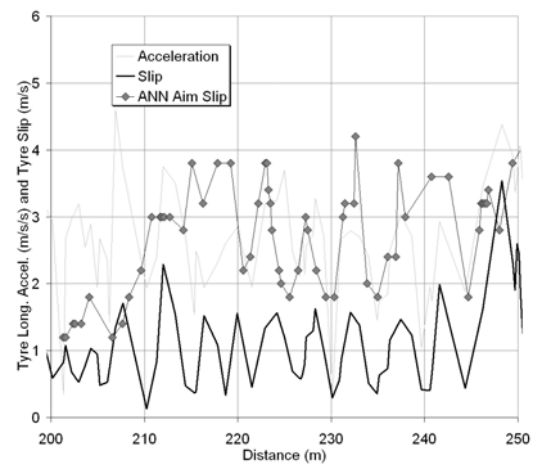


Figure 8.54: DANNSCO prediction of aim slip for best constant circle acceleration for 1km/hr DEMTC

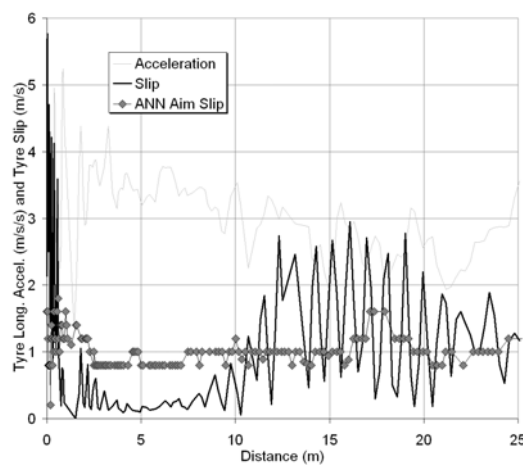


Figure 8.52: DANNSCO prediction of aim slip for best straight-line acceleration for 5km/hr METC

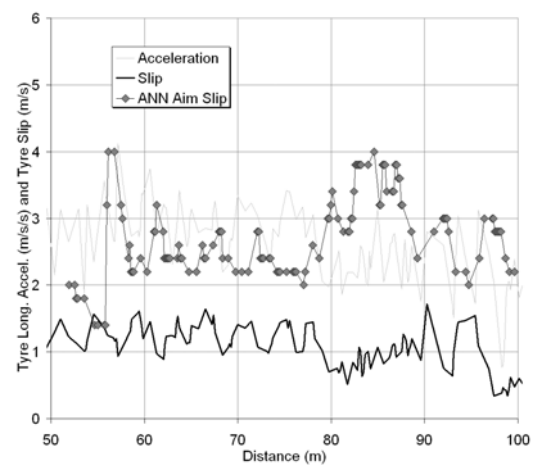


Figure 8.55: DANNSCO prediction of aim slip for best constant circle acceleration for 2km/hr DEMTC

Figure 8.50 to Figure 8.53 shows the ANN optimum aim slip predictions for the better straight-line METC acceleration runs (at different METC aim slips). Figure 8.54 and Figure 8.55 shows the ANN optimum aim slip predictions for the circle manoeuvre.

For the straight-line case, it can be seen that the ANN optimal aim slip varies through approximately the 0.8 to 1.6m/s range, but mostly falls at 1.0m/s. This is slightly lower than the values stated as optimal earlier within this chapter, but closer observation of Figure 8.13 to Figure 8.15 shows that this is still extremely close to the maximum longitudinal acceleration value, and is a very encouraging result.

Furthermore, the fact that the optimum slip value seems to alter with changes in vehicle state is a promising feature. In particular, each of the straight-line launches show a clear increase in the ANN optimal slip. This is consistent with the concept of “launch control” and shows that the ANN has learnt that controlling the tyre for optimum acceleration at launch is a special case.

Focusing on the circle manoeuvre cases, the optimal slip also varies to a significant level, but have a mean of around 2.7m/s. This mean value is consistent with the previous observed maximum, and shows that the controller has a good grasp of the dynamics of the process. In Figure 8.54, the large variations in actual slip (as a result of the DEMTC operation) cause a partially corresponding variation in ANN optimum slip, while Figure 8.55 has a smaller variation in actual slip and in optimum slip. This could be for two reasons. One possibility that has been discussed earlier, is that when there is a large difference between the current condition (the actual slip) and the predicted optimum condition (the ANN slip) the ANN prediction loses accuracy. Another possibility is that the constant variation in actual slip (and vehicle acceleration) introduces significant transient effects within tyres, which in turn alters the optimum slip as the results indicate.

Additional evidence on the performance of the ANN controller can be found in Figure 8.56 to Figure 8.61. Here, the average slip curves at different speeds presented previously, are overlaid with the predictions of maximum acceleration at optimum slip for the same off-line data set.

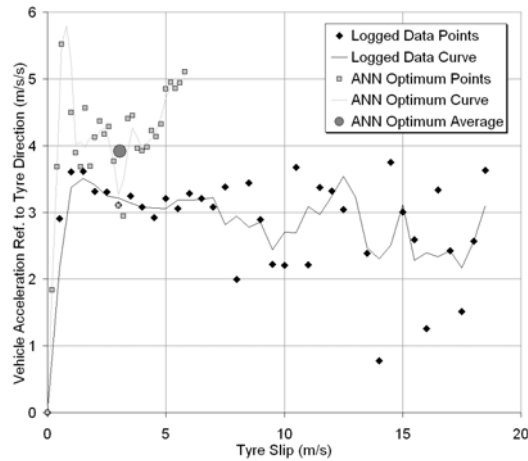


Figure 8.56: Average slip and vehicle straight-line acceleration DANNSCO comparison for 0 to 2.5m/s speed

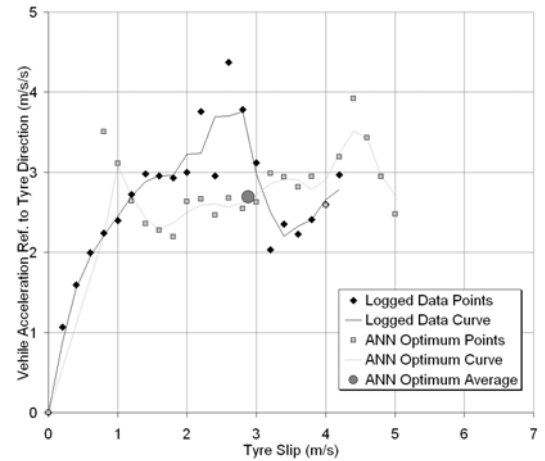


Figure 8.59: Average slip and tyre long. accel. DANNSCO comparison for circle manoeuvre 6.5 to 7.5m/s speed

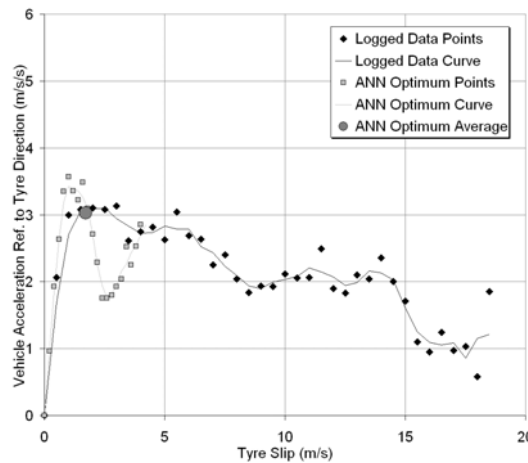


Figure 8.57: Average slip and vehicle straight-line acceleration DANNSCO comparison for 2.5 to 7.5m/s speed

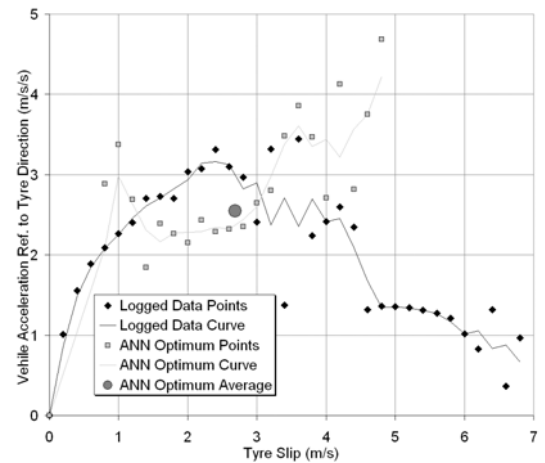


Figure 8.60: Average slip and tyre long. accel. DANNSCO comparison for circle manoeuvre 7.5 to 8.5m/s speed

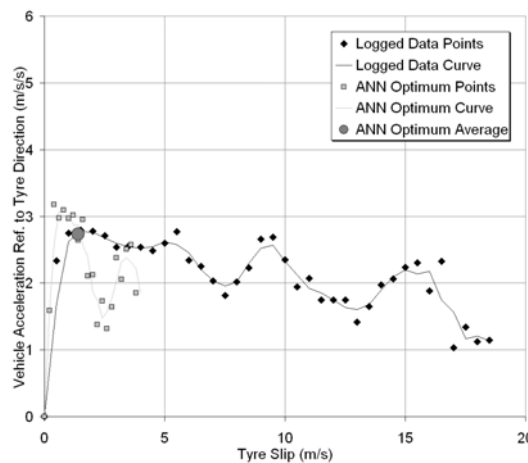


Figure 8.58: Average slip and vehicle straight-line acceleration DANNSCO comparison for 7.5 to 12.5m/s speed

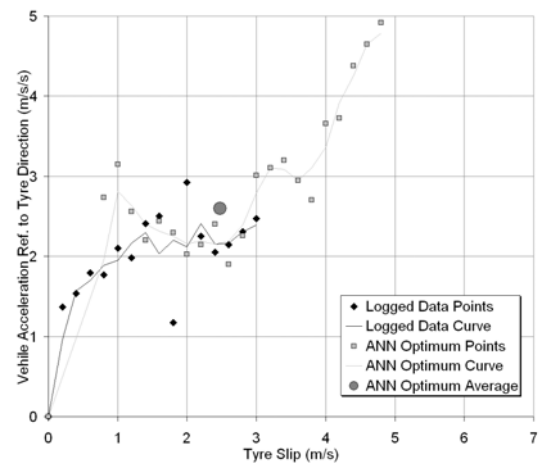


Figure 8.61: Average slip and tyre long. accel. DANNSCO comparison for circle manoeuvre 8.5 to 9.5m/s speed

It is important to realise that the overlaid curves are not directly comparable. The logged data simply shows average acceleration performance of the vehicle for each specific speed/slip combination, in an attempt to produce general slip curves for the surface. The ANN optimum slip curves represent a different process entirely. Here, the ANN takes the vehicle parameters and predicts the optimum slip and corresponding maximum acceleration, with this data averaged for different speed and slip conditions. As such, one curve represents the general characteristic of the surface, while the other represents the general optimum values.

Considering the straight-line conditions first, there are a number of observations that can be made. Firstly, the optimum predicted slips are confined within the approximate 0.2 to 5m/s region, which clearly shows the ANN model has determined that large slips correlate with reduced acceleration. The 2.5-7.5m/s and 7.5-12.5m/s curves also show another feature, with the predictions of maximum acceleration at low optimum slips higher than with increased slip. In these cases, optimum slips in the 0.2 to 2.0m/s range are predicted to consistently produce greater acceleration than the off-line testing data realised. It can be inferred that if the ANN predicted aim slips are implemented on the vehicle (with rapid response and accuracy) then the achieved vehicle acceleration should surpass the METC and DEMTC systems by up to 16%.

Worthy of note, high acceleration gains can only be realised through part of the off-line data. This is evident at slips above 2.0m/s, because the ANN predictions show there are some conditions where maximum acceleration should be less than the general curve suggests. This seems counter-intuitive at first glance, but is still consistent with accurate ANN predictions. The logged data is simply what has been observed, and the ANN data consists only of optimum slip conditions. As such, it can be inferred from the data that when conditions arise that require unusually high optimum slips, that maximum accelerations will generally be lower.

These observations are based on assumptions of the dynamics of the process. While it is fairly apparent in these two cases that the ANN is behaving as might be expected (with some conditions requiring different optimum slips), no mathematical 'rule' that may prove its performance has been presented. To this end, the concept of average ANN prediction of optimum slip will be introduced.

The logged data slip curve provides a very good indication of what the general optimum slip value is, being the slip at the peak of the transition region. This value can be considered the average optimum slip for all of the off-line data. Furthermore, because the ANN optimum slip evaluation was completed for the same data set, the average ANN optimal slip should correspond to the average logged optimal slip. In this way, the performance of the ANN predictions can be directly evaluated. This is a very valuable comparison and, as can be seen for the two straight-line cases, the ANN accuracy is extremely good (because the ANN optimum average dot overlaps the critical slip for the general surface). In addition, the average ANN prediction of maximum acceleration should also correlate to the critical acceleration, which is also evident in these two cases. Worthy of note is that this value is not required for control and is significantly susceptible to error due ANN limitations and the way it is derived.

Now considering the 0-2.5m/s straight-line case three features are evident, and include the constant high prediction of maximum acceleration, a higher average ANN optimum slip and a higher average ANN maximum acceleration. The logged data contains a large degree of scatter, which is a result of the vibration and launch dynamics complexities when first accelerating.

Moving now to the three circle cases, they are each very similar, with the only notable differences being that acceleration decreases at increasing speed and that the 8.5-9.5m/s curve is incomplete. Most notably is that the average optimum values in the first two cases correlate very well. For the 6.5-7.5m/s case the ANN optimum and logged optimum slips are 2.9 and 2.6m/s respectively. For the 7.5-8.5m/s case these values are 2.7 and 2.4m/s. Clearly, the ANN predictions of optimum slips are of high quality in a general sense. A noteworthy observation is that the ANN seems to be under-predicting optimum acceleration except at high slips. This produces an interesting question as to how the ANN in predicting optimum acceleration and how it will operate within a closed-loop controller. According to the ANN model, maximum acceleration can be obtained at very high and very low slips, while moderate slips produce moderate acceleration. If this is simply how the dynamics of the system work (which is entirely possible due to transient effects) then the ANN should provide very good control. However, if the ANN has mislearned the process dynamics, this will probably result in divergent behaviour (where the controller will either allow no slip, or very high slip). This would be clearly undesirable, and would

become evident very quickly during closed-loop on-line testing. As such, this form of testing provides another performance verification tool.

8.8.2 On-Line ANN Controller Performance

On-line testing provides a number of benefits above all of the off-line testing to date. Of greatest benefit, however, is the ability to compare the ANN control to other methods so it can be determined if it provides improved control. In this way, if its control is proved to be similar or better than current systems, then the internal ANN prediction accuracy can be assumed to be high. Furthermore, on-line testing highlights the ability of the controller to be utilised in a simple manner in a real-life scenario, which is in stark contrast to other ANN investigations that rely on simulated control. In short, a positive outcome in on-line testing would provide a compelling argument for ANN adoption into stability control.

Before this can happen the DANNSCO method must be integrated into a wheel slip controller. The DANNSCO prediction of aim slip can be used as an additional input to a traditional wheel slip controller to produce ANN traction control. The ANN part of the traction controller can determine the optimum (aim) slip for the driven wheels for the given dynamic condition, and the traditional controller can control the wheels to try and realise this value. To this end, the DANNSCO model is fitted in series with a simple gain controller identical to the one used in the DEMTC model, where measured slip above the aim slip induces a proportional engine cut voltage. The amount of engine cut is therefore determined from the slip difference and the static gain of the system, which must be manually tuned (as was necessary for the METC and DEMTC models).

An unfortunate side effect of the required high level of computation of the DANNSCO model, however, is that it can only just maintain a 50Hz sampling rate. Furthermore, the Microsoft Windows 98 operating systems uses resources in an unpredictable way, and sampling rates of as little as 10Hz were observed in practice. This would have a large and negative effect on the performance of the system. As a small “stop gap” to this problem, however, the DAQ control program was altered so that the ANN aim slip was made available to the slip controller for every while loop iteration, not simply every time the ANN computes a new value. This improved performance to a small extent.

The first stage of on-line ANN testing required the best gain value to be chosen, and was completed in a similar way to METC and DEMTC gain parameters. Specifically, many

straight-line runs were made at different gain amounts, and the gains that repeatedly showed the best performance were chosen. This produced the results shown in Table 8.4.

Controller Gain (Vs/m)	Speed at 25m (m/s)	Average Accel. 0m to 25m (m/s/s)	ANN Average Optimum Slip 0m to 25m (m/s)	Cumulative ANN Average Optimum Slip 0m to 25m (m/s)	Average Slip 0m to 25m (m/s)	Cumulative Average Slip 0m to 25m (m/s)	ANN Average Optimum Slip 5m to 25m (m/s)	Cumulative ANN Average Optimum Slip 5m to 25m (m/s)	Average Slip 5m to 25m (m/s)	Cumulative Average Slip 5m to 25m (m/s)
1.5	13.60	3.42	1.10	1.10	0.81	0.81	1.10	1.10	0.72	0.72
1.5	13.52	3.17	1.28	1.19	0.76	0.79	1.11	1.11	0.91	0.82
1.5	13.47	3.22	1.18	1.19	0.46	0.68	1.12	1.11	0.65	0.76
1.5	13.44	3.38	1.13	1.17	0.48	0.63	1.11	1.11	0.63	0.73
1.5	13.40	3.05	1.28	1.19	0.67	0.64	1.11	1.11	0.86	0.75
0.5	13.10	3.30	1.20	1.20	2.94	1.02	1.20	1.13	2.24	1.00
0.1	13.10	4.37	1.17	1.17	2.84	2.84	1.15	1.15	3.27	3.27
0.5	13.07	3.05	1.21	1.19	1.56	1.32	1.17	1.13	1.28	1.32
1.0	13.00	3.10	1.28	1.20	0.57	1.23	1.19	1.14	0.46	1.22
1.0	12.92	3.07	1.28	1.21	0.94	1.20	1.18	1.14	0.65	1.17
1.0	12.89	3.30	1.16	1.21	0.74	1.16	1.13	1.14	0.89	1.14
0.5	12.85	3.44	1.18	1.20	3.12	1.32	1.21	1.15	2.41	1.25
1.0	12.83	3.08	1.22	1.21	0.62	1.27	1.15	1.15	0.59	1.20
0.5	12.82	3.81	1.19	1.20	3.48	1.43	1.20	1.15	3.08	1.33
0.5	12.80	3.63	1.17	1.20	2.60	1.51	1.15	1.15	2.30	1.40
1.0	12.79	2.81	1.34	1.21	0.86	1.47	1.15	1.15	0.88	1.36
0.1	12.48	3.97	1.18	1.21	1.92	1.49	1.23	1.16	1.89	1.39
2.0	11.73	2.50	1.36	1.22	2.06	1.52	1.34	1.17	1.95	1.43
2.0	11.71	2.60	1.30	1.22	2.50	1.58	1.33	1.18	2.54	1.48
2.0	11.62	2.41	1.38	1.23	2.40	1.62	1.39	1.19	2.31	1.53
0.1	11.59	2.46	1.40	1.24	6.25	1.84	1.52	1.20	6.88	1.78
2.0	11.55	2.45	1.37	1.24	1.97	1.84	1.32	1.21	2.13	1.80
0.1	11.46	2.27	1.54	1.26	7.03	2.07	1.61	1.22	6.54	2.00
0.1	11.43	3.48	1.44	1.26	2.12	2.07	1.64	1.24	1.83	2.00
2.0	1.73	2.60	1.39	1.27	1.51	2.05	1.29	1.24	1.60	1.98

Table 8.4: Summary of top five DANNSCO straight-line accelerations for different controller gains

The gain of 1.5Vs/m produces the best results, and this value was used for all following investigations. However, the controller is limited in its ability of actually realising the ANN aim slip. In particular, the best acceleration run shows an ANN average aim slip of 1.1m/s and an actual average slip of 0.7m/s, which seems to be a common with other cases. In principle, this should limit vehicle performance to a degree, although it is noted that this level of variation is also the case for the METC and DEMTC methods. As such, some deviation from the optimal performance can be expected. However, because each of the METC, DEMTC and DANNSCO control methods exhibit similar control limitations, they are comparable to a degree. In fact, the slightly slower sampling time of the DANNSCO controller puts it at the greatest comparable disadvantage, meaning a positive result will have increased bearing.

Figure 8.62 and Figure 8.63 show the closed-loop on-line DANNSCO control results for the best performing straight-line and circle manoeuvres. By presenting the results in this way, the DANNSCO performance can be observed by comparing the aim and measured slips. Since these are the best runs, both of these curves should be similar, although it is noted that controller limitations means that the aim slip can rarely be accurately realised. In particular, the “ANN Aim (Optimum) Slips” are updated at a slower rate than for the

DEMTC case, indicating a slower rate of control. This means that the DANNSCO controller has less ability to react to rapid changes to wheel slip, and that excessive slip is sometimes countered too late and that the corrective engine cut can be too severe.

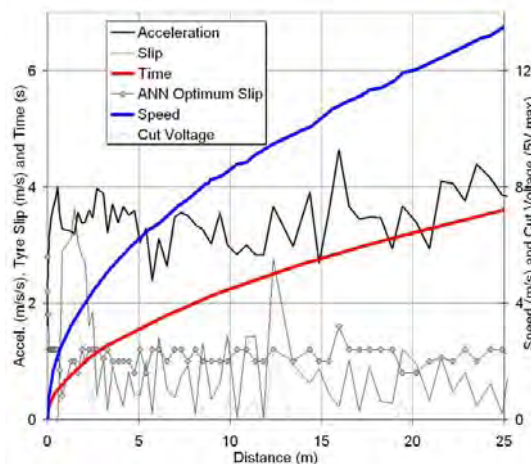


Figure 8.62: DANNSCO performance for best straight run

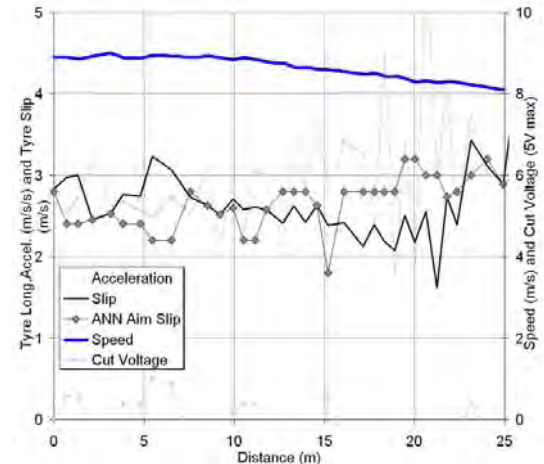


Figure 8.63: DANNSCO performance for best 25m circle segment

Regardless of this problem, however, the DANNSCO control exhibits a number of appealing features. Most notably, the best performing straight-line and circle manoeuvres also happen to be the manoeuvres that most closely match ANN aim slip and actual slip. This is a very strong indication of the capacity of the DANNSCO model to predict optimum slip.

The curve optimisation processes that were used to identify the ANN optimum slips are also given in Figure 8.64 and Figure 8.65. The ANN predicts the slip/longitudinal acceleration curve for every sample point. In addition the predicted curves and the maximum accelerations for different vehicle conditions vary to a significant extent, although the critical slip does not change much. In particular, the transition region of the vehicle stability seems to be modelled well, which is the region this type of control is most concerned with. While there is no way of knowing if these curves are correct without high quality simulation and access to comprehensive tyre data, they do seem to exhibit the sort of behaviour that would be expected. In particular, regardless of tyre condition, the optimal slip should not vary greatly on a constant surface, otherwise existing stability controllers would be of little benefit. Further, the amount of acceleration a tyre can transmit is highly dependant on tyre condition, and factors such as vibration, transitional effect and normal load variation should significantly alter instantaneous maximum achievable acceleration.

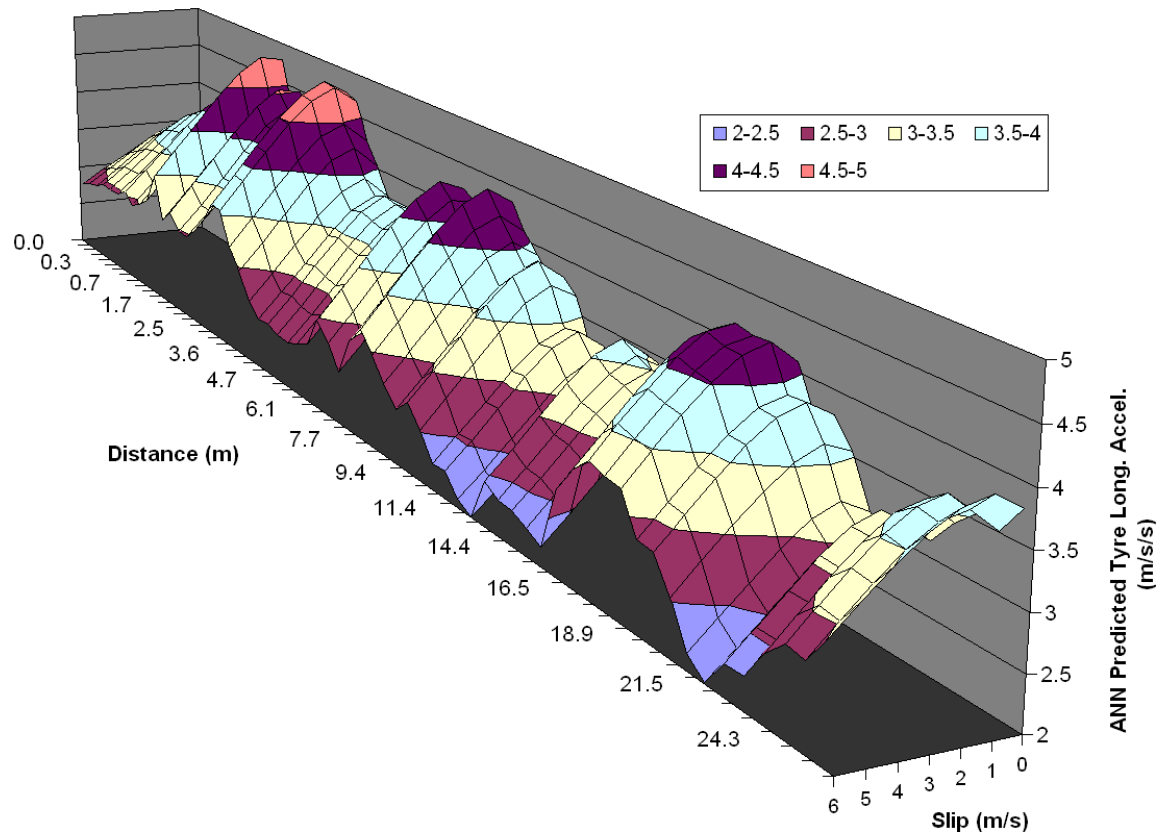


Figure 8.64: DANNSCO dynamic slip curve prediction for best straight run

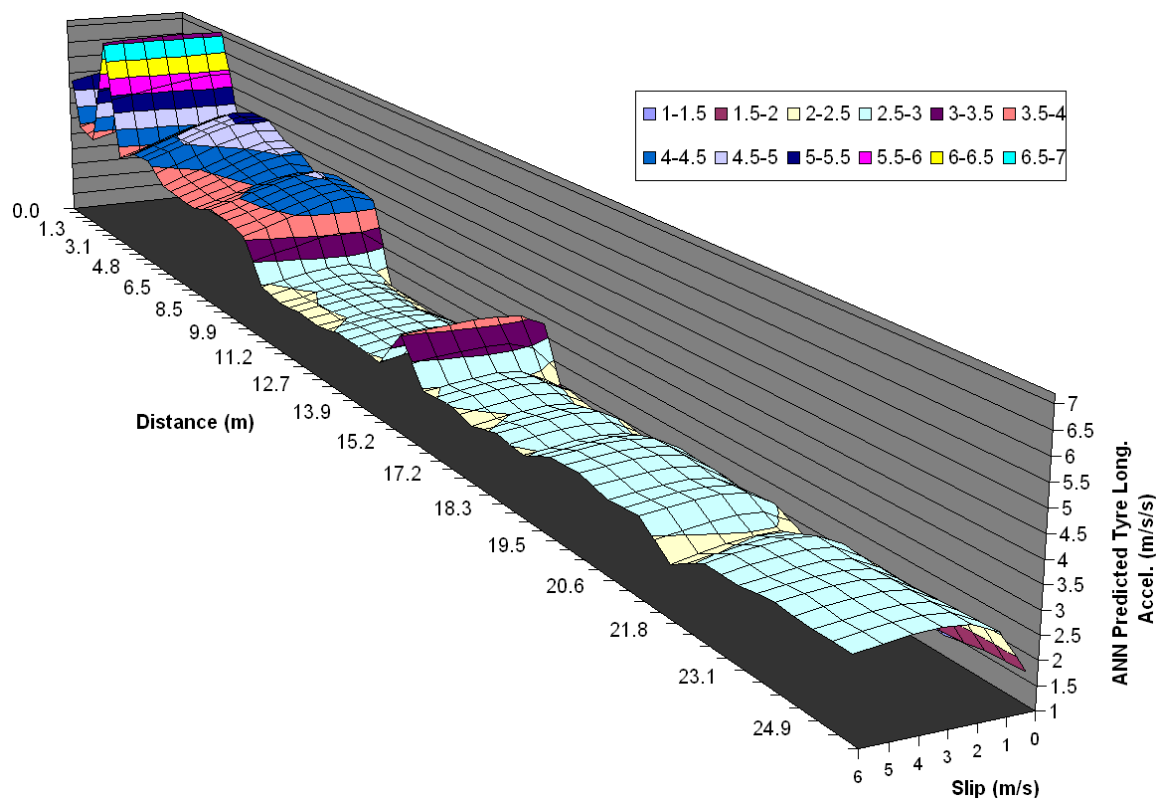


Figure 8.65: DANNSCO dynamic slip curve prediction for best 25m circle segment

All of the DANNSCO control tests that have been conducted above are only concerned with simple manoeuvres. This is important from the aspect of providing consistent analysis baselines and showing that the ANN model is accurate from one end of the spectrum to the other, but it does not show that the traction controller performs well generally. To address this Figure 8.66 shows the operation of the DANNSCO controller during miscellaneous manoeuvres.

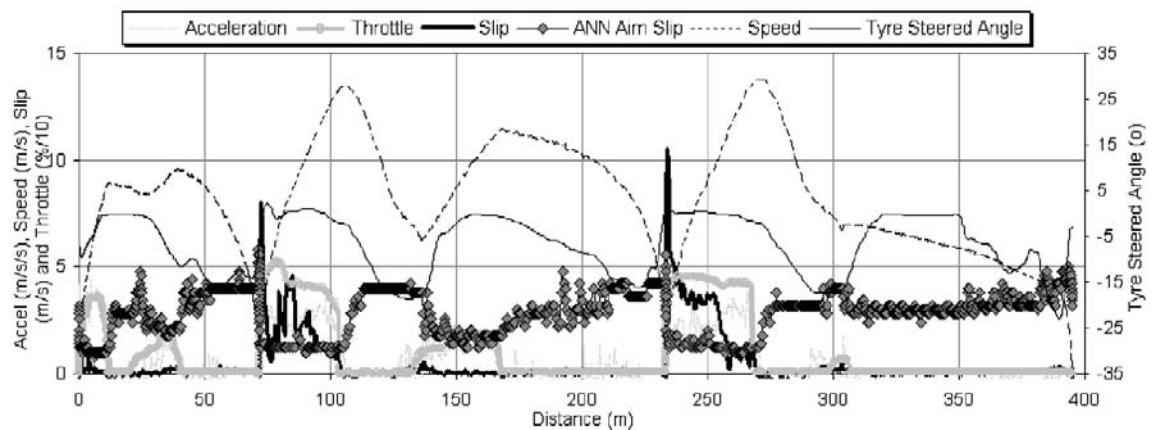


Figure 8.66: DANNSCO performance for miscellaneous driving (0-400m)

Much of this logged data is for 0% throttle, further when the vehicle is accelerating (>0% throttle) the ANN choses the aim slip that it determines is appropriate for the prevailing conditions. For instance, at 0-50m that the aim slip varies with vehicle speed and steering angle. As such, the DANNSCO controller provides ability over and above other stability controllers, in that it can vary optimum aim slip based on the manoeuvre the car is completing. If this were applied to ABS, for instance, the control strategy would allow maximum braking force in a straight line as needed, but also vary aim slip as the steering wheel is turned to provide steering control when required. This is a significant potential benefit.

8.8.2.1 Unsealed Surface Performance

While these results provide compelling evidence towards the ANN application, they are so far applicable to one surface type. It has been argued previously that these results can be extended to other surfaces due to the generic nature of ANN models, and forms an important potential characteristic for ANN chassis control. As such, this section presents the performance of the generic DANNSCO on-line controller on an unsealed surface.

To complete the ANN evaluation on the unsealed surface, the DANNSCO model had to be re-trained for the new surface. In this way for instance, the ANN stability controller and

the ANN surface identification method could be utilised in combination to activate different DANNSCO controllers for different surfaces. Furthermore, this method of re-training for specific roads would also be directly applicable for racing applications and provide some insight into the possibilities of DANNSCO adaptive learning. It was decided that the amount of the ANN training data that was acquired should be small. By testing in this way it would be possible to not only evaluate the performance of the DANNSCO model, but to gain some insight into the potential of racecar and adaptive learning applications (which would both require good ANN generalisations to be made with minimal training data).

With this in mind, the ANN training data was acquired by driving the test vehicle along a 4.4km section of the test track at a variety of safe wheel slips. The newly trained ANN model was transported in the DANNSCO controller, and its abilities in unsealed pavement traction control evaluated by driving along the same stretch of road. The resultant logged data for a typical stretch of this road is shown in Figure 8.67.

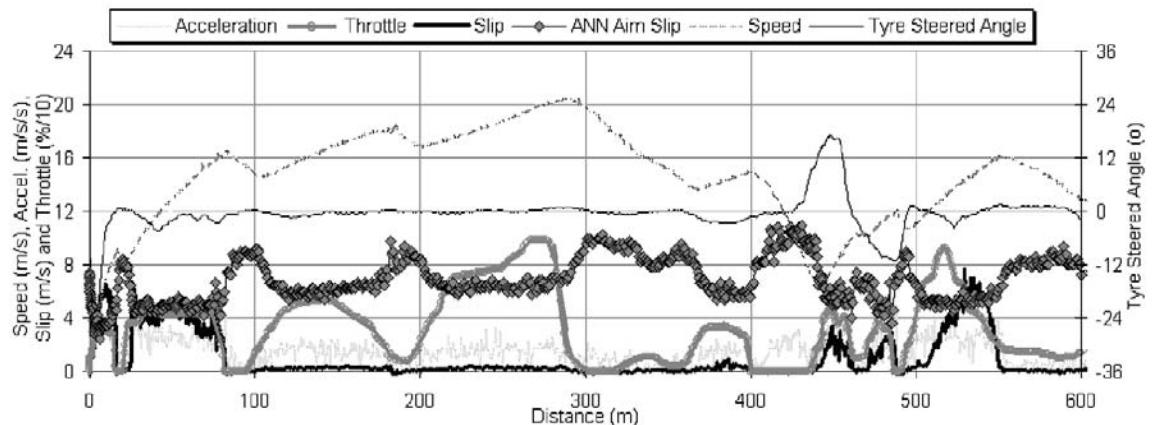


Figure 8.67: DANNSCO performance for unsealed road section – 0 to 600m

The ANN predicted aim slips are much higher than for the wet cement case of the previous tests. Further, the throttle position seems to have a large effect on the aim slip (as in the previous case) even though it is not used to determine this value. This is a curious effect, and is either based on transient abilities of tyres to produce increased acceleration when quickly ramped from low slip to high slip (which may or may not be true), or problems with the ANN model in predicting aim slips from one extreme to another (which has been discussed previously). Of most importance, however, maximum longitudinal acceleration is realised only when the actual slip is similar to the ANN prediction of aim slip. Lower slips, in the order of the optimum values for wet cement, simply do not produce high

acceleration. This clearly shows that the ANN model has been able to model the new surface reasonably well, and with much greater performance than if the METC or DEMTC were used. The reason for this, and the properties of the surface, can be seen in Figure 8.68 to Figure 8.71.

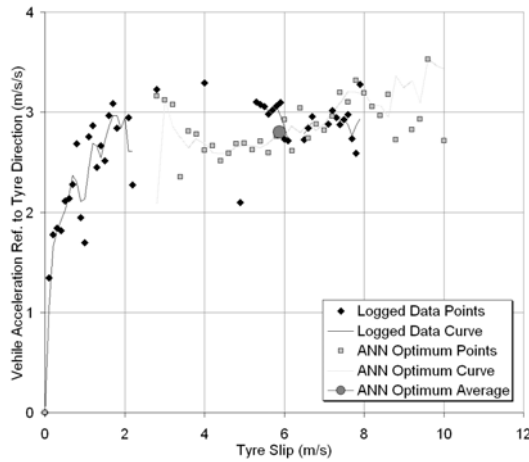


Figure 8.68: Average slip and tyre long. accel. DANNSCO comparison for 2.5 to 7.5m/s on unsealed surface

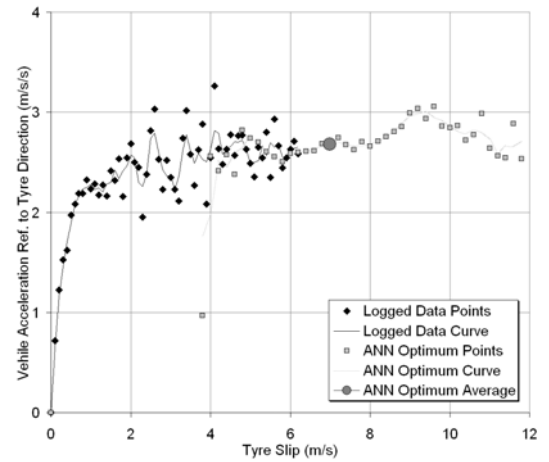


Figure 8.70: Average slip and tyre long. accel. DANNSCO comparison for 12.5 to 17.5m/s on unsealed surface

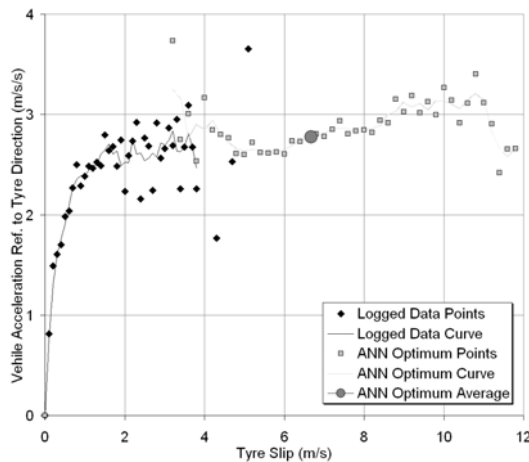


Figure 8.69: Average slip and tyre long. accel. DANNSCO comparison for 7.5 to 12.5m/s on unsealed surface

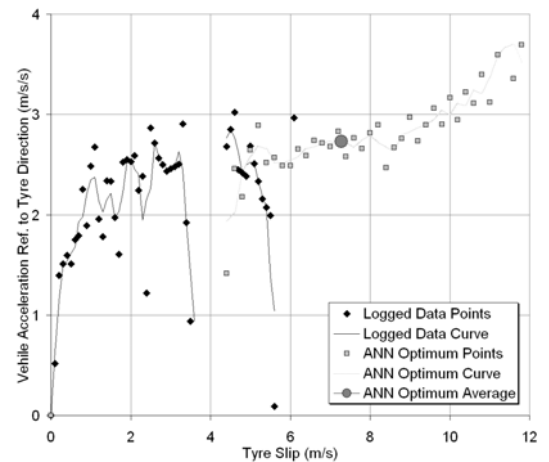


Figure 8.71: Average slip and tyre long. accel. DANNSCO comparison for 17.5 to 22.5m/s on unsealed surface

The most obvious feature of these graphs is that the logged data provides no indication of the critical slip. In fact, the transition zone appears to extend indefinitely with no point where increased slip will result in decreased acceleration. This is typical of unsealed surfaces, which exhibit similar properties to the “loose sandy soil” slip/coefficient of friction curve provided in the theory (Figure 2.10). It is also why traditional traction controllers have a renowned lack of ability on dirt surfaces. As such, the ANN model

should be able to identify this, and place the aim slip at a high value. The training data, which only consists of comparably low slip values makes this difficult, however, because these conditions are not represented well. Nonetheless, the abilities of ANN to learn from incomplete data come into play here, with the ANN predictions of aim slips clearly exceeding the slips within the training set. This produces a significant level of uncertainty into the determination of aim slips, which is evident in the spread of optimum slips in the 6 to 12m/s range, but is not considered a problem because these values fall outside the actual driving conditions.

Even so, Figure 8.67 still shows that situations arise where the ANN predicts there is a relatively low optimal slip (of around 5m/s in this case). It is anticipated that this is because at high slips the tyre actually “digs” through the loose gravel and makes contact with the compacted dirt, which is a feature the ANN prediction would not be able to recognise until it started to happen. In this case, a critical slip would exist, and the ANN seems able to identify it. It cannot identify it at low slips however, because the ANN curve optimisation logic is based on the “if everything else is constant” principle (which would assume a loose sandy soil).

8.8.2.2 Appraisal against Other Controllers

Comparing the DANNSCO controller to other controller performances has been argued to provide the best evidence of the application of ANN for stability control. Figure 8.72 and Figure 8.73 provide information for the wet conditions, with each of the runs ranked in order of ultimate speed. Furthermore, because some types of control are represented in greater numbers than others, the process of ranking runs 1 to 10 (for ten runs) was replaced with a normalisation process. Here, all of the runs for each controller are placed into the order of highest to lowest ultimate speed and (1=fastest, 10=slowest) and the runs between these extremes given a corresponding fraction in this range. This allows each type of control to be directly compared for performance, and performance repeatability.

Clearly, the METC (“MoTeC ECU Control”) has better performance than each of the other controllers. This is expected, as discussed above, because of the faster control the ECU is capable of and the tuning method employed. As such, this does not provide a good comparison for the DANNSCO and DEMTC control. Another feature is that the “No Control” option, while capable of high accelerations, does not provide repeatable

performance. This is also expected, and shows the clear benefits of any type of traction control.

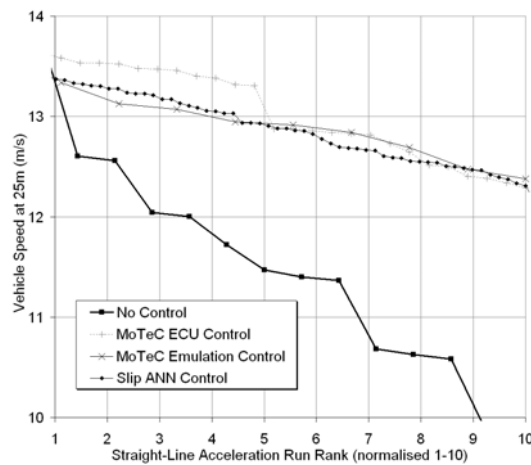


Figure 8.72: Straight-line acceleration performance comparison of different controllers by normalised 1-10 rank

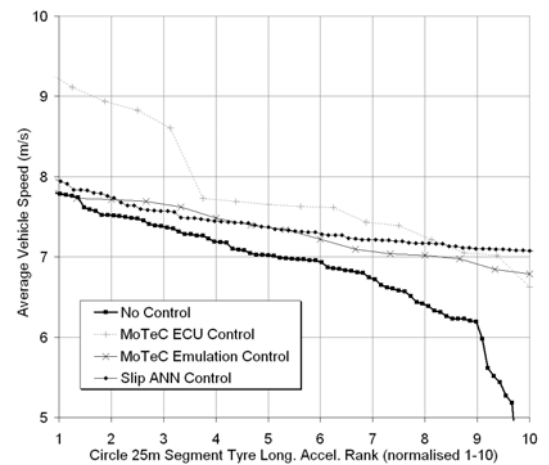


Figure 8.73: Circle run performance comparison of different controllers by normalised 1-10 rank

As such, the most important comparison made on these two graphs is between the DEMTC and the DANNSCO controllers. The slip control methods between these two techniques are identical and the control rates are very similar, which means they provide a very good comparison basis. In fact, the only significant difference between the two methods is that the DEMTC has a pre-tuned static aim slip, while the DANNSCO model varies aim slip based on ANN predictions of optimum slip.

To this end, that the DANNSCO and DEMTC models generally produce similar performance, which alone prove the potential of ANN control. However, the DANNSCO model has constantly higher performance than the DEMTC model at the faster end of the rank spectrum. This shows that the ANN prediction of optimum aim slips actually produces better performance than the traditional method, despite the slightly slower control rate of the model. In addition, the DEMTC aim slips were tuned separately for the two cases, while the DANNSCO control did not have to be, which further highlights the capability of the ANN control. Therefore, the performance of ANN control on the wet and slippery surface of the police academy test track is proven to be at least as good as the traditional control method, if not better.

8.9 Remarks

The development of the “Intelligent Traction Controller” involved a number of significant steps. This included determining the philosophy of control, finding appropriate test tracks, training a number of ANN model for improved accuracy, evaluating a range of ANN controllers to find the most promising and conducting off-line and on-line performance tests of the chosen controller. This process lead to the development, appraisal and performance verification of the Direct ANN Slip Curve Optimisation (DANNSCO) controller, which provided a number of very positive results.

In particular, the DANNSCO controller was appraised as being highly adept at determining optimum slips for maximum driven wheel longitudinal acceleration in all tested conditions, and in a generic manner. In practice, it performed as well, if not better, than comparable traditional controllers due to its ability to modify aim slip for different manoeuvres. This provides very good verification that intelligent traction control exhibits benefits above those provided by traditional controllers. It is noted, however, that these results are not conclusive due to the limitations in testing equipment, infrastructure, tyre testing data, and test-driving ability. There are many aspects of the ANN modelling accuracy that could not be explored in this work, although general performance results could be obtained.

These positive results for traction control are considered generic for all stability controllers, and were highlighted by its simple transportation to unsealed road conditions. The DANNSCO model is a generic tool used within a specific application here. The model is capable of optimising many parameters to achieve maximum acceleration in the longitudinal direction, and should be easily modified to provide other forms of wheel control. Furthermore, the goal of optimising longitudinal acceleration could be replaced with optimising acceleration in the driver desired direction, which would enable many new forms of stability control with additional actuation devices. If this can be done, which this research suggests it can, then very significant inroads will made into vehicle safety systems in regards to performance and cost.

The potential of using ANN models to predict the driver’s desired acceleration direction and an acceptable yaw rate was also briefly discussed in this chapter. As it stands, these crucial parameters are determined using traditional methods. ANN models could be used

to replace this process, in a fashion well suited to ANN modelling but seemingly unexplored. By modelling the driver's behaviour during stable conditions using ANN, their control actions in different situations can be linked to the vehicle acceleration direction and yaw rate. In this manner, ANN models would be able to observe the driver responses when the vehicle is unstable to determine the vehicle dynamics the driver is expecting. This would have the clear benefit over traditional algorithms because the model would be able to adaptively take driving style into account, as well as providing capacity to finely determine the driver's desired acceleration direction and yaw rate.

CHAPTER

- 9 -

CONCLUDING REMARKS AND PROPOSED FUTURE WORK

The work has resulted in a new and functional ANN surface identifier for stable driving conditions, an ANN traction controller that exceeds the performance of comparable traditional controllers, the development of a test vehicle in preparation for hydrogen conversion and a highly flexible research tool for many automotive applications.

This chapter highlights the outcomes of this research, discusses where it fits with current technology and expectations, and presents avenues for possible future work.

Current ABS, TCS and VDC stability controllers represent only the beginning of the performance advances active safety systems can realise. As new technologies become more developed and cheaper to implement, it is anticipated that large inroads will be made into vehicle safety. The effectiveness of these systems are dependent on the volume and quality of controller input data, design of controller output actuators, type of control implemented and control algorithm quality. A number of these emerging technologies are discussed below.

Large quantities of sensor data will improve the accuracy of control algorithms. With this in mind, there are many new sensors that are in development to provide new data, and older ones that require cost reductions to become widely adopted. Vehicle velocity sensors allow wheel slip to be directly measured, but are currently uneconomical for widespread use. The same can be said of chassis attitude sensors, which measure vehicle roll, pitch and yaw, and road surface sensors [27, 23]. Mobile telephone, radio broadcasting and Global Positioning Systems (GPS) have an application here, allowing the vehicle to collect and transmit data with external sources. Further, vision, radar and laser based systems have the capacity to monitor surrounding traffic and the preceding road conditions to add forecasting capability to active safety controllers [44, 45, 46]. Finally, other sensors are available to determine driver state, such as Blood Alcohol Content (BAC) and fatigue, which have already been shown to be major factors in crash risk.

Control actuator advances also produce significant capacity for active safety system improvements. The “x by wire” concept [27, 55] aims to remove the mechanical linkages between the driver and the vehicle, and replace them with electronic ones. In this way “brake by wire”, “throttle by wire” and “steer by wire” have the capacity to improve the scope of active safety system control to a large extent. Active rear wheel steering [25, 43, 50], differential control [33, 38, 50, 51, 52, 53, 54], real-time damping [25, 47, 48, 49], active spring rate, active anti-roll bar stiffness [25, 43, 47] and active camber also show significant promise in improving vehicle safety and performance.

As these sensor and actuator technologies develop, so does the scope for various information and control systems in vehicles. The autonomous road vehicle concept [135], for instance, has been under constant and extensive research for some time. This ambitious technology attempts to totally replace the driver, surrendering all control decisions to the onboard computer. Such a system clearly requires extremely

comprehensive sensory data and “x by wire” technology, not to mention advanced control algorithms. Collision avoidance systems [47, 55] use traffic and road obstacle information to determine whether an accident is imminent and makes avoidance manoeuvres regardless of driver inaction. Other systems attempt to improve stability control through a range of measures. Anti-rollover technology [43, 136, 137] has gained much attention in this area, and attempts to reduce the rollover propensity of vehicles such as semi-trailers, trucks and SUVs. Other systems use communication tools to provide road condition advice to stability controllers, and cover aspects such as speed zone identification, recommended corner speeds and weather conditions.

Further, improved performance does not rely solely on new sensors, new actuators and new types of control. Performance will increase as new methods are developed to derive more information from existing sensors, determine additional control possibilities from existing actuators, implement different types of controller architectures and integrate separate automotive systems. As such, future active safety systems will integrate more sensory data, control actuators, control strategies and intelligent use of these systems to improve vehicle safety. This will significantly increase system complexity, as Versmold suggests.

A clear trend for the development of system architectures can be predicated, which is influenced by the rising number of functionalities in future vehicles, the accompanying increase in complexity of vehicle system architecture and increasing requirements on system integrity.

V. Versmold [56]

Artificial Neural Networks (ANN) provide significant potential in overcoming all of these problems. Not only do they possess an ability to model complex non-linear systems, they can be taught instead of programmed. ANN models offer potential to provide better control through existing data acquisition and control hardware, new and more complicated combinations of control actuation, integration of more data from additional sensors, increased information from existing sensors and development of entirely new vehicle control concepts. They offer this with decreased mathematical complexity, faster computation, and adaptive control capabilities.

The greatest potential benefit of ANN based active safety systems in stability control applications lies in overcoming the most significant limitation in current control methodology. This difficulty is determining the optimal control strategy to achieve

maximum acceleration in the driver's desired direction and vehicle attitude, and places severe limitations on the overall performance of new technologies. In particular, as numbers of controlled variables expand passed the single tyre slip parameter used currently, significant modeling problems will severely limit performance. In such a case, any performance benefits from increased stability controller system complexity will be marginal and expensive. ANN modeling offers a solution to this problem, by providing a tool that is capable of optimally controlling complex systems with little programming complexity and few computation resources. This would provide greater performance increases at reduced costs and in shorter timeframes, and would have a significant effect of overall road safety. Particularly, ANN stability control has significant potential in integrating all of the approaching new technologies into an efficient and highly capable safety and performance package for new vehicles.

While this is the case, there is an enormous difference between "potential" and "application", and much of ANN potential is yet to be explored. Most of the research into this area has been very limited in scope, resources and budget, and for these reasons has failed to make compelling arguments for widespread ANN application. There is a clear need for more work to provide this information.

A reason for slow uptake of ANN technology can be explained by how it is potentially perceived by current industry. The "white box" nature of current stability controllers means that the control process is fully understood, and any controller limitations can be highlighted relatively easily. As such, the controller can be marketed with a clear understanding of where any flaws and litigation liabilities may lay. In contrast an ANN controller is a "black box" and can produce unpredictable actions. Even though such a system may be safer overall, this would still be a cause for concern. Furthermore, the "learning" abilities of ANN could produce problems because it is harder to determine liability for an accident. In such a case the argument could be put forward that the artificial intelligence aspect of the vehicle could cause it to be considered similarly to a trained animal, where its actions may be a result of its physiology, its environment and the quality of training that its owner provides. This is a philosophical question of how much intelligence an object must have before its possible erratic operation is not considered the responsibility of its manufacturer. Before industry will pursue systems that can think for themselves, especially in areas where safety is concerned, this issue will need to be addressed.

Such as discussion is still dependent on the quality of ANN control, which will rely very heavily on technical outcomes. This investigation advanced this technical argument on two fronts, namely through ANN surface identification in stable conditions and through ANN stability control. These two technologies are closely related, and form a foundation for highly robust stability control over a wide range of surfaces when integrated.

When accomplishing these goals, a significant component of the research included the development of a test vehicle to allow flexible research into a broad range of automotive research areas. This installation is discussed in detail through three chapters, and covers sensor, engine management, data acquisition and control hardware installation, as well as calibration and ANN controller development within NI LabVIEW. The resulting systems provide flexible tools for hydrogen, engine and chassis investigation, and were designed so additional devices could be plugged in with minimal effort and so simple system performance upgrades. In particular, the vehicle provides a platform from which previous “Intelligent Car” technologies can be developed further. These include GPS identification of speed zones, GPS and SMS integration into vehicle security systems, and ANN engine modeling and tuning. The MoTeC M400 ECU provides scope for real-time adjustment and control of all engine parameters, which can be exploited in on-line ANN engine tuning and control. Capacity also exists to combine this with hydrogen engine tuning for hybrid operation, to produce new and innovative ANN applications.

The surface identification research discussed in Chapter 5 builds on literature to provide a tool that operates in actual driving conditions, predicts more surface features, and operates in the stable tyre region. Of highlight, the model can provide information that was previously considered by literature to be impossible to obtain, at a small increase of hardware cost. In particular, when the vehicle is driven normally the model can predict whether surfaces are rough or smooth at 87% accuracy, sealed or unsealed at 94% accuracy, and wet or dry at 100% accuracy. This also means that it can be used to build statistical models to predict future conditions and enhance stability controller information and performance. This is in stark contrast to the current methods of surface identification, which can only operate after the vehicle has become unstable. Since surface characteristics are integral to efficient stability control, this new surface identifier provides the foundation for significantly increased vehicle performance. Furthermore, the ANN surface identifier opens new avenues of exploration in this field because it operates using wheel vibration data instead of kinematic relationships, and provides information that the

literature considers impossible to derive using traditional techniques. Potential limitations of the application are also highlighted through the apparent “overfitting” of the ANN model, which is assumed to be the result of the large ANN models and complex tyre elastic properties within the linear region. It is expected that further investigation will enhance these research outcomes on many fronts. This work has proved that ANN models can be used for surface identification in stable conditions, which remains a critical and unsolved area of stability control.

The ANN stability control research presented in Chapter 8 replaces the empirical and mathematical modelling required for traditional stability control with ANN tools. The ANN stability controller that was developed is based on the premise that the primary controller goal is to maximise the vehicle acceleration vector magnitude, in the driver desired direction. Under wheel speed regulation this relies on determining optimal wheel slip to achieve maximum vehicle acceleration, and formed the focus of the investigation. This approach was used to develop an intelligent traction controller as a simplified example to highlight generic ANN capability in present and future stability controllers.

The “Intelligent Traction Controller” was developed and performance verified in an actual vehicle in real-life tests, which is in contrast to the simulated conditions that form the mainstay of ANN research in this field. This is a significant research contribution, as the controller utilised ANN models to identify optimal control parameters by determining the slip / driven tyre longitudinal acceleration relationships, which are at the core of achieving optimal performance. In operation, the controller was shown to exceed the performance levels of comparable traditional traction controllers, and also provided increased functionality by determining optimal slip values that varied under different operating conditions. While it was observed that the infrastructure and resources were not available to make complete quantitative comparisons of the ANN model performances, the statistical, quantitative and qualitative comparisons that could be made showed very promising ANN control capacity. The immediate result of this research is the direct utilisation of the “Intelligent Traction Controller” in racecar traction control tuning for reduced tuning complexity and greater performance. Moreover, the generic nature of the ANN training showed a high capacity to learn new operating conditions, which could be developed further for adaptive control possibilities. The underpinning concept of this work provides broad scope for future ANN stability controller application, and presents a basis for significant and rapid advancements in automotive performance and safety.

REFERENCES

- [1] M. OLLEY, "Road Manners of the Modern Car", Society of Automotive Engineers, 1961
- [2] L. EVANS, "Traffic Safety", Science Serving Society, 2004
- [3] J. KOOPMANN and W. NAJM, "Analysis of Off-Roadway Crash Countermeasures for Intelligent Vehicle Applications", Volpe National Transportation System Center, Society of Automotive Engineers, 2002
- [4] M. MARINE, J. WIRTH and T. THOMAS, "Characteristics of On-Road Rollovers", Thomas Engineering, Inc., Society of Automotive Engineers, 1999
- [5] A. HAC, "Rollover Stability Index Including Effects of Suspension Design", Delphi Automotive Systems, Society of Automotive Engineers, 2002
- [6] W. NAJM, M. DASILVA and C. WIACEK, "Estimation of Crash Injury Severity Reduction for Intelligent Vehicle Safety Systems", Volpe National Transportation System Center, Society of Automotive Engineers, 2000
- [7] E. GOHRING, "Electronic Traction Control Systems ASR and its Integration in the Anti-Lock Braking Systems ABS to Form a Safety System (ABS/ASR) for Commercial Vehicles", Daimler-Benz AG., Society of Automotive Engineers, 1988
- [8] A. T. van ZANTEN, R. ERHARDT and G. PFAFF, "VDC, The Vehicle Dynamics Control System of Bosch", Robert Bosch GmbH, Society of Automotive Engineers, 1995
- [9] VAGVERKET, "ISA: Intelligent Speed Adaptation", Swedish National Road Administration
- [10] M. A. DILICH, D. KOPERNIK and J. GOEBELBECKER, "Evaluating Driver Response to a Sudden Emergency", Triodyne Inc., Society of Automotive Engineers, 2002
- [11] G. BROOKS and P. BELLION, "Close Up - Engineering Safety is Only Part of the Solution", Autoengineer Australasia, Issue 7, p10, Society of Automotive Engineers Australasia, March 2002
- [12] L. EVANS, "ABS and Relative Crash Risk Under Different Roadway, Weather, and Other Conditions", General Motors Corp., Society of Automotive Engineers, 1995
- [13] W. BARTLETT, O. MASORY and B. WRIGHT, "Driver Abilities in Closed Course Testing", Mechanical Forensics Engineering Services LLC, Society of Automotive Engineers, 2000
- [14] H. BAUER, "Driving-Safety Systems", 2nd Edition, Robert Bosch GmbH, 1999

-
- [15] D. DENNEH, R. JONES and J. MOTTRAM, "Foresight Vehicle: Drive-by-Tyre", University of Warwick, Society of Automotive Engineers, 2002
 - [16] C. ROUELLE, "OptimumG", Course notes, MoTeC Pty Ltd, 2002
 - [17] W. MILLIKEN and D. MILLIKEN, "Race Car Vehicle Dynamics", Society of Automotive Engineers International, 1995
 - [18] C. SMITH, "Tune to Win", Aero Publishers, Inc., 1978
 - [19] V. IVANOV, B. SHYROKAU and U. SIAKHOVICH, "Identification of Road Properties in Advanced Active safety Applications: Overview and Conceptual Solutions", Belarusian National Technical University, Society of Automotive Engineers, 2005
 - [20] J. DIXON, "Tires, Suspension and Handling", Second Edition, Society of Automotive Engineers, 1996
 - [21] K. CHEOK, F. HOOGTERP, W. FALES, K. KOBAYASHI and S. SCACCIA, "Fuzzy Logic Approach to Traction Control Design", Oakland University, Society of Automotive Engineers, 1996
 - [22] A. HAC and M. SIMPSON, "Estimation of Vehicle Side Slip Angle and Yaw Rate", Delphi Automotive Systems, Society of Automotive Engineers, 2000
 - [23] Z. FAN, Y. KOREN and D. WEHE, "Practical Rule-Based Vehicle Traction Control", University of Michigan, Society of Automotive Engineers, 1994
 - [24] M. GINDY and L. PALKOVICS, "Possible Application of Artificial Neural Networks to Vehicle Dynamics and Control: A Literature Review", National Research Council of Canada, International Journal of Vehicle Design, vol. 14, Inderscience Enterprises Ltd., 1993
 - [25] D. McLELLAN, J. RYAN, E. BROWALSKI and J. HEINRICY, "Increasing the Safe Driving Envelope - ABS, Traction Control and Beyond", General Motors Corp., Society of Automotive Engineers, 1992
 - [26] A. ZANTEN, W. RUF and A. LUTZ, "Measurement and Simulation of Transient Tire Forces", Robert Bosch GmbH, 1989
 - [27] S. ROHR, R. LIND, R. MYERS, W. BAUSON, W. KOSIAK and H. YEN, "An Integrated Approach to Automotive Safety Systems", Delphi Automotive Systems, Society of Automotive Engineers, 2000
 - [28] R. BANNATYNE, "Future Developments in Electronically Controlled Braking Systems", Transportation Systems Group, Motorola Inc., 1998
 - [29] T. MATHUES, "ABS Extending The Range", ITT Automotive Brake Systems, Society of Automotive Engineers, 1994
 - [30] M. J. SCHEIDER, "Use of a Hazard and Operability Study for Evaluation of ABS Control Logic", Ford Motor Company, Society of Automotive Engineers, 1997
 - [31] H. SAITO, N. SASAKI, T. NAKAURA, M. KUME, H. TANAKA and M. NISHIKAWA, "Acceleration Sensor for ABS", Sumitomo Electric Industries, Society of Automotive Engineers, 1992
 - [32] W. MAISCH, W. JONNER, R. MERGENTHALER and A. SIGL, "ABS5 and ASR5: The New ABS/ASR Family to Optimize Direction Stability and Traction", Robert Bosch GmbH, Society of Automotive Engineers, 1993

-
- [33] H. DEMEL and H. HEMMING, "ABS and ASR for Passenger Cars - Goals and Limits", Robert Bosch GmbH, Society of Automotive Engineers, 1989
 - [34] A. STRICKLAND and K. DAGG, "ABS Braking Performance and Steering Input", Royal Canadian Mounted Police, Society of Automotive Engineers, 1998
 - [35] T. BACH, H. SCHMITT, W. SCHWANKE and H. J. TUMBRINK, "ROADRUNNER - Realtime Simulation in Antilock Brake System Development", Lucas Braking Systems, Society of Automotive Engineers, 1995
 - [36] K. ISE, F. INOUE and S. MASUTOMI, "The Lexus Traction Control (TRAC) System", Toyota Motor Corp., Society of Automotive Engineers, 1990
 - [37] R. K. JURGEN, "Automotive Electronics Handbook", 2nd Edition, McGraw-Hill, 1999
 - [38] A. SIGL and H. DEMEL, "ABS-Traction Control, State of the Art and Some Prospects", Robert Bosch GmbH, Society of Automotive Engineers, 1990
 - [39] B. A. JAWAD, N. A. HACHEM, S. CIZMIC, J. LEESE and W. BOWERMAN, "Traction Control Applications in Engine Control", International Truck & Bus Meeting & Exposition, Society of Automotive Engineers, 2000
 - [40] D. BUTLER, "Traction Control Using Artificial Neural Networks", Masters of Engineering Science Thesis, University of Tasmania, 2002
 - [41] K. ASAMI, Y. NOMURA and T. NAGANAWA, "Traction Control (TRC) System for 1987 Toyota Crown", Toyota Motor Corp., Society of Automotive Engineers, 1989
 - [42] T. SHINOMIYA, T. TODA, M. NISHIKIMI, H. SAITO, H. TANKA and F. MANKINO, "The Sumitomo Electronic Antilock System", Sumitomo Electric Industries, Society of Automotive Engineers, 1988
 - [43] A. HAC, "Influence of Active Chassis Systems on Vehicle Propensity to Maneuver-Induced Rollovers", Delphi Automotive Systems, Society of Automotive Engineers, 2004
 - [44] A. KAWASHIMA, K. KOBAYASHI and K. WATANABE, "Implementation of Human-Like Driving for Autonomous Vehicle", Hosei University, Society of Automotive Engineers, 2001
 - [45] H. KAWAZOE, T. MURAKAMI, O. SADANO, K. SUDA and H. ONO, "Development of a Lane-Keeping Support System", Nissan Motor Co. Ltd., Society of Automotive Engineers, 2001
 - [46] M. TSUJI, R. SHIRATO, H. FURUSHO and K. AKUTAGAWA, "Estimation of Road Configuration and Vehicle Attitude by Lane Detection for a Lane-Keeping System", Nissan Motor Co. Ltd., Society of Automotive Engineers, 2001
 - [47] "Vehicle Stability Enhancement Systems - TRAXXAR", Delphi Automotive Systems, www.delphiauto.com, 2001
 - [48] S. SOMMER, "Electronic Air Suspension with Continuous Damping Control", "AutoTechnology, Vol. 3, p52", International Federation of Automotive Engineering Societies, April 2003
 - [49] J. FENG, Y. ZHAO and G. XU, "Design of a Bandwidth-Limited Active Suspension Controller for Off-Road Vehicle Based on the Co-Simulation

- Technology”, Shock and Harshness Institute of Automotive Engineering, Society of Automotive Engineers, 2004
- [50] J. HE, D. CROLLA, M. LEVESLEY and W. MANNING, “Integrated Active Steering and Variable Torque Distribution Control for Improving Vehicle Handling and Stability”, University of Leeds, Society of Automotive Engineers, 2004
- [51] “Active Torque Dynamics Evaluated”, AutoTechnology, Vol. 3, p12, International Federation of Automotive Engineering Societies, June 2003
- [52] R. HOLZWARTH and K. MAY, “Analysis of Traction Control Systems Augmented by Limited Slip Differentials”, Zexel-Gleason USA, Inc., Society of Automotive Engineers, 1994
- [53] “AWD Vehicle Dynamics Improvement using Active Limiting Slip Devices”, MIRA - New Technology 2001, www.atalink.co.uk/mira/html/p071.htm, 2001
- [54] H. HUCHTKOETTER and T. GASSMANN, “Vehicle Dynamics and Torque Management Devices”, GKN Driveline, Society of Automotive Engineers, 2004
- [55] D. WARD and H. FIELDS, “A Vision of the Future of Automotive Electronics”, Delphi Delco Electronics Systems, Society of Automotive Engineers, 2000
- [56] H. VERSMOLD, “Architectures of Future Automotive Systems”, Auto Technology, Vol. 5, p60, International Federation of Automotive Engineering Societies, December 2005
- [57] A. HADRI and J. CADIOU, K. M'SIRDI and Y. DELANNE, “Wheel-Slip Regulation Based on Sliding Mode Approach”, Universite de Versailles, Society of Automotive Engineers, 2001
- [58] M. BIAN, K. LI, N. FENG and X. LIAN, “An Empirical Model for Longitudinal Tire-Road Friction Estimation”, Tsinghua University, Society of Automotive Engineers, 2004
- [59] W. R. PASTERKAMP and H. B. PACEJKA, “Application of Neural Networks in the Estimation of Tire/Road Friction Using the Tire as Sensor”, Delft University of Technology, Society of Automotive Engineers, 1997
- [60] F. ASSADIAN, “Mixed H and Fuzzy Logic Controllers for the Automobile ABS”, Peugeot-Citroen, Society of Automotive Engineers, 2001
- [61] “Technical Innovations”, Northstar systems, www.cadillac.com/tech/northstar_r_cntrl.htm, 2001
- [62] T. UMENO, E. ONO, K. ASANO, S. ITO, A. TANAKA, Y. YASUI and M. SAWADA, “Estimation of Tire-Road Friction Using Tire Vibration Model”, Toyota Central R&D Lads, Inc., Society of Automotive Engineers, 2002
- [63] <http://en.wikipedia.org>, “Fourier Transforms”, Wikipedia, 2006
- [64] <http://en.wikipedia.org>, “Spectral Density”, Wikipedia, 2006
- [65] www.cbi.dongnocchi.it/glossary/PowerSpectralDensity.html, “Power Spectral Density”, CBI, 2006
- [66] www.wavemetrics.com, “Igor Pro - Power Spectra”, WaveMetrics, 2006
- [67] www.cygres.com/OcnPageE/Glosry/Spec.html, “Data Analysis”, Cygnus Research International, 2006

-
- [68] L. JUN, Z. JIANWU and Y. FAN, "An Investigation into Fuzzy Control for Anti-Lock Braking Systems Based on Road Autonomous Identification", Shanghai Jiao Tong University, Society of Automotive Engineers, 2001
 - [69] G. MAUER, G. GISSINGER and Y. CHAMAILLARD, "Fuzzy Logic Continuous and Quantising Control of an ABS Braking System", University of Nevada, Society of Automotive Engineers, 1994
 - [70] S. MEYER and A. GREFF, "New Calibration Methods and Control Systems with Artificial Neural Networks", IAV Automotive Engineering Inc., Society of Automotive Engineers, 2002
 - [71] D. BUTLER and V. KARRI, "Using Artificial Neural Networks to Predict Vehicle Acceleration and Yaw Angles", University of Tasmania, Proceedings of 9th International Conference on Neural Information Processing, Singapore, 2002
 - [72] P. SCHOEGGL and E. RAMSCHAK, "Vehicle Drivability Assessment using Neural Networks for Development, Calibration and Quality Tests", AVL List GmbH, Society of Automotive Engineers, 2000
 - [73] H. KIM and P. RO, "A Tire Side Force Model by Artificial Neural Network", Hyundai Motor Co., Society of Automotive Engineers, 1995
 - [74] "Artificial Neural Network Technology", www.dacs.dtic.mil/techs/neural, 1993
 - [75] T. SHIOTSUKA, A. NAGAMATSU and K. YOSHIDA, "Real Time Identification and Classification of Road Surface with Neural Network", Tokyo Institute of Technology, Society of Automotive Engineers, 1993
 - [76] S. MOHAN and R. WILLIAMS, "A Survey of 4WD Traction Control Systems and Strategies", New Venture Gear, Society of Automotive Engineers, 1995
 - [77] R. BRACH and R. BRACH, "Modeling Combined Braking and Steering Tire Forces", Exponent Corp., Society of Automotive Engineers, 2000
 - [78] K. GORDER, W. JANITOR and T. DAVID, "Vehicle Dynamics Fingerprint Process", Ford Motor Co., Society of Automotive Engineers, 1999
 - [79] W. KRANTZ, J. NEUBECK and J. WIEDEMANN, "Estimation of Side Slip Angle Using Measured Tire Forces", FKFS - Research Institute of Automotive Engineering and Vehicle Engines, Society of Automotive Engineers, 2002
 - [80] W. J. MANNING, M. SELBY, D. A. CROLLA and D. BROWN, "IVMC: Intelligent Vehicle Motion Control", University of Leeds, Society of Automotive Engineers, 2002
 - [81] K. BUCKHOLTZ, "Use of Fuzzy Logic in Wheel Slip Assignment - Part I: Yaw Rate Control", Delphi Automotive Systems, Society of Automotive Engineers, 2002
 - [82] K. BUCKHOLTZ, "Use of Fuzzy Logic in Wheel Slip Assignment - Part II: Yaw Rate Control with Sideslip Angle Limitation", Delphi Automotive Systems, Society of Automotive Engineers, 2002
 - [83] H. SASAKI and T. NISHIMAKI, "A Side-Slip Estimation Using Neural Network for a Wheeled Vehicle", Japan Defense Agency, Society of Automotive Engineers, 2000

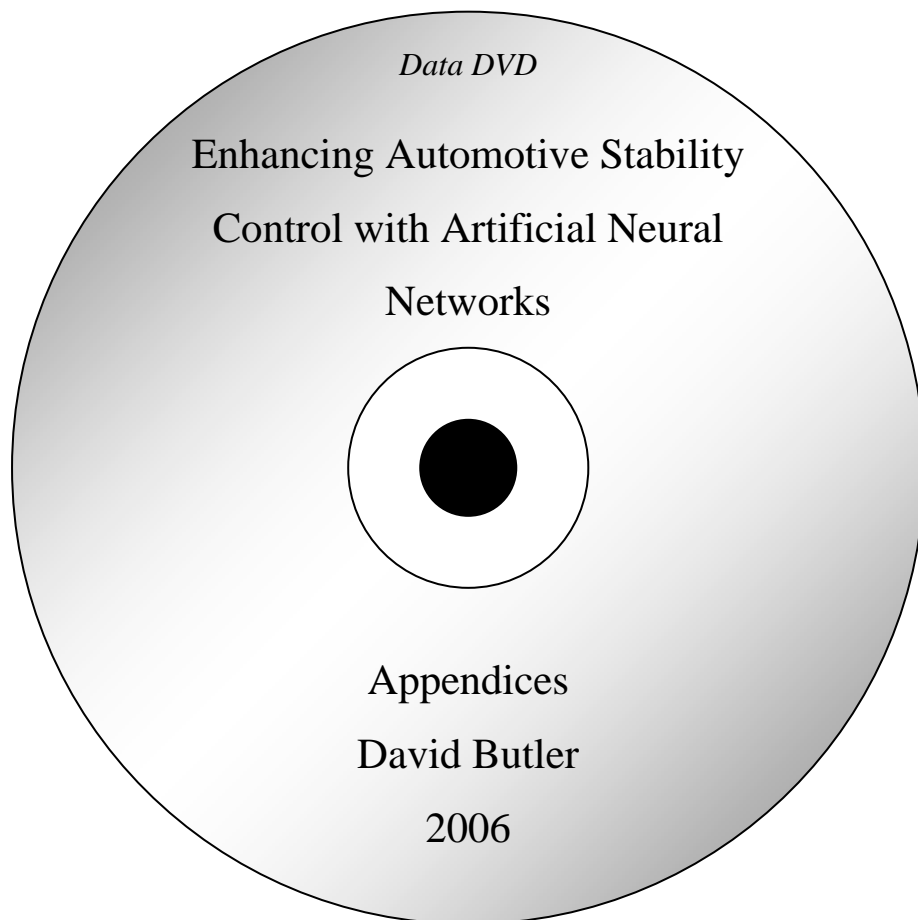
-
- [84] T. SHIOTSUKA, A. NAGAMATSU, K. YOSHIDA and M. NAGAOKA, "Active Control of Drive Motion of Four Wheel Steering Car with Neural Network", Tokyo Institute of Technology, Society of Automotive Engineers, 1994
 - [85] M. BURNETT, A. DIXON and J. WEBB, "Damper Modelling Using Neural Networks", Auto Technology, Vol. 4, p62, International Federation of Automotive Engineering Societies, August 2003
 - [86] N. LIGHTOWLER and H. NAREID, "Artificial Neural Network Based control Systems", AXEON Ltd., Society of Automotive Engineers, 2003
 - [87] G. HERON, "Estimation of Brake Force on an Open Wheel Racing Car Using Artificial Neural Networks", Masters of Engineering Science Thesis, University of Tasmania, 2003
 - [88] H. CUNNINGHAM, "Prediction of Parameters to Avoid Roll Over Using Neural Networks", Masters of Engineering Science Thesis, University of Tasmania, 2004
 - [89] D. BUTLER and V. KARRI, "An Intelligent Traction Controller", University of Tasmania, Controller Proceedings of the HiPC 2002 Workshop on Soft Computing, Bangalore, India, 2002
 - [90] D. BUTLER and V. KARRI, "Race Car Chassis Tuning Using Artificial Neural Networks 2003", University of Tasmania, Proceedings of the 16th Australian Conference on AI, Advances in Artificial Intelligence, Perth, Australia, 2003
 - [91] "LabVIEW 7", National Instruments Corporation, 2002
 - [92] C. WANG, G. CHEN, S. GE and D. HILL, "Smart Neural Control of Pure-Feedback Systems", City University of Hong Kong, Hong Kong RGC, 2002
 - [93] D. HEBB, "Organisation of Behaviour", McGill University, John Wiley & Sons, Inc., 1964
 - [94] M. ARBIB and J. ROBINSON, "Natural and Artificial Parallel Computation", Massachusetts Institute of Technology, 1990
 - [95] F. FROST, "Neural Network Applications to Aluminum Machining", PhD Thesis, University of Tasmania, 1998
 - [96] V. KARRI, "ANN for Performance Estimation in Wood Turning", University of Tasmania, ICMA Hong Kong, 1997
 - [97] R. P. KING, D. A. CROLLA and A. S. ASH, "Identification of Subjective-Objective Vehicle Handling Links Using Neural Networks for the Foresight Vehicle", University of Leeds, Society of Automotive Engineers, 2002
 - [98] V. KARRI and F. FROST, "Selecting Optimum Network Conditions In BP Neural Networks with respect to Computation Time and Output Accuracy", University of Tasmania
 - [99] D. LIU, "Neural Network-Based Adaptive Critic Designs for Self-Learning Control", University of Illinois at Chicago, National Science Foundation, 2001
 - [100] M. ZEIDENBURG, "Neural Networks in Artificial Intelligence", University of Wisconsin, Ellis Horwood, 1990
 - [101] M. CAUDILL and C. BUTLER, "Understanding Neural Networks", Vol. 1, The MIT Press, 1994

-
- [102] I. ARSIE, F. MAROTTA, C. PIANESE and G. RIZZO, "Information Based Selection of Neural Networks Training Data for S.I. Engine Mapping", University of Salerno, Society of Automotive Engineers, 2001
- [103] T. KIATCHAROENPOL, "Application of Neural Networks to Tool Condition Monitoring in Drilling Operations", PhD Thesis, University of Tasmania, 2004
- [104] S. ERGEZINGER and E. THOMSEN, "An Accelerated Learning Algorithm for Multilayer Perceptrons: Optimization Layer by Layer", University of Hannover, IEEE Transactions on Neural Networks, vol. 6, 1995
- [105] R. HECHT-NIELSEN, "Neurocomputing", University of California, Addison-Wesley Publishing, 1989
- [106] K. JAYAKUMAR, K. RAJARAM and A. FARUQI, "Machine Intelligence for Crisis Handling in Navigation Vehicles using Neuro-Controllers", 6th International Conference on Neural Information Processing, Institute of Electrical and Electronics Engineers
- [107] P. JENNINGS, J. FRY, G. DUNNE and R. WILLIAMS, "Using Neural Networks to Predict Customer Evaluation of Sounds for the Foresight Vehicle", University of Warwick, Society of Automotive Engineers, 2002
- [108] S. KALOGIROU, T. CHONDROS and A. DIMAROGONAS, "Development of an Artificial Neural Network Based Fault Diagnostic System of an Electric Car", University of Patras, Society of Automotive Engineers, 2000
- [109] R. TAWEL, N. ARANKI, G. PUSKORIUS, K. MARKO, L. FELDKAMP, J. JAMES, G. JESION and T. FELDKAMP, "Custom VLSI ASIC for Automotive Applications with Recurrent Networks", Ford Motor Company, 1999
- [110] C. ALIPPI, C. DE RUSSIS and V. PIURI, "A Fine Control of the Air-To-Fuel Ratio with Recurrent Neural Networks", Instrumentation and Measurement Technology Conference, Institute of Electrical and Electronics Engineers, 1988
- [111] J. SITTE, "Low Cost Neural Network Hardware for Control", Queensland University of Technology, Society of Automotive Engineers, 2001
- [112] "Honeywell Online Catalogue", <http://content.honeywell.com/sensing/prodinfo/auto/wheelspeed.asp>, 2002
- [113] "MoTeC Advanced Dash Logger", Software, MoTeC Pty Ltd, 2005
- [114] "Gefran Online Catalogue", http://www.gefran.com/ing/istituzione/m_map.htm, 2002
- [115] S. McBEATH, "Competition Car Data Logging - A Practical Handbook", Haynes Publishing, 2002
- [116] "Crossbow Online Catalogue", <http://www.xbow.com/html/gyros/dmuahrs.htm>, 2002
- [117] T. MURO, "Traffic Performance of a Rubber Tracked Vehicle Travelling Up and Down a Sloped Pavement", Journal of Terramechanics, Vol. 29, No. 6, 1992
- [118] L. PALKOVIC, M. EL-GINDY and H. PACEJKA, "Modelling of the Cornering Characteristics of Tyres on an Uneven Road Surface: A Dynamic Version of the Neuro-Tyre", International Journal of Vehicle Design, Vol. 15, 1994

-
- [119] V. V. VANTSEVICH, M. S. VYSOTSKI and S. V. KHARITONT, "Control of Wheel Dynamics", International Congress & Exposition, Society of Automotive Engineers, 1998
 - [120] R. ALLEN, T. MYERS, T. ROSENTHAL and D. KLYDE, "The Effect of Tire Characteristics on Vehicle Handling and Stability", "Systems Technology, Inc.", Society of Automotive Engineers, 2000
 - [121] "SmartTire for Passenger Vehicles", www.smarttire.com, SmartTire Systems Inc., 2004
 - [122] "Tasmanian Towns Street Atlas", Dept. of Primary Industries, Water and Environment, Tasmanian Government, 2001
 - [123] O. SORENSEN, "Neural Networks in Control Applications", PhD Thesis, Department of Control Engineering, Aalborg University, 1994
 - [124] "Toyota Corolla Electrical Wiring Diagrams", Toyota Motor Corp., 2001
 - [125] "Toyota Corolla Engine Maintenance 1ZZ-FE VVTi", Toyota Motor Corp., 2002
 - [126] "Toyota Corolla Electrical Diagrams", Toyota Motor Corp., 2002
 - [127] B. BONING, R. FOLKE and K. FRANZKE, "Traction Control (ASR) Using Fuel-Injection Suppression - A Cost Effective Method of Engine-Torque Control", Robert Bosch GmbH, Society of Automotive Engineers, 1992
 - [128] "M400 Engine Management System", Specifications, MoTeC Pty Ltd, 2004
 - [129] Online Documentation, Robert Bosch GmbH, www.boschmotorsandcontrols.co.uk, 2006
 - [130] Online Documentation, National Instruments Corp., www.ni.com, 2005
 - [131] D. STOLARZ, "Car PC Hacks - Tips & Tools for Geeking Your Ride", First Edition, O'Reilly Media, Inc., 2005
 - [132] K. HOSOMI, A. NAGAE, S. YAMAMOTO, Y. TAKAHIRA, M. KOIZUMI and T. ISHIKAWA, "Development of Active-Traction Control System", Toyota Motor Corp., Society of Automotive Engineers, 2000
 - [133] J. FORBES, T. HUANG, K. KANAZAWA and A. RUSSELL, "The BAT Project", UC Berkeley, www.cs.berkeley.edu/~zasio/bat/, 2001
 - [134] T. WIELENGA, "A Method for Reducing On Road Rollovers - Anti Rollover Braking", Dynamotive L.L.C., Society of Automotive Engineers, 1999
 - [135] H. PENG, "Vehicle Stability Control Panel Discussion: Anti-Rollover Braking and Yaw Control - Design and Evaluation", SAE Dynamics & Stability Conference 2000, Society of Automotive Engineers, 2000

APPENDICES

All appendices are contained within the attached data DVD



“Documents – Thesis and Appendix Summary” folder contains electronic copies of the Thesis and the Appendix documents

“Information – Appendices” folder contains all relevant data and programs including:

Appendix A – ADL and Sensor Information

Appendix B – ANN Generic Programs

Appendix C – Pavement Feature Recognition Programs and Data

Appendix D – Pavement Feature Recognition Results

Appendix E – MoTeC ECU Information

Appendix F – NI DAQ Information

Appendix G – Stability Control Programs and Data

Appendix H – Stability Control Results

Appendix I – Photos, Movies and Presentations